Heterogeneous photocatalysis for selective formation of high value-added molecules: some chemical and engineering aspects

F. Parrino, M. Bellardita*, E.I. García-López, G. Marcì, V. Loddo, L. Palmisano*

"Schiavello-Grillone" Photocatalysis Group, University of Palermo, Department of Energy, Information Engineering and Mathematical Models (DEIM), Viale delle Scienze, 90128 Palermo, Italy. Corresponding authors e-mails: marianna.bellardita@unipa.it, leonardo.palmisano@unipa.it

Abstract

This article reviews the parameters that influence heterogeneous photocatalysis (PC) for selective synthesis of high value chemicals alone or coupled with other technologies. In particular, the parameters related to the photocatalysts as crystallinity degree, type of polymorph, surface acid-base properties, exposure of particular crystalline facets, coupling of different semiconductors, position of the valence and conduction band edge, addition of doping agents, and those related to the reaction system as setup configuration and reactor geometry, type of solvent, type and amount of photocatalyst, affecting the selectivity towards specific products, are described and discussed. The presented results highlight that a precise evaluation of the efficiency of the process is a challenging but necessary task to be approached in order to allow real applications of photocatalytic processes.

Keywords: Selective photocatalysis, Selectivity enhancement, Photocatalyst features, High value-added chemicals, Reactor configuration optimization.

Introduction

Since the publication of the first papers on the application of light to chemical reactions [1-5], great attention has been devoted by the scientific community to heterogeneous photocatalysis. During the first years this technology has been developed mainly in the field of environmental remediation, with particular attention to the degradation of toxic compounds present both in liquid and in gaseous effluents,[6-9] but in recent years the attention has moved towards organic synthesis,[10-12] which include selective partial oxidations,[13] reduction reactions,[14] coupling reactions,[15,16] fuels production.[17]

Heterogeneous photocatalysis is universally recognized as a "green" and inexpensive technology because it can be carried out under mild experimental conditions (ambient temperature and pressure in the presence of cheap and non-toxic semiconductors as photocatalysts), often by using water as the solvent, O_2 as the oxidizing agent and solar light or artificial light with low-energy consumption as the irradiation sources.[18] This technology can, therefore, compete with the traditional chemical routes, which generally require drastic experimental conditions as the presence of noxious oxidant agents, toxic solvents, high temperatures and pressures. Nevertheless, photocatalysis also presents some drawbacks as the low selectivity towards the partial oxidation products (especially by using water as the solvent), the impossibility to work with solutions at high concentration, and the need of UV light irradiation to activate some photocatalysts. The efficiency of photocatalytic organic syntheses can be improved by operating different strategies, both on the typical parameters of the photocatalysts (crystallinity degree, type of polymorph, surface acid-base properties, exposure of particular crystalline facets, coupling of different semiconductors, position of the valence and conduction band edge, addition of doping agents) and on parameters related to the reaction system (setup configuration and reactor geometry, type of solvent, type and amount of photocatalyst, initial pH, presence of gases, temperature).[19] Selective photocatalytic formation of high value organic compounds can occur either through oxidation reactions or reduction of the starting substrate, therefore parameters that influence the oxidizing or reducing power, respectively, are to be taken into account.

Moreover, strictly speaking, a chemical reaction can be defined a "synthesis reaction" when the target product is separated from the reaction mixture and purified. This step is generally not reported in papers describing photocatalytic processes, and only in few works the main product has been isolated and its yield has been determined.[20-25] Nevertheless, most of the published papers on this topic can be considered only as preliminary fundamental studies, just to verify the feasibility of the process and to identify the kinetics and reactor parameters, and the structural and surface physico-chemical properties of the photocatalysts which can be optimized to enhance the selectivity/yield.

Various reviews have been published reporting papers dealing with different aspects of the synthetic photocatalysis as type of reactions, photocatalysts, use of visible or UV light, parameters that influence the reaction efficiency, biomass which can be efficiently utilized, etc.[10-12,19,26-31]

Photocatalytic syntheses have been generally performed in batch reactors. As a matter of fact, this reactor configuration perfectly suits to studies where novel reactions are under investigation. In fact, the concentration of the relevant compounds can be easily retrieved as a function of time and phenomena related to mass transport and radiant field distribution can be better controlled. Furthermore, batch reactors are very versatile and their use is well established, especially for slow reactions and when treating slurries or products with a tendency to fouling. Even if this is generally the case of heterogeneous photocatalytic reactions, the widespread use of batch systems in synthetic photocatalysis indirectly confirms the nascent level of this application. In fact, large scale synthetic processes are generally carried out in continuous systems.

Very few industrial synthetic processes are based on the use of visible light including the low-cost synthesis of rose oxide,[32] and the production of the anthelmintic drug ascaridole via solar irradiation of alpha-terpinene carried out since 1943.[33] Even more, the high cost of irradiation due to the poor efficiency of most electric light sources (until the advent of LEDs in the early 2000s), and the limited quantum efficiency discouraged chemical companies from introducing light photons as chemical reagents, no matter how clean they could be.

However, it is evident that only in a continuous reactor system it is possible to unambiguously observe, for example, catalyst poisoning or improvements of the reaction rate, whilst in batch regimen these effects will be hidden due to the interference of the products which can in turn degrade according to their kinetic law. Furthermore, continuous systems allow to reduce the size of the reactor and enable higher mixing rates, thus showing superior heat and mass transfer capacities. Even if activation energy values of photocatalytic reactions are some orders of magnitude lower than those typical of thermally activated reactions (thus making the heat transfer a secondary issue), it is necessary to avoid mass transfer limitations which result in the existence of concentration gradients in the reaction space. Furthermore, it is worth to mention that the comparison of photocatalytic results obtained in different researches is almost meaningless if mass transfer is the rate limiting step. This problem is of paramount importance for synthetic applications. In fact, the product of interest is generally a reaction intermediate and, as such, its concentration profile presents a maximum at the optimum residence time, followed by a decreasing part where its degradation is faster than its generation. Therefore, in order to enhance the selectivity towards the target compound, its residence time must be carefully optimized. In a batch system this can be achieved only by stopping the reaction when the target compound concentration reaches its maximum, with relevant disadvantages in terms of plant flexibility and operational costs. On the other hand, in a continuous reactor the residence time distribution can be simply controlled by optimizing the fluid dynamics of the system.

The aim of this paper, is not only to describe the advances of using heterogeneous photocatalysis for selective formation of fine chemicals (not only organics) with the exception of H_2, reporting in more detail the papers published recently, but also to comment on the strategy for the enhancement of process performance in terms of selectivity and photon efficiency. Moreover, the influence of the reactor type, the process set-up and the coupling of the photocatalytic reactor with a membrane system is examined. The main goal for researchers involved in heterogeneous selective photocatalysis is to prepare and to test new photocatalysts (composites, sensitized, coupled oxides etc.) or to modify the structural and surface physico-chemical properties of well-known photocatalysts to optimize the efficiency and the selectivity of the process under investigation (process intensification) and to synthetize new products.

1. Selectivity enhancement by tuning photocatalyst features

Figure 1 shows the main parameters, related to the photocatalyst properties, which can be tuned to enhance the selectivity.
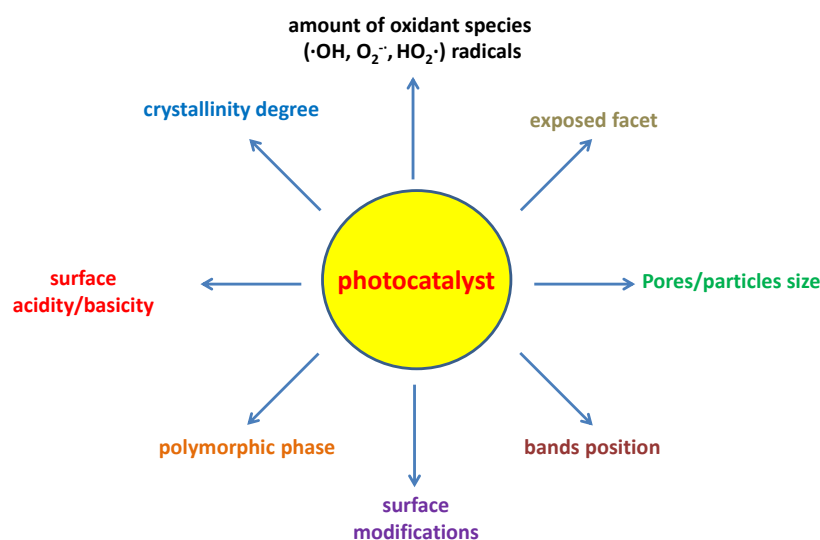

Figure 1: Scheme of the photocatalyst physico-chemical and electronic properties.

1.1. Influence of the phase of TiO$_2$, the most used photocatalyst

The various polymorphs of a semiconductor possess different intrinsic electronic and surface physico-chemical properties (conduction and valence band edges position, band-gap, charge recombination rate, charge mobility, surface concentration and strength of acid-base sites, hydroxylation degree, specific surface area, zero charge point, hydrophilicity, oxygen interaction with the surface)[34-39] which result in a different photocatalytic activity, and in particular in a different selectivity. TiO$_2$ is the most popular photocatalyst because of its high efficiency and versatility in different reaction media, chemical stability, nontoxicity, and low cost. The three most used TiO$_2$ polymorphs are anatase, brookite, and rutile. Rutile is the most thermodynamically stable form, whilst anatase and brookite are metastable phases that turn into rutile at high temperatures. From the photocatalytic point of view, anatase is considered the most active one, rutile is believed scarcely active while, until a few years ago, the photocatalytic activity of brookite was not known because of its difficult preparation as a pure phase.

Genarally, rutile and brookite are less active than anatase in total oxidation reactions,[40] but they can be used effectively in synthetic reactions in which catalysts with a low oxidizing power are preferred. In particular, rutile and brookite powders were more efficient than anatase in the partial oxidation of 4-methoxybenzyl alcohol (4-MBA) to para-anysaldehyde (PAA) in pure water because of their higher hydrophilicity due to surface hydroxyl groups

which favor PAA desorption from the catalyst surface avoiding its subsequent oxidation.[41-43] This hypothesis was confirmed by Li et al.[44] who reported the partial oxidation of benzyl alcohol (BA) over TiO_2 rutile nanorods: they found, in fact, an increase of selectivity with the surface hydroxyl groups density.

The photoactivity of Au nanoparticles supported on nanofibers of TiO_2 with different phases was compared under visible light irradiation towards the coupling of nitroaromatic compounds.[45] The samples containing a higher percentage of brookite showed a greater nitroaromatics reductive coupling efficiency.

Brookite TiO_2 nanosheets in aqueous H_2O_2 solution allowed a BA conversion of ca. 51%, with a selectivity to benzaldehyde close to 100%.[46] The high activity was attributed to the formation of superoxide radicals on the catalyst surface due to the low adsorption energy between brookite TiO_2 surface and H_2O_2.

Ohno et al.[47] studied the adamantane oxidation in acetonitrile/butyronitrile mixtures in the presence of various TiO_2 anatase, rutile and anatase-rutile samples and O_2 or H_2O_2 as the oxidants. Anatase was more efficient than rutile under aerated conditions, whilst an inversion of the activity was noted after H_2O_2 addition with an enhancement of the quantum efficiency from 6.4 % in the presence of anatase to 25 % in the presence of rutile. This behavior has been attributed to the higher formation rate of $^.$OH radicals, as confirmed also by Hirakawa et al.[48] Moreover, a different distribution of the hydroxylation adamantine products was obtained at various anatase amounts. Thus, by selecting an appropriate catalyst, it is possible to maximize the yield of a given product.

A difference in the amount of hydroxylation products was found also in the photocatalytic oxidation of phenol to catechol in water (Table 1) by using anatase and rutile samples calcined at different temperatures.[49] An increase and a decrease of conversion of the substrate was noted after NaF addition for anatase and rutile, respectively, whilst selectivity improved for both phases. In particular it reached very high values (>90%) by using pure rutile.[49]

Table 1 Anatase and rutile percentage and particle size, conversion of phenol and selectivity towards catechol during the photocatalytic oxidation of phenol in water over bare TiO_2 or fluoride modified TiO_2 at pH=3. Reproduced with permission from ref 49. Copyright 2008 Wiley and Sons.

Catalyst	Anatase (wt %)	Rutile (%)	[NaF] = 0 mM		[NaF] = 1 mM	
			Phenol conversion (%)	Catechol selectivity (%)	Phenol conversion (%)	Catechol selectivity (%)
AT200[a]	100	0	1.2	33	4.0	53
AT400[a]	100	0	6.0	59	10	76
AT600[a]	100	0	20	64	54	75
AT800[b]	3	97	0.64	60	12	81
RT200[b]	0	100	18	66	5.0	95
RT400[b]	0	100	10	51	2.4	90
RT600[b]	0	100	12	64	2.7	97
RT800[b]	0	100	5.4	76	1.9	100
P25[a]	70	30	39	63	84	76
P25[b]	0	100	6.4	60	3.6	90

[a]Values of conversion and selectivity were calculated after 1.0 h of irradiation.
[b]Values of conversion and selectivity were calculated after 6.0 h of irradiation.

The reduction of m-dinitrobenzene (m-DNB) in a deareated water/2-propanol (50% v/v) mixture in the presence of P25 TiO_2 samples calcined at different temperatures under UV light produced selectively m-phenylenediamine (m-PDA) with the untreated P25 and m-nitroaniline (m-NA) with pure rutile after 8 h of irradiation.[50] Also in this case rutile exhibited a lower photoreactivity than anatase.

As reported in Table 2, during the alanine oxidation both conversion and selectivity were related to the TiO_2 polymorph.[51] Moreover, a different formation rate of the various products can be observed: acetamide was preferentially formed in the presence of pure anatase and in rich anatase samples, whilst pyruvic acid was the main product by using rutile. The two products were formed following two different routes: pyruvic acid directly from alanine and acetamide from condensation of acetaldehyde and ammonia.

Table 2: Decomposition and formation rates in photocatalytic decomposition of alanine in deuterated aqueous TiO_2 suspension after 10 h of UV irradiation. Reproduced with permission from ref 51. Copyright 2007 Elsevier.

Sample	Anatase content (%)	Alanine decomposition rate (μmol/min)	Formation rate (μmol/min)			
			Acetaldehyde	Acetic acid	Pyruvic acid	Acetamide
AMT-100	100	20.4	4.2	16.1	0.09	0.25
ST-01	100	15.0	2.3	6.3	0.10	0.26
UV-100	100	13.0	3.4	4.7	0.11	0.19

ST-21	100	14.4	2.7	8.5	0.11	0.24
F4	88	10.4	4.1	4.4	0.10	0.35
AMT-600	100	24.6	6.5	8.0	0.14	0.20
P25	80	13.8	4.0	3.8	0.15	0.24
MT-500B	0	6.4	1.8	2.4	0.45	0.09
PT-101	0	9.9	1.2	4.9	0.40	0.06

During the oxidation of benzene to phenol in water and in the presence of O_2, a higher selectivity was observed by using anatase samples (Figure 2).[52] Moreover, it was possible to differentiate the oxygen present in phenol by using isotopically traced oxygen ($H_2^{18}O$ and $^{18}O_2$). In the presence of rutile most of oxygen present in phenol derived from O_2, whilst an opposite behavior was observed for anatase.
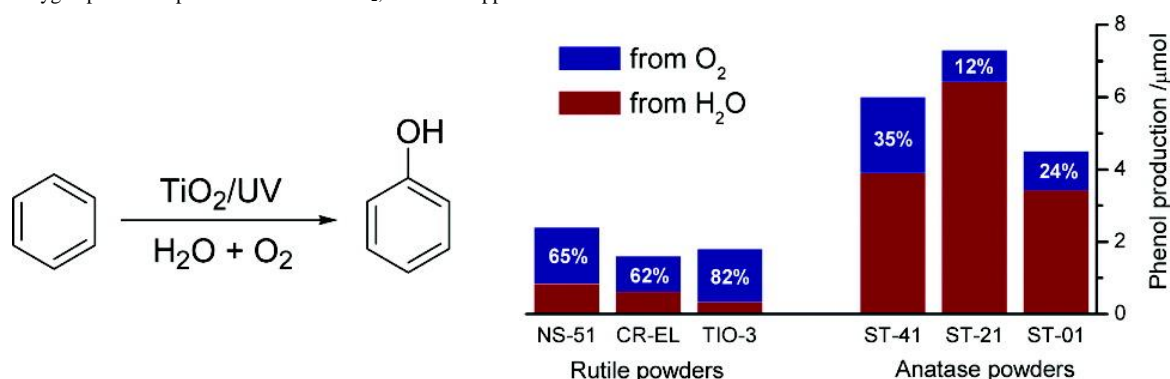
Figure 2: Amount of phenol obtained from benzene in the presence of different anatase and rutile TiO_2 commercial samples irradiated under UV-vis light for 100 minutes. Reproduced with permission from ref 52. Copyright 2010 American Chemical Society.

In the selective anaerobic conversion of glucose in aqueous solution, a different behavior of anatase and rutile TiO_2 samples towards the distribution of partial oxidation products has been noticed (Tables 3) by two different research groups.[53,54] Rutile was more efficient than anatase in glucose conversion; gluconic acid was preferentially produced in the presence of anatase, whilst arabinose and erythrose in the presence of rutile; pure brookite (for the first time employed for glucose conversion) exhibited the same behavior of rutile. The different behavior was tentatively attributed to the formation of $^\cdot$OH radicals on the anatase surface and of peroxy species on rutile. In the presence of a mixed CH_3CN/H_2O solvent, on the contrary, P25 showed a higher glucose conversion than rutile and anatase and also in this case a slight difference in the distribution of the oxidation products was noted.[55]

Table 3A: Glucose aqueous conversion and selectivity for runs carried out in anaerobic conditions.

Sample	Phase[1]	Conversion [%]	Selectivity [%]				
			Fructose	Arabinose	Erythrose	Gluconic Acid	Formic Acid
Pt-P25	A+R	36	25	41	-	-	45
Pt-BDH	A	40	85	-	-	41	7
Pt-HP-Rutile	R	77	-	54	47	-	116
Pt-HP-Brookite	B	53	4	22	5	-	29

[1] A = Anatase, R = Rutile, B = Brookite.

Table 3B: Glucose aqueous conversion and selectivity for runs carried out in anaerobic conditions.

Sample	Phase[1]	Conversion [%]	Selectivity [%]		
			Arabinose	Erythrose	Gluconic Acid
Rh-P25	A+R	17	60.7	9.0	9.6
Rh-TiO$_2$-A	A	16	49.4	4.5	3.2
Rh-TiO$_2$-R	R	47	74.7	20.6	-

[1] A = Anatase, R = Rutile

Shiraishi et al.[56] found a high activity of rutile for hydrogenation of nitroaromatics to the corresponding anilines (yield > 94%) in the presence of alcohols as H source. The higher performance of rutile with respect to anatase was attributed to the higher concentration of surface oxygen vacancies,

with a resulting more significant presence of reduced Ti^{3+} atoms. The latter can contemporaneously work as preferential adsorption sites for the nitroaromatics substrates and as trapping sites for e^-, favoring selectively the hydrogenation of nitro to amino-group (Figure 3).
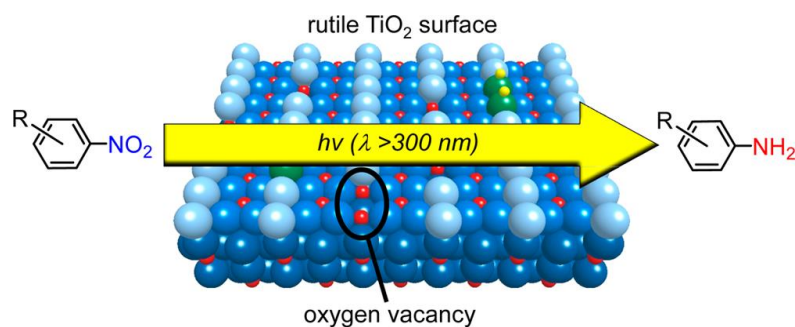

Figure 3. Scheme of nitroaromatics hydrogenation to anilines. Reproduced with permission from ref 56. Copyright 2012 American Chemical Society.

However, it is not possible to infer a general behavior of one phase with respect to another, because the photocatalytic activity of a catalyst depends on many factors and it can not be, generally, foreseen by considering only one of them. This explains the different reactivity of the same TiO_2 polymorph which is prepared in different ways and used under different experimental conditions.

Moreover, generally, a higher activity of rutile and brookite with respect to anatase has been found when polyhydroxylated substrates, as the carbohydrates, are used.[53,54]

1.2. Crystallinity degree

When a powdered photocatalyst, as for instance TiO_2, is used for environmental applications, a way to increase the oxidation power is to enhance the crystallinity degree, because the higher the percentage of the amorphous phase the higher the presence of lattice defects and the higher the recombination probability among the photogenerated charges. On the contrary, catalysts with a low oxidizing power can be more effective for photocatalytic syntheses because they limit the further oxidation of the obtained high value products. For this purpose, catalysts with a low degree of crystallinity can give better results with respect to very crystalline samples. For photocatalytic materials, and generally for oxides, only the crystalline phase is taken into account for the evaluation of the catalytic properties as the amorphous fraction is considered inactive. This assumption is correct when the amount of amorphous phase present in a solid is small, but it is not valid when the amorphous phase becomes an important fraction of the sample. Yurdakal et al.[57] demonstrated that, during the selective oxidation of 4-MBA, also the fraction of amorphous phase present in TiO_2 influences the reaction providing active sites for the alcohol partial oxidation and hindering the electron transfer between the particles as a consequence of the strong basic character of the terminal hydroxyls of the amorphous titania chains. It is difficult to quantify and to characterize the amorphous portion of the materials, and only few papers report experimental methods to calculate the extent of crystallinity.[58-64] Moreover, some features, as the crystallinity of the photocatalyst, can change under irradiation. In particular, Zhang et al.[65] observed un amorphization of few superficial layers of anatase crystals in the presence of light and water vapor.

Low crystalline home made TiO_2-rutile samples showed better performances than highly crystalline commercial samples towards partial oxidation of 4-MBA and benzyl alcohol (BA) to the corresponding aldehydes.[41] Poorly crystallized N-doped TiO_2 samples were very effective in the selective formation of PAA from 4-MBA under solar light irradiation.[66] Also in the aqueous synthesis of vitamin B3 (pyridine-3-carboxylic acid) from its corresponding alcohol, the less crystalline home prepared TiO_2 samples were more efficient, reaching a selectivity under UV light irradiation of ca. 75 % for 50 % of conversion.[67]

Carneiro et al.[68] observed a decrease in the cyclohexanone formation by increasing the crystallinity during the selective oxidation of cyclohexane by using TiO_2 anatase calcined at different temperatures. In the partial oxidation of glucose in aqueous dispersion of different TiO_2 commercial and home made (HP) photocatalysts, the least crystalline samples gave rise, generally, to the greatest conversions (considered as sum of the partial oxidation to high value chemicals and isomerization to fructose).[53] It is not possible to obtain a perfectly monotonous trend because different factors can contribute, in various ways, to the determination of photoactivity/selectivity.

On the contrary, during the selective hydroxylation of phenol (aromatic compound with an electron donor group) and benzoic acid (aromatic compound with an electron withdrawing group) the highest selectivity towards mono-hydroxy species was obtained by using the most crystalline samples (Figure 4).[69] The same trend was found for the partial oxidation of glycerol: the very crystalline commercial TiO_2 P25 gave rise to the best selectivity to 1,3-dihydroxyacetone, glyceraldehyde and formic acid.[70] These findings suggest that the results are not general and depend on the type of substrate and the interactions between the catalyst surface and the substrate and/or intermediates and products.
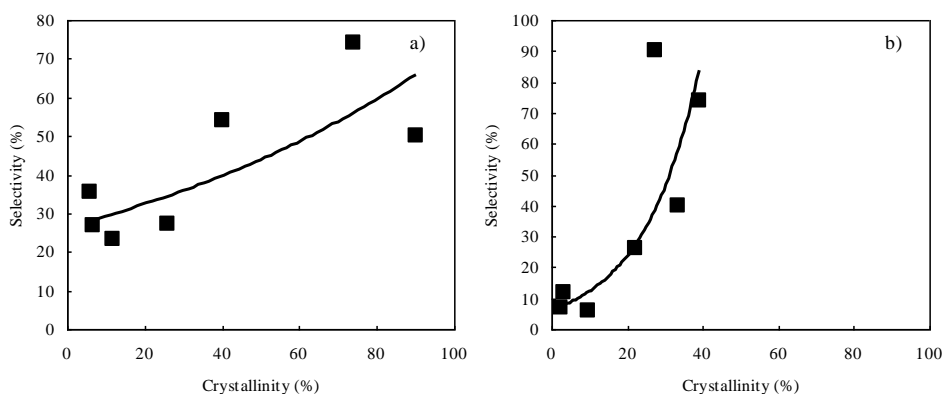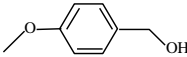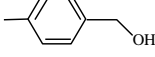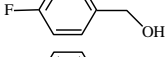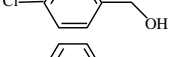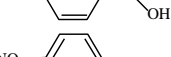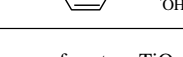
Figure 4: Selectivity to mono-hydroxylated species vs. samples crystallinity. a) Phenol, b) benzoic acid. Reproduced with permission from ref 69. Copyright 2012 Elsevier.

1.3. Influence of the crystal facet

In the last years, an increasing attention has been devoted to the synthesis, characterization and understanding of the physical, chemical and photocatalytic properties of the different facets of a semiconductor. The most investigated photocatalyst has been anatase TiO_2, while less attention has been dedicated to the other TiO_2 polymorphs and other photocatalysts.[71,72] In anatase the most abundant facet is the most thermodynamically stable {101} (surface energy 0.44 J m^{-2}), whilst the facets {001} (surface energy 0.90 J m^{-2}) and {010} (surface energy 0.53 J m^{-2}) are less common and their growth can be prevalently favored by varying appropriately the synthesis condition. The most employed method foresees the use of capping agents (fluorine prevalently) which bind to a facet during the synthesis, allowing the growth of another one. It is reported that the anatase TiO_2 facets have different properties and different photocatalytic behavior. In the aqueous selective oxidation under UV irradiation of some benzylic alcohols (Table 4), anatase with predominance of the {001} facet (T001: 80% {001})[73] showed superior activity (than the sample with a majority of the {101} facet (T101: 8% {001}). The better performance of the sample T001 was ascribed to a higher value of the surface energy of the {001} facet that favors the activation of the adsorbed reagents, a better O_2 adsorption and a higher number of oxygen vacancies.

Table 4: Photocatalytic performances of TiO_2 anatase home prepared samples in the selective oxidation of benzylic alcohols to the corresponding aldehydes. Reproduced with permission from ref 73. Copyright 2016 Elsevier.

Reactant	Conversion (%)		Selectivity (%)	
	T101	T001	T101	T001
(methoxy-benzyl alcohol)	40	63	98	99
(methyl-benzyl alcohol)	38	60	100	99
F— (fluoro-benzyl alcohol)	28	49	98	97
Cl— (chloro-benzyl alcohol)	30	51	99	97
Br— (bromo-benzyl alcohol)	32	53	99	100
NO_2— (nitro-benzyl alcohol)	26	35	95	96

The evaluation of the performance of anatase TiO_2 samples prepared in the presence of different amounts of HF acid towards the selective oxidation of two alcohols, i.e. 2-propanol (in gas phase) and 4-MBA (in liquid phase) evidenced that both the presence of the {001}, {101} and {010} facets and residual fluorine influenced the features and the photocatalytic proprieties of the samples.[74] The contemporaneous presence of the three TiO_2 facets allowed heterojunction with an efficient separation of the photo-generated pairs, as schematized in Figure 5, while the presence of fluorine, as revealed by EIS measurements, enhanced the conductivity of fluorine-doped samples.
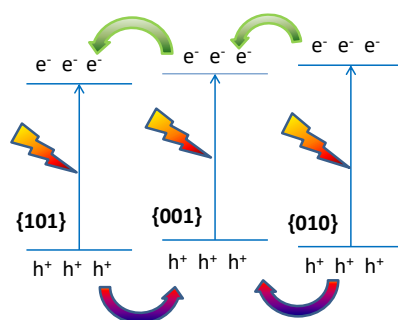
Figure 5: Electronic band position in the TiO$_2$ anatase {101}, {001} and {010} facets.

Yu et al.[75] examined the photocatalytic activity of anatase TiO$_2$ samples containing different percentages of {001} and {101} facets in gaseous CO$_2$ reduction under simulated solar light irradiation. A commercial P25 TiO$_2$ sample was used for the sake of comparison. The maximum CH$_4$ production rate was obtained with the sample HF4.5 containing 58% and 42% of the {001} and {101} facets, respectively (Figure 6). These findings indicate that the activity was not directly proportional to the amount of {001} facet but was related to an optimal ratio between the two facets. In the light of DFT (Density Functional Theory) calculations, which revealed a different band edge position for the {001} and {101} facets, the results were explained by considering a surface heterojunction that allowed an efficient separation of the photogenerated charges. Similar results were obtained by Cao et al.[76]
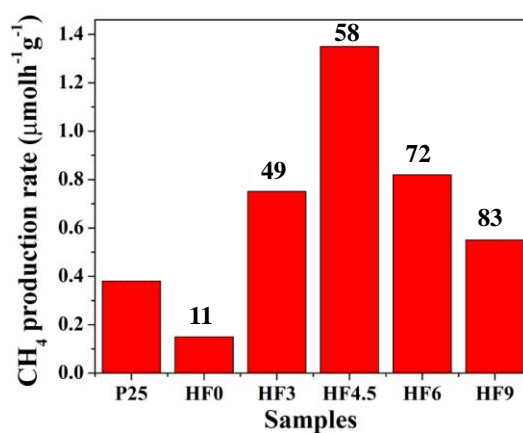

Figure 6: CH$_4$-production rate on P25 and TiO$_2$ samples prepared by varying HF amount. On the bars the percentage of {001} facet is reported. Reproduced with permission from ref 75. Copyright 2014 American Chemical Society.

Mao et al.[77] carried out the CO$_2$ photoreduction to CH$_4$ by using anatase TiO$_2$ samples with exposed {001} and {010} facets with and without Pt-loading. They found a different trend in CH$_4$ production: in the absence of Pt the best catalyst was that containing prevalently the {010} facets, the opposite was found after Pt deposition (see Figure 7). This behavior was explained by considering the different electronic structure of the {001} and {010} facets, responsible for a different distribution of Pt on the two surfaces; in particular, Pt was present on the {010} facet as nanoparticles aggregates, whilst it was uniformly distributed on the {001} facet.
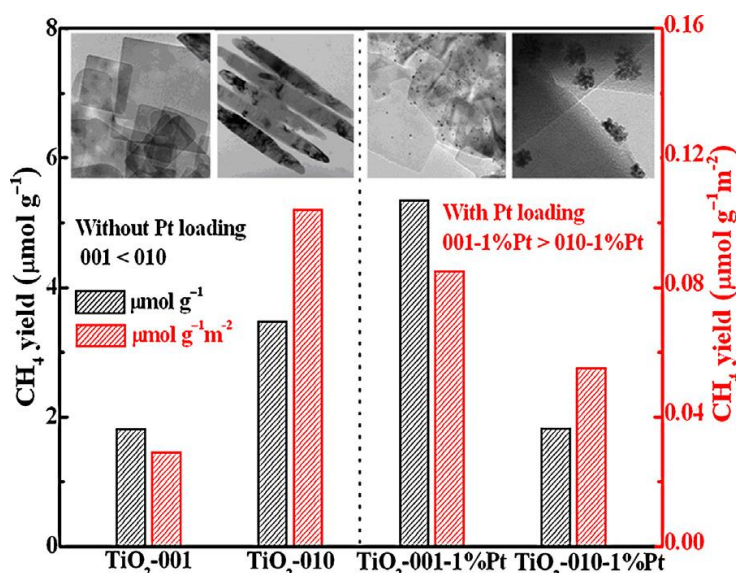
Figure 7: CH_4 yield over bare and Pt-TiO_2 samples. Reproduced with permission from ref 77. Copyright 2014 Elsevier.

CO_2 photoreduction on brookite TiO_2 exposing the {001} and {210} facets allowed to tuning the CO/CH_4 ratio by varying the amount of loaded Ag nanoparticles.[78] The CO amount showed a bell shaped trend with the Ag percentage: for percentages of Ag ≤ 0.5%, the particles were mainly distributed on the {210} facet, whilst for higher amounts Ag was mainly present on the {210} facet as aggregates, and in less amount on the {010} facet as dispersed nanoparticles, thus favoring the enhancement of CH_4 evolution.

Recently the CO_2 reduction under simulated solar light irradiation has been reported on TiO_2 anatase exposing {001} and {101} facets supported on carbon nanofibers (CNFs).[79] The high activity of the composite system has been attributed, as depicted in Figure 8, to the formation of an efficient heterojunction between CNFs and the TiO_2 facets.
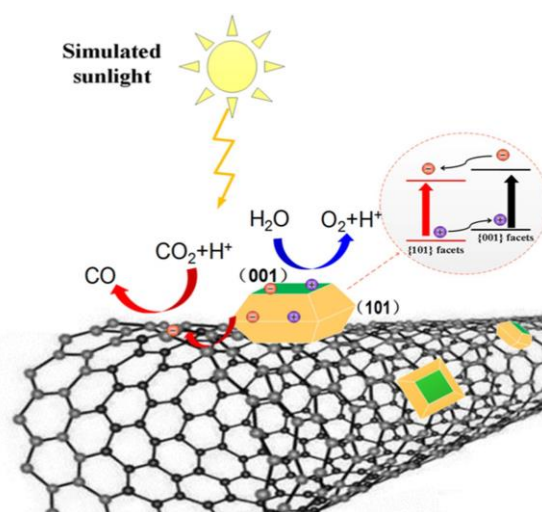

Figure 8: Hypothesized mechanism of CO_2 photoreduction on CNFs/TiO_2 system. Reproduced with permission from ref 79. Copyright 2018 Elsevier.

Nevertheless, the above results are not generally valid because they depend on the reaction type, reaction conditions and preparation of the photocatalytst. Notably, anatase samples obtained starting from different precursors can present different photocatalytic behaviors due to different structural and surface physico-chemical properties, while showing the same facets distribution. Liu et al., in fact, found that the crystal facets of TiO_2 samples tested in selective reduction and oxidation reactions exhibited different photocatalytic efficiency, as shown in Figure 9.[80] In particular, the facets order of activity was {101} > {001} > {100} for reduction of nitrobenzene to aniline, whilst {101} ≈ {001} ≈ {100} for BA oxidation to benzaldehyde (BAD).
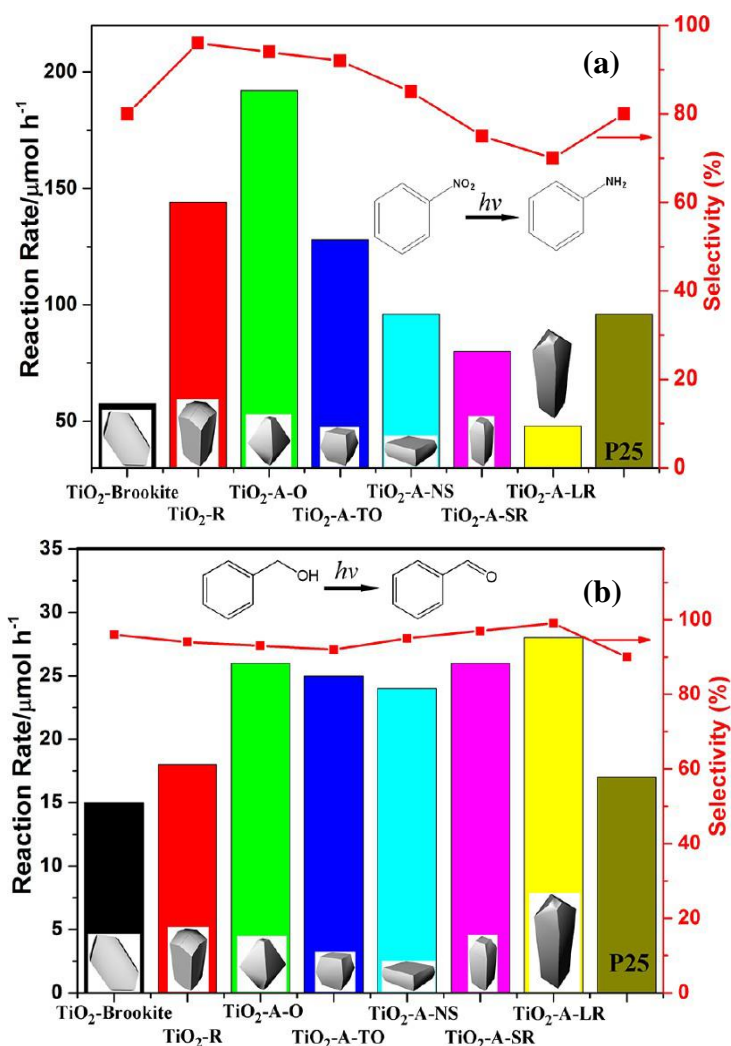
Figure 9: Photocatalytic activity of the different samples for reduction of nitrobenzene to aniline (a) and oxidation of benzyl alcohol to benzaldehyde (b). Reproduced with permission from ref 80. Copyright 2013 American Chemical Society.

The reduction of nitrate in water under simulated solar light irradiation was performed with high efficiency (95 % of conversion with N_2 selectivity over 90%) by selectively depositing Ag nanoparticles on {101} facet of anatase containing both {001}and {101} facets.[81]

The glycerol selective photocatalytic conversion in water under anaerobic conditions produced hydroxyacetaldehyde (HAA), formic acid (FA), trace of glyceraldehyde (GA) in the liquid phase and H_2 in the gas phase.[82] The products selectivity depended both on TiO_2 polymorph and crystal facet (Figure 10): both conversion and selectivity to HAA were higher by using rutile with a high percentage of {110} facet. The different results were ascribed to the prevalent formation of peroxo species on rutile surface and $^-$OH radicals on anatase surface which gave rise to a different glycerol reaction pathway.

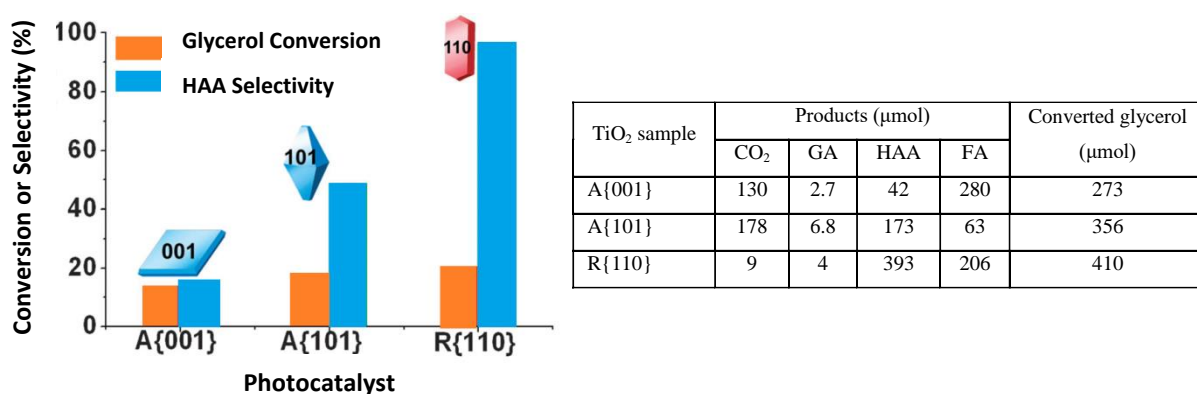| TiO_2 sample	Products (µmol)				Converted glycerol
	CO_2	GA	HAA	FA	(µmol)
A{001}	130	2.7	42	280	273
A{101}	178	6.8	173	63	356
R{110}	9	4	393	206	410

Figure 10: Photocatalyst performances during glycerol conversion with TiO_2 anatase (A) and rutile (R) exposing different facets.

In the following are reported two examples in which the influence of the crystal facet on the photocatalytic activity was observed in the case of materials different from TiO_2.

Bi_2WO_6 nanoplates exhibiting a high percentage of {001} facet showed good performance in CO_2 gas phase reduction under visible light irradiation.[83] The authors demonstrated that {001} facet is more reactive than the other facets towards CO_2 reduction and the main observed products was CH_4.

Bai et al.[84] analyzed the facet selectivity of Pd {111} and Pd {100} used as co-catalyst with two-dimensional $g-C_3N_4$ nanosheets in the presence of liquid water for CO_2 reduction under Xe lamp irradiation. By molecular adsorption and activation simulations based on geometry optimization, different CO_2 and H_2O adsorption configurations, at wich corresponded different adsorption energies, where found for Pd {100} and Pd {111} surfaces.

The facet-dependent photocatalytic activity of $BiVO_4$ is also reported in the literature[85-89] and, similary to TiO_2, the diverse facets exhibited different features. In particular, it has been found that the {010} and {110} facets of monoclinic $BiVO_4$ presented reduction and oxidation sites, respectively.[85] Xie et al.[88] studied the photocatalytic coupling of formaldehyde to ethylene glycol and glycoaldehyde in the presence of $BiVO_4$ single crystals with controllable amount of {010} and {110} facets. The samples exhibiting an equal fraction of {010} and {110} facets showed the best yield due to their highest electron-hole separation ability.

1.4. Influence of the valence band (VB) and conduction band (CB) edge positions of the semiconductor

In a photocatalytic process the photogenerated e^-/h^+ pairs can give rise to oxidation and reduction processes if the edge potentials of the valence band, VB, and the conduction band, CB, of the photocatalyst, are higher and lower, respectively, than the potentials of the redox couples present in the solution. Thus, known the redox potential of the species that must be oxidized/reduced, it is possible to choose the photocatalyst with the most suitable bands edges position.[90] The thermodynamic driving force is strictly related to the difference between CB and VB potentials of the semiconductor and to the redox potentials of the target compounds.

Many semiconductors have been used as photocatalysts: TiO_2, ZnO, WO_3, CdS, NiO and C_3N_4 can be found among the best performing ones. Each photocatalyst is characterized by a different band gap energy and band edges position. In Figure 11 are reported the band edges positions of the most employed photocatalysts calculated at pH = 7 in aqueous solution. For reduction reactions, semiconductors with more negative CB edges are more efficient whilst semiconductors with more positive VB edge are more effective for oxidation reactions. The reported values, of course, are not absolute and undergo variations when the pH is different from 7, in solvents different from water, by varying the concentration of the species to be oxidized/reduced, and when species present in the solution are adsorbed on the catalyst. Indeed, a cathodic shift is observable by increasing the pH value in aqueous solvent; the flat band potential of Bi_2S_3 in a S^{2-} ions solution is pH-insensitive and shifts negatively with increasing S^{2-} concentration.[91] Weber aand Kirchner[92] verified the band shift in the presence of ionic liquids by computational measurements on anatase TiO_2. In particular it was found that the cations induced an energetic downward shift of the TiO_2 band levels whilst the anions raised the energy levels. In the case of anatase and rutile controversial results are reported in the literature on the relative position of theirs CB and VB edges. Usually, it has been reported that the anatase CB lies at a slightly more negative potential than that of rutile,[93,94] but some authors found that the CB of rutile lies above that of anatase.[95,96] The apparent contradictory results have been explained considering the differences occurring between pristine surface and water adsorbed in different concentrations on the anatase and rutile surfaces.[96] This emphasizes the importance of the experimental conditions in which the measures are carried out. In addition, for the same catalyst there may be shifts depending on the size of the particles (quantum effect).[97,98]
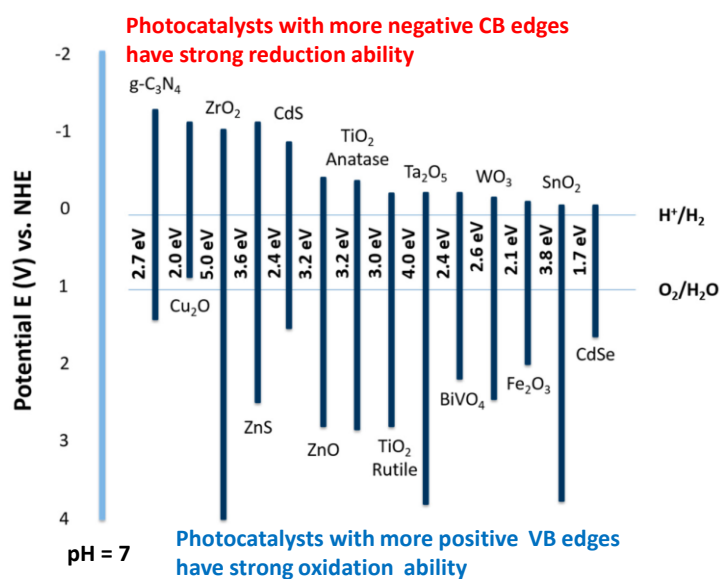

Figure 11: Band positions and potential applications of some typical photocatalysts (at pH = 7 in aqueous solutions).

Carbon nitride, as consequence of the very negative value of CB edge, is a good candidate for reduction reaction, moreover it is possible to negatively shift the band edge potential by means of structural and morphological modifications. Graphic bulk (Bulk-CN) and ultra-thin nanosheets (NS-CN) carbon nitrides were compared for CO_2 reduction.[99] Although the CB of both samples is more negative than the reduction potential of the possible products, higher CH_4 and CH_3OH yields were observed in the presence of NS-CN (Figure 12a), due to its more negative CB, and consequently stronger reduction power than Bulk-CN (Figure 12b).
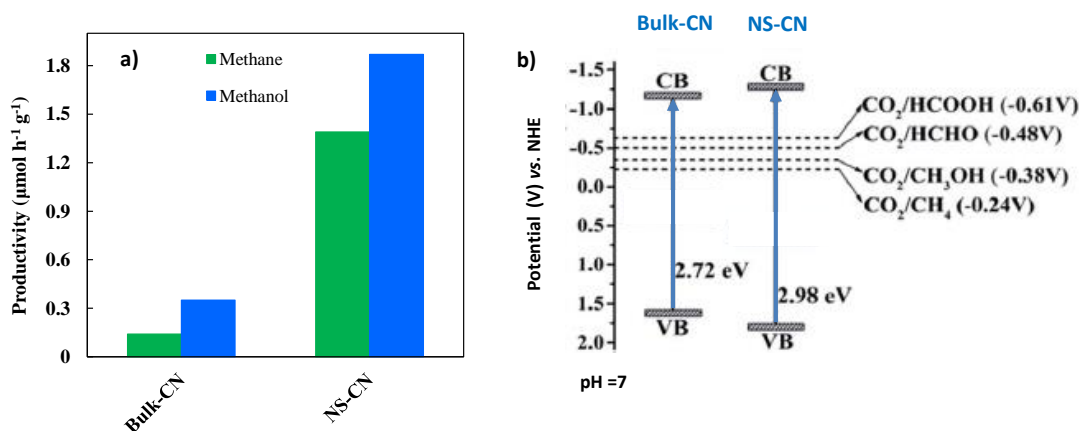

Figure 12: Productivity for CO_2 reduction (b) and bands position of Bulk-CN and NS-CN (a).

Xu et al. prepared anatase TiO_2 samples in the form of nanocubes (TC) and nanofibers (TW), and calculated the position of CB and VB edge by capacitance measurements (Figure 13a).[100] The higher amounts of CH_4 and CH_3OH (Figure 13b) produced by the TC sample was ascribed to its more negative CB potential with respect to TW sample.
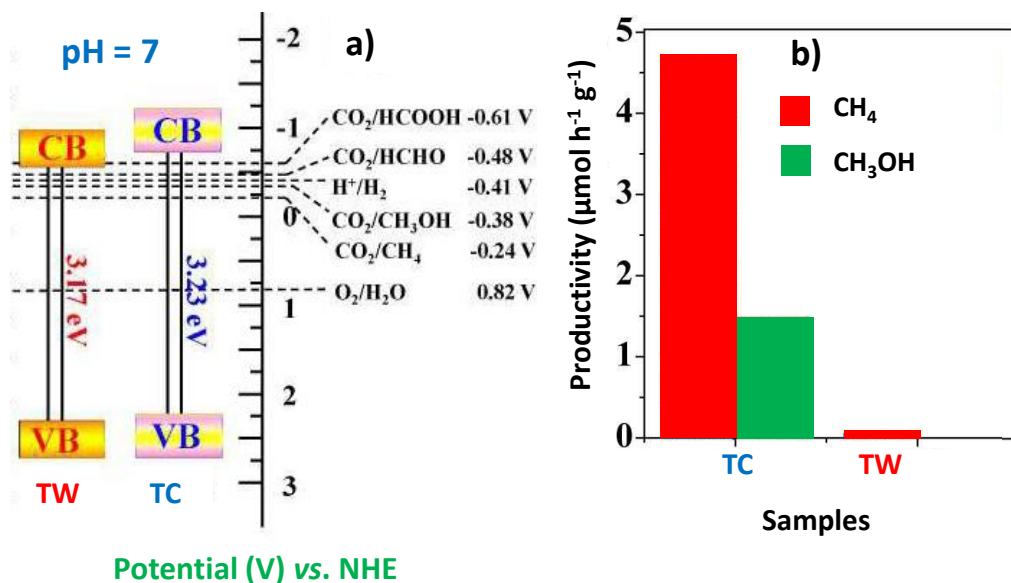

Figure 13: Calculated band positions of the TW and TC samples (a) and products formation rate (b).

Chen et al.[101] observed the absence of activity of commercial massive WO_3 sample towards CO_2 reduction in the presence of water and artificial solar irradiation, whilst a good CH_4 production was found by using laboratory made WO_3 nanosheets (Figure 14a). This difference was explained by considering the more negative CB edge (−0.42 eV) of nanosheets than microcrystalline WO_3 (0.05 eV) (Figure 14b), thus allowing the CO_2 reduction to CH_4, being the reduction potential -0.24 V.
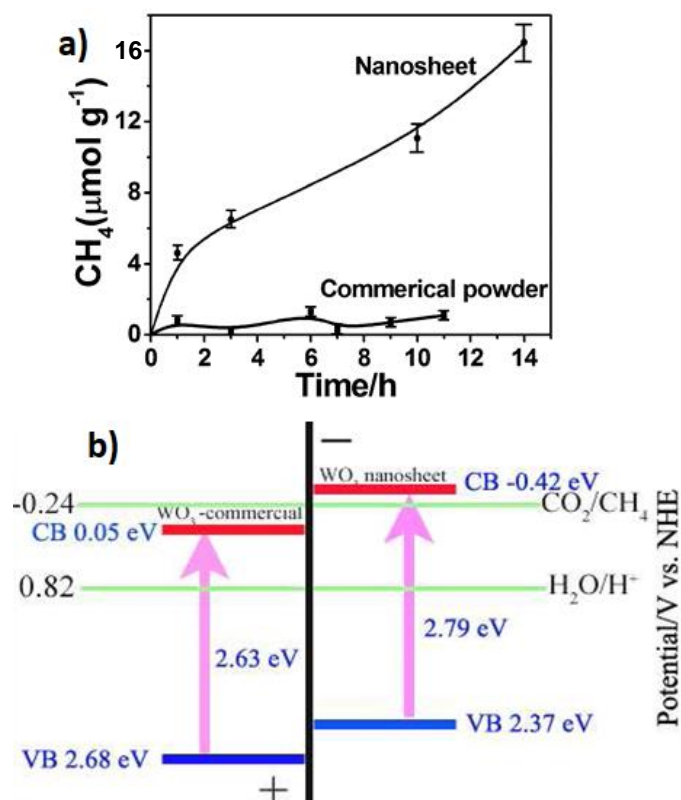
Figure 14: CH$_4$ generation over the nanosheet and commercial powder as a function of visible light irradiation times ($\lambda > 420$ nm) (a) and band positions of the WO$_3$ nanosheet and commercial WO$_3$, relative to the redox potential of CO$_2$/CH$_4$ in the presence of water (b). Reproduced with permission from ref 101. Copyright 2012 American Chemical Society.

The different distribution of the products obtained from CO$_2$ gas phase reduction in the presence of home-prepared anatase and rutile samples was attributed to the different CB edges position of the two polymorphs (Figure 15).[102]
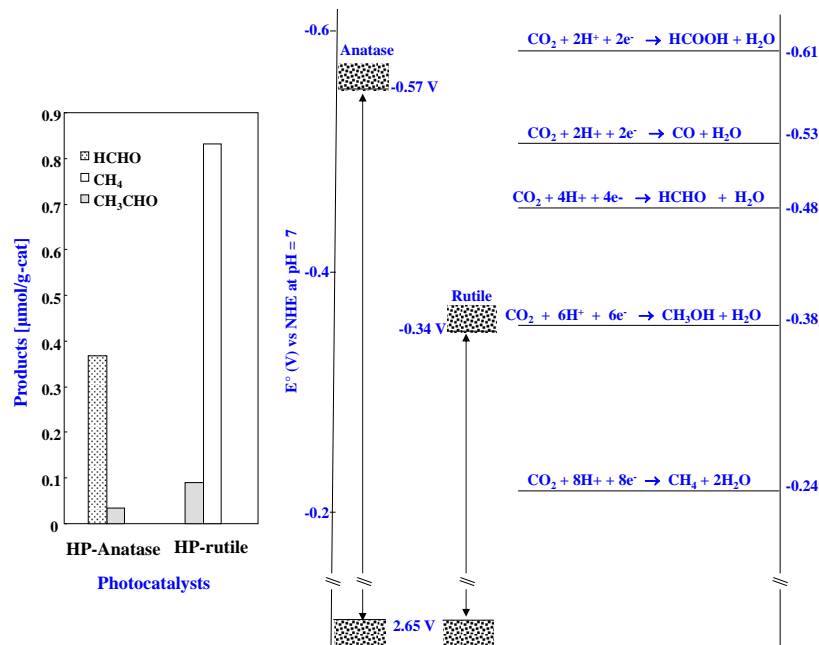

Figure 15: Amounts of the main compounds obtained by photocatalytic reduction of CO$_2$ on home-prepared samples, relationship between the band structures of anatase and rutile, and the thermodynamic potentials for CO$_2$ reduction to various products versus NHE at pH = 7.

To favor CO$_2$ reduction, TiO$_2$ (Evonik P25) was coupled with commercial GaP that exhibits more negative CB value than TiO$_2$.[103] Figure 16 shows the positions of VB and CB of the semiconductors along with the reduction potentials of the CO$_2$/CH$_4$ couple. GaP/TiO$_2$ composite was effective in the gaseous CO$_2$ reduction under simulated solar light irradiation, and CH$_4$ was the main product. The high efficiency was attributed to the formation of a

Z scheme between TiO_2 (both anatase and rutile present on P25) and GaP. In detail, the photogenerated electrons on TiO_2 recombine with the photogenerated holes on GaP while the photogenerated electrons on GaP are available for CO_2 reduction.
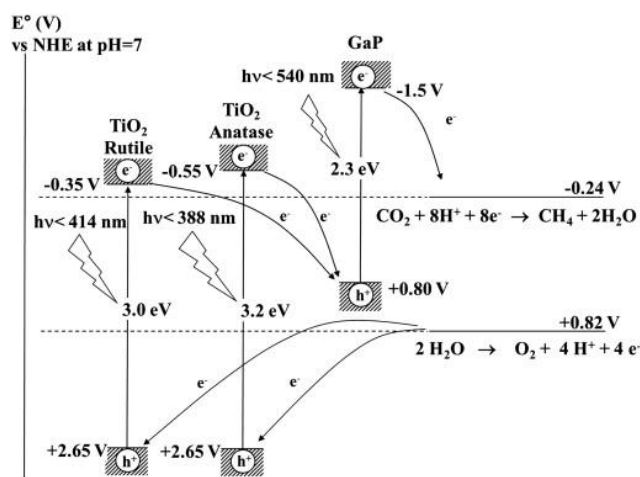

Figure 16: Relationship between the band structures of TiO_2 and GaP, and the reduction potentials (versus NHE at pH=7) for the most favorite processes of oxidation and reduction. Reproduced with permission from ref 103. Copyright 2014 Elesevier.

The band tuning can be realized also by doping the semiconductor. It is reported that the presence of foreign ions can introduce localized levels near the VB and CB, which modify the reaction mechanism. Tripathy et al.[104] observed a change in the distribution of the partial oxidation products of toluene after Ru doping, and in particular no benzoic acid was formed by using Ru-doped TiO_2 nanotubes. This finding was explained by considering the different electronic properties of the samples: Ru introduces a level below the TiO_2 CB with a more positive potential than the $O_2/O_2^{\cdot-}$ couple hindering the $O_2^{\cdot-}$ formation, which was considered the species responsible for benzoic acid formation.

Among the emerging photocatalysts, bismuth oxyhalides (BiOX, X = Cl, Br, and I), showed a good activity in the selective syntheses.[105,106] By using BA as the probe molecules in aqueous solution under LED irradiation, a conversion higher than 99% and a benzaldehyde (BAD) selectivity higher than 99% was obtained and attributed to the suitable energy band of the samples.

Reducing the size of particles to quantum dots results in relevant changes of the edges of their valence and conduction bands causing major changes in their optical features (quantum effect). In Figure 17 it is reported, as an example, the band gap variation of CuO by varying the particles size with the consequent shift of the VB and CB edges.[107]

This figure shows that, if these samples are used for H_2 production, the most efficient will be those with the smallest particles size as a progressive negative shift of the CB edge occurs by reducing the dimensions until the achievement of values more negative than the redox potential of hydrogen.

Colloidal semiconductor quantum dots (QDs) generally present broad and intense absorption spectra in the visible region. This feature, along with their high surface-to-volume ratio, makes them promising candidates for organic synthesis under visible light. CdSe QDs have been recently applied for the coupling of thiols to disulfides and hydrogen,[108] for the oxidation of alcohols to carbonyl compounds,[109] β-alkylation, β-aminoalkylation, amine arylation, decarboxylative radical formation, dehalogenation,[110] reduction of aromatic azides[111] and nitrobenzene[112] to the corresponding amines.
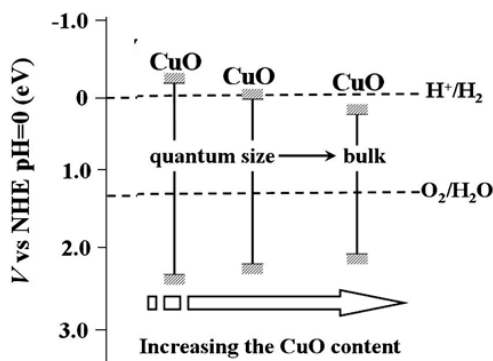

Figure 17: Energy levels of the conduction and valence band edges vs normal hydrogen electrode (NHE, at pH 0) for CuO with various sizes (the quantum size effect is proven by the band gap increase). Reproduced with permission from ref 107. Copyright 2011 Elsevier.

1.5. Influence of the surface acidity/basicity

In order to determine the activity of a photocatalytic reaction, the interaction between the catalyst surface and the reagents/products is essential (both the adsorption and desorption steps are important). For selective syntheses better results are obtained, notably, by favoring the adsorption of the reagents but also the desorption of the products before their further transformation. The degree of interaction depends on the nature of adsorbate and adsorbent and it can be tuned by varying the surface acid-base properties of the photocatalyst modifying both the amount and the type of acid-base sites. Moreover, the type and the strength of surface sites can influence the products distribution as in the case of 2-propanol photocatalytic oxidation in gas-solid regime. In particular, propanone (formed by dehydrogenation) was mainly formed in the presence of basic or acid–base pair sites, whilst propene (formed by dehydration) was the principal product when strong Brønsted sites were present on the catalyst surface. Marcì et al.[113] carried out the photo-assisted oxidation of 2-propanol in gaseous phase by using a fixed bed reactor in the presence of bare and Keggin type ($H_3PW_{12}O_{40}$) polyoxometalates (POM) impregnated TiO_2, commercial (P25) and home prepared (HP) TiO_2 samples. Polyoxometalates were used as they display very strong Brønsted acid sites and are known as effective oxidant catalysts. Data reported in Table 5 show that commercial TiO_2 was the most efficient sample for 2-propanol conversion and mineralization; the presence of POM had a negative effect on both TiO_2 samples; propanone was the main intermediate for bare TiO_2, whilst propene was selectively formed with samples containing POM.

Table 5: Reactivity results for 2-propanol conversion.

Sample	Conversion (%)	Selectivity (%)					B/L[a] ratio
		Propanone	Propene	Acetaldehyde	Isopropylether	CO_2	
POM/P25	63	14	80	2	4	0	2.35
POM/HP	49	7	82	2	8	0	2.24
P25	99	47	0	1	0	52	-
HP	37	90	0	8	0	0	-

[a] Brønsted (B) and Lewis (L) acid sites determined by FT-IR investigation.

An analogous behavior was found for propene hydration in the presence of Keggin heteropolyacid (POM) supported on different oxides (commercial and HP TiO_2, SiO_2, WO_3, ZrO_2, ZnO, Al_2O_3).[114] 2-Propanol formation rate per gram of POM was higher for the samples exhibiting the strongest acid sites.

Also in the selective conversion of glycerol to acrolein in liquid-solid regime, the surface acidity of POM played a crucial role.[115] The runs were carried out by comparing bare TiO_2 with different binary POM/TiO_2 materials obtained by impregnation of three Keggin type POM ($H_3PW_{12}O_{40}$, $H_3PMo_{12}O_{40}$, $H_4SiW_{12}O_{40}$) on TiO_2. Both the glycerol conversion and the acrolein selectivity were higher by using the binary samples, containing a greater amount of acid center than bare TiO_2 (see Figure 18).
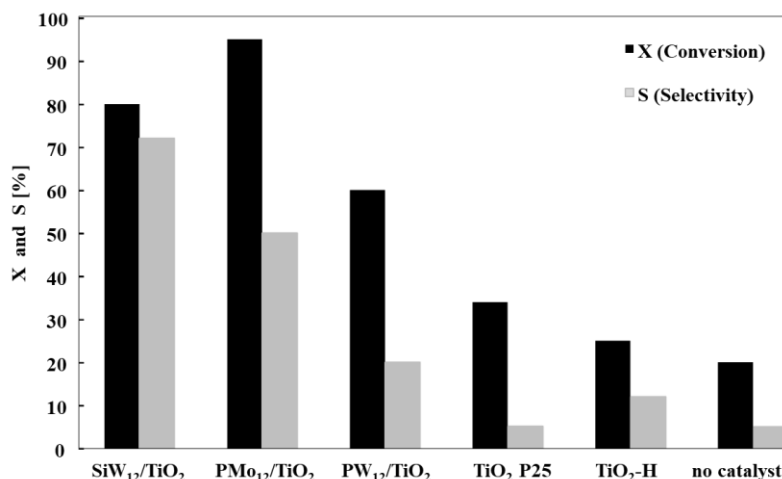

Figure 18: Glycerol conversion (X%) and acrolein selectivity (S%) after 65 min of irradiation in the presence of HPA/TiO_2 photocatalysts, bare TiO_2 samples and in the absence of photocatalyst. Reproduced with permission from ref 115. Copyright 2017 Elsevier.

In the aqueous conversion of glucose under UV light irradiation, a different reaction mechanism was found on bare TiO_2 (both commercial and home prepared) and binary POM/TiO_2 samples, obtained by functionalizing TiO_2 with a commercial Keggin heteropolyacid $H_3PW_{12}O_{40}$ (PW_{12}) or with a home prepared $K_7PW_{11}O_{39}$ salt (PW_{11}).[116] By using both TiO_2 bare samples, the glucose conversion (Table 6) was ca. 40 % and the main obtained products were fructose, arabinose and erythrose with TiO_2-P25 and only fructose and erythrose with TiO_2-HP; fructose selectivity increased when POMs were present and reached 99% with bare PW_{11}, and also gluconic acid was formed in the binary samples. This behavior was attributed to the

different types and distribution of acid sites present in these samples with respect to bare TiO_2 and was in accord to data in the literature reporting that glucose isomerization to fructose occurs in the presence of acid catalysts.

Table 6: Glucose conversion, selectivity to identified products, after 360 minutes of UV irradiation in the presence of different samples.

Sample	Glucose Conversion (%)	Fructose Selectivity (%)	Gluconic acid Selectivity (%)	Arabinose Selectivity (%)	Erythrose Selectivity (%)
TiO_2-P25	41	14	0.6	42	28
TiO_2-HP	40	20	-	-	13
PW_{12}/P25	64	68	22	-	-
PW_{12}/HP	39	56	20	-	-
PW_{11}	20	99	-	-	-
PW_{11}/ HP	20	34	9	-	23

The TiO_2 surface acidity played a determing role in the photocatalytic reduction of NO_3^- in aqueous formic acid solution under UV light.[117] TiO_2 samples displaying different properties were used and it was found that Lewis acid sites favors the non-selective N_2 evolution, whilst the presence of surface defects endorses the reduction of NO_3^- to NH_3 (selectivity ca. 97%). The enhanced selectivity to NH_3 was attributed to the strong adsorption of NO_2^- (a reaction intermediate) that remained anchored on the catalyst surface and evolved to NH_3. On the contrary, the NO_2^- ions easily desorb from the Lewis acid surface sites and form N_2 (Figure 19). By preparing photocatalysts having few Lewis acid sites and a large amount of defects it is possible, therefore, to address selectively the reduction of NO_3^- to NH_3.
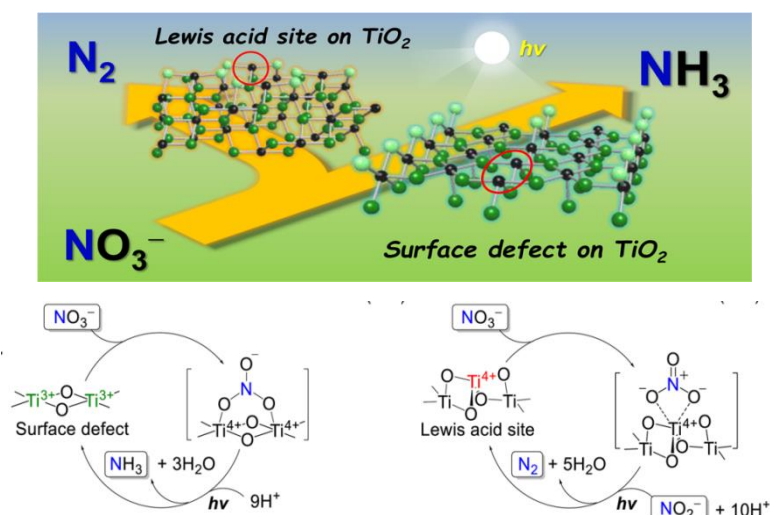

Figure 19: Proposed mechanisms for photocatalytic reduction of NO_3^- on surface defect and Lewis acid site of TiO_2. Reproduced with permission from ref 117. Copyright 2017 American Chemical Society.

Ma et al.[118] used very acid TiO_2 simultaneously functionalized with active carbon (AC) and sulfonic groups (TiO_2/AC/SO_3H) having different TiO_2/AC ratios, to synthesize 2-quinoline carboxamide starting from quinoline and formamide under simulated solar light irradiation in the presence of H_2O_2. The best results (yield of 39%, selectivity 100%) were obtained with an acid density of 1.55 mmol g^{-1} (TiO_2/AC ratio = 1:1). Figure 20 shows the hyphotesized reaction mechanism. The acidic groups of the solid protonate quinoline while $^{\cdot}$OH radicals formed after the interaction of H_2O_2 with e^-, react with formamide giving rise to the formamide radical. The latter reacts with protonated quinoline to form 2-quinoline carboxamide. The use of a sulfonated photocatalyst avoids the addition of acid in solution and represents a green process that can be potentially used in industrial application.
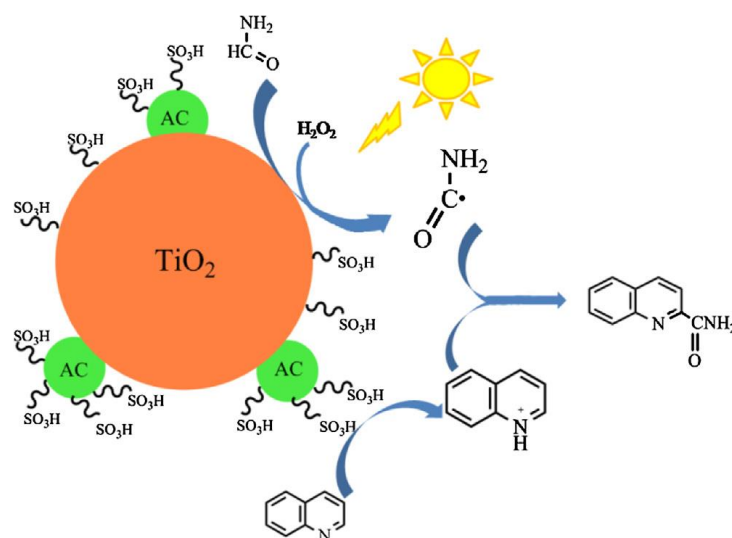
Figure 20: Scheme of the reaction mechanism of the photosynthesis of 2-quinoline carboxamide using TiO$_2$/AC/SO$_3$H catalyst. Reproduced with permission from ref 118. Copyright 2016 Elsevier.

Hakki et al.[119] compared the activity of different commercial and home-made TiO$_2$ samples towards the reduction of m-nitrotoluene (m-NT) in ethanol under Ar atmosphere. The distribution of the products and the selectivity depended on the TiO$_2$ phase and on the surface acidity of the samples, evaluated by FTIR spectroscopy after pyridine adsorption. By observing Figure 21 and Table 7 it can be noticed that m-toluedine (1) was selectively formed on pure rutile with a yield of 72% due to its poor acidity; its imine (2) was obtained with a higher yield (44%) in the presence of pure anatase, which exhibits a higher Lewis acidity than rutile; P25, that shows both Lewis and Brønsted acid sites, promoted, in turn, the cyclization of the imine to dimethyl quinoline (3) with a yield of 31%. In this case imine formed on the Lewis sites, whilst cycles on the Brønsted sites.
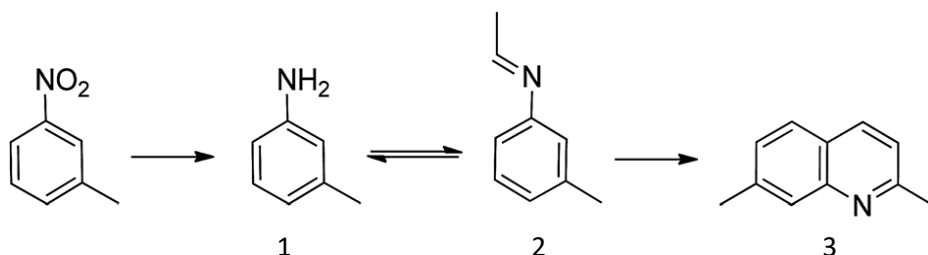

Figure 21: Sequence of the cyclization and N-alkylation reactions of m-NT in EtOH.

Table 7: Results of the photocatalytic conversion of m-nitrotoluene in EtOH with various TiO$_2$ catalysts under UV(A) irradiation. R= Rutile, A= anatase.

Catalyst	Phase	Yields (%)		
		1	2	3
Rutile	R	72	2	7
UV100	A	49	44	4
P25	A-R	21	13	31
Mesoporous A	A	32	44	3
UV100 + R	A-R	48	47	5

Moreover, the presence of Brønsted and Lewis acidic sites is beneficial in the photocatalytic partial oxidation of alcohols as they favor the adsorption of substrate on the catalyst surface with the formation of complexes, thus promoting the activation under visible light irradiation, as in the case of HNb$_3$O$_8$ nanosheets.[120]

Also the influence of surface basic sites has been investigated. Leow et al.[121] found that Al$_2$O$_3$, when used in the presence of dyes, had a positive effect in the benzyl alcohol partial oxidation due to the surface complexation of the alcohol with the Brønsted basic sites of the oxide, which reduces its oxidation potential and causes an upshift of its HOMO for electron abstraction by the dye. The same mechanism was responsible for the photocatalytic hydroxylation of boronic acids to alcohols in the presence of different basic oxides such as MgO, ZnO, Al$_2$O$_3$.[122] Furthermore, it was demonstrated that also the strength of the basic sites was important, by finding a relationship between the yields of alcohol and the quantity of strong basic sites of Al$_2$O$_3$. This finding opens a new road for the successful realization accomplishment of photosynthetic reactions.

1.6 Influence of surface OH density

Water in contact with the TiO_2 surface undergoes a dissociative adsorption giving rise to a certain hydroxylation degree. After irradiation, the photogenerated holes oxidize the hydroxyl groups to $^\cdot OH$ radicals, which are responsible, together with $^\cdot HO_2$ radicals, for the oxidation processes taking place in a photocatalytic system. Surface OH density plays a key role in determining the photocatalytic efficiency. During the photocatalytic oxidations, a high concentration of OH groups favors O_2 adsoption and it has a beneficial effect on the photoactivity.[123,124] On the other hand, scarce information is available on the influence of OH surface density on synthetic reactions. Di Paola et al.[125] examined the role of OH density of some home prepared and commercial TiO_2 samples on the photocatalytic activity by considering the partial oxidation of 4-MBA as a probe reaction. An EPR study demonstrated that higly hydroxylated samples (Figure 22a) were the most selective ones towards p-anysandehyde formation, but the least active in the formation of tempone (Figure 22b). Tempone concentration is related to the formation of $^\cdot OH$ radicals because it derives from reaction between TEMPO and $^\cdot OH$ (Figure 22c). This study demonstrated that not all the total amount of surface OH species can be transformed in the highly reactive OH radicals. An opposite behavior was found for phenol and benzoic acid hydroxylation (Figure 23): a selectivity decrease towards the mono hydroxylated species both of phenol and benzoic acid was observed by increasing the total OH amount.[69] The above findings indicate that the results are strictly related to the substrate-catalyst coupling and can not be generalized.

The surface OH group density of different TiO_2 samples played a key role also in the selective oxidation of cyclohexane to cyclohexanol and cyclohexanone.[126] A series of TiO_2 samples prepared in HCl aqueous concentrations with different concentration were compared in the propene oxidation.[127] The best results were obtained with the samples exhibiting the higher surface OH density.

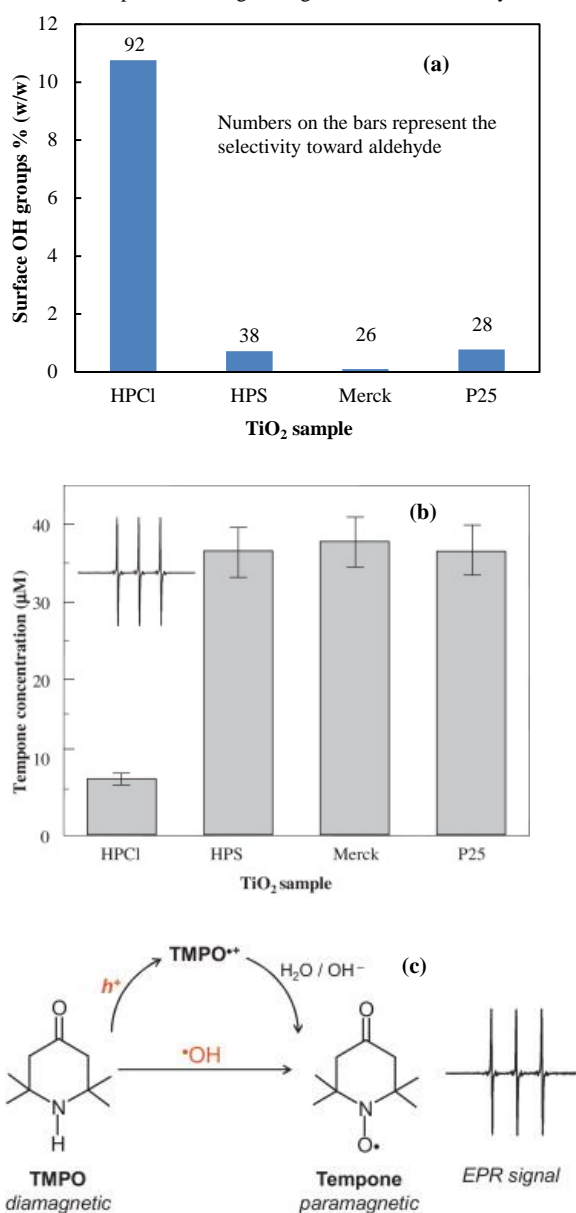**Figure 22:** Surface OH amount (a), Tempone concentration monitored after 365 nm irradiation of deoxygenated acetonitrile suspensions of TiO_2 samples (b) and mechanisms of TMPO oxidation to nitroxide radical Tempone in the irradiated (λ = 365 nm) deoxygenated acetonitrile TiO_2 suspensions, along with EPR spectrum of Tempone (c). Reproduced with permission from ref 125. Copyright 2014 Elsevier.
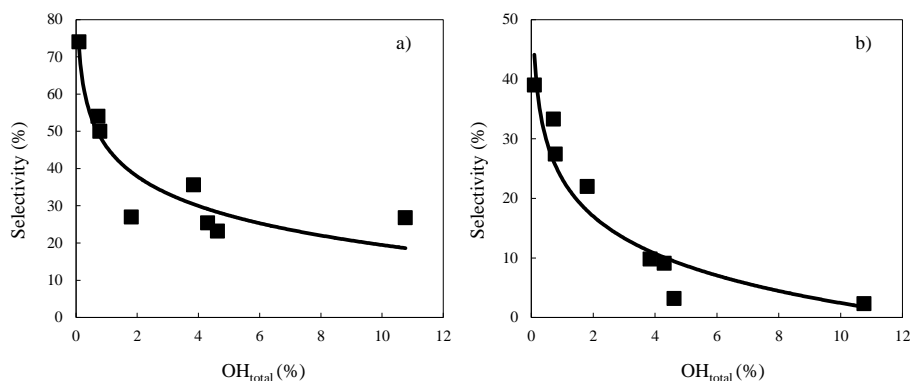
Figure 23: Selectivity to mono-hydroxylated species vs. samples global hydroxylation determined by TGA for the used photocatalysts. (a) Phenol; (b) benzoic acid. Reproduced with permission from ref 69. Copyright 2012 Elsevier.

Surface OH groups of anatase TiO_2 influenced also the distribution products of gaseous toluene oxidation in a fixed-bed continuous reactor.[128] Partial oxidation to benzaldehyde with a selectivity of ca. 20% was observed in the presence of air and water. By FTIR investigation it was demonstrated that toluene was weakly stabilized by hydrogen bond onto hydrate TiO_2 surface and it was successively oxidized to benzaldehyde only if surface OH groups were present. A reduction of toluene conversion rate was observed after the first hours of irradiation in the absence of water due to the poisoning of the photocatalyst, whilst the formation of benzaldehyde was almost wholly inhibited because of the surface OH groups consumption.

1.7 Surface modifications

Photocatalytic reactions always take place on the surface of a photocatalyst, therefore the selective adsorption ability of the photocatalyst towards reactants and products is crucial for the selective photoreactions, a thought that has been mostly ignored for a long period. It is viable to promote the selectivity by surface adjustment, e.g., transforming the surface charge/functional group, constructing specific structures[129] and by adsorption of Brønsted acid.[130] Actually, the weaker interaction between target product and photocatalyst is beneficial for the selective reaction, because the desired products can easily desorb from the photocatalyst surface once reactant-to-product transformation is over, which has been proved not only by density functional theoretical calculations but also by experiments.[131-133] Therefore, achieving control over adsorption is a relevant approach to affect the selectivty of photocatalytic processes.[134] Furthermore, adsorption is also strongly related to surface properties such as zeta potential, which can be controlled by the pH of the solution, or by the presence of specific surface functional groups. Ohtani et al. highlighted the importance of surface adsorption on selectivity in their studies on the synthesis of cyclic secondary amines starting from diamines.[135-137] The optical purity of the product significantly changed by changing the photocatalyst. The presence of CdS gave rise to a racemic mixture, while one isomer was preferentially produced in the presence of TiO_2. The difference of the optical purity of the products was attributed to the different position of the adsorbed amino group onto the surface of the photocatalyst.

Augugliaro et al.[138-139] attributed the higher selectivity towards aldehydes obtained in the presence of home prepared TiO_2 based photocatalysts with respect to commercial ones, to the competition between water and aldehyde for the adsorption. The selectivity was higher for highly hydrophilic TiO_2 samples, in which water was able to displace the aldehyde molecules from the surface, thus facilitating their desorption and avoiding further oxidation. Notably, the competition between water and organics on the surface of TiO_2 has been recently quantitatively estimated by means of fast field cycling NMR analysis.[140]

Similarly, the selectivity towards cyclohexanone in the partial oxidation of cyclohexane was strongly influenced by product desorption.[141] Cyclohexanone, in fact, desorbs significantly more slowly from an irradiated surface than under dark. In fact, the surface hydroxylation degree was higher under irradiation, so that cyclohexanone could bind more strongly to the catalyst surface, resulting in slow desorption.

Maira et al.,[142] by carrying out the toluene oxidation in gas phase in a continuous photoreactor, showed that the rate of toluene photo-oxidation to benzaldehyde was the same on differently hydroxylated TiO_2 samples, while toluene photo-oxidation to CO_2 was faster on the more hydroxylated ones, showing that the latter process occurred on different adsorption sites, maybe characterized by multiple anchoring of the aromatic ring interacting with more acidic OH groups.

Photocatalysts with well-defined textural characteristics have been described to address the selectivity of the photocatalytic processes.[143] The use of one-dimensional nanostructure-based material continues to receive more attention as a method to achieve improved selectivity of organic photocatalytic synthesis.[144]

1.7.1 Molecular Recognition Sites (MRS)

Molecular imprinting is defined as ''the construction of ligand selective recognition sites in synthetic polymers where a template (atom, ion, molecule, complex or a molecular, ionic or macromolecular assembly, including micro-organisms) is employed in order to facilitate recognition site formation during the covalent assembly of the bulk phase by a polymerization or polycondensation process, with subsequent removal of some or all of the template being necessary for recognition to occur in the spaces vacated by the templating species''.[145]

Recently, creation of molecular recognition sites (MRS) on the surface of suitable oxides has attracted increasing attention for plenty of applications.[145] The resulting materials present highly selective sites capable to selectively interact with specific substrate with a "lock and key"-type mechanism. Photocatalytic applications of these materials have been mostly proposed for the preferential degradation of specific toxic pollutants present in complex organic mixtures.[146] For instance Ghosh-Mukerji et al.[147] chose thiolated β-cyclodextrin (TCD) as the MRS, whose well-defined cavity facilitated the hosting of 2-methyl-1,4-naphthoquinone with respect to other molecules such as benzene. The target pollutant was degraded 11 times faster with respect to benzene in the presence of the TCD, while the two molecules degraded similarly in its absence. However, due to the organic nature of MRS, some precautions have to be observed to prevent the degradation of the MRS which might be slowly deteriorated during a long period of UV-light illumination. For this reason synthetic applications of MRS are rare. However, to increase the stability of the nanocomposite under UV irradiation, inorganic molecularly imprinted polymers (IMIPs) coated TiO_2 photocatalysts have been investigated for the degradation of phthalate esters.[148] This idea has been used for shape-selective synthetic reactions. Canlas and co-workers[149] showed that indiscriminately reactive catalyst surfaces can be made reactant shape-selective through the use of partial overcoating with an inert oxide. For example, TiO_2 coated with a porous very thin Al_2O_3 layer is a selective photocatalyst for both reduction and oxidation reactions (template nanocavities). Using this photocatalyst, nitrobenzene and benzyl alcohol were photocatalytically reduced and oxidised, respectively, while the ortho methylated derivatives did not react. Molecularly imprinted photocatalysts (MIP) are very promising for synthetic applications but they are rarely used. In fact, design of a new MIP system suitable for a specific template molecule often requires a lot of time and work for synthesis, washing and testing. Generally, many attempts need to be made, changing various experimental parameters, before finding the optimum conditions. Combinatorial Chemistry has been recently used in order to accelerate the optimization of MIPs to attain the desired performance.[150] Other important critical points are the design of water-compatible MIPs and their stability under irradiation.

1.7.2 Modification with organics

Selectivity and conversion of photocatalytic synthetic reactions can be improved by functionalizing the semiconductor with suitable organics. The shuttle molecule grafted on the surface of the photocatalyst may influence the process in various ways according to its properties and to the specific interaction with light and with the photocatalyst surface.

One of the most used technique to extend the light absorption capability of some metal oxides from UV to the visible range, is the surface sensitization with suitable dyes. The resulting photocatalytic mechanism is generally indicated as "indirect" because the excited dye injects electrons into the conduction band of the semiconductor upon visible light absorption, giving rise to an efficient spatial charge separation. The resulting process not only is driven by visible light but generally it shows improved selectivity and conversion towards target molecules in synthetic applications.

Chen et al.[151] report the simultaneous reduction of nitroaromatics and oxidation of alcohols to the corresponding amines and aldehydes, respectively, by using a dye sensitized TiO_2 photocatalyst in organic solvents. Both reactions occur with high selectivity (ca. 90% in the optimized conditions). Notably, the photoexcited electron transfer from the excited dye molecule to the CB of TiO_2 generates the corresponding dye radical which can selectively oxidize the alcohol to aldehyde. The radical is simultaneously reduced back to the starting dye which is therefore reformed.

Oxidation of amines to imines has been carried out in acetonitrile and in the presence of dye sensitized TiO_2 by using (2,2,6,6-tetramethylpiperidin-1-yl)oxyl (TEMPO) as a suitable redox mediator to relay the electron transfer (see Figure 24).[152]
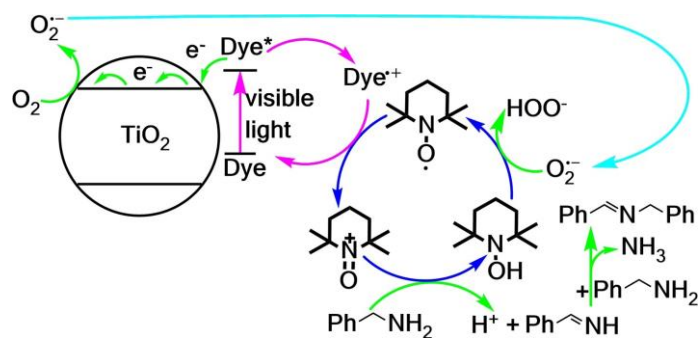
Figure 24: Mechanism for the photocatalytic oxidation of amine to imine with O_2 by dye-sensitized TiO_2 and TEMPO under visible light irradiation. Reproduced with permission from ref 152. Copyright 2018 Elsevier.

Upon visible light excitation, the dye molecules on the surface of TiO_2 inject electrons into its conduction band, thereby generating dye radical cations. The latter oxidize TEMPO to $TEMPO^+$ which in turn oxidizes amines to imines, forming TEMPOH in the meantime. Finally, superoxide anion species,

formed through oxygen reduction at the TiO_2 interface, oxidize back TEMPOH to TEMPO. The complex synergy between TiO_2, dye and redox mediator, although if mimicking some mechanisms reported for hydrogen and oxygen generation by means of electron relay molecules,[153] represents an interesting proof of concept to be used for novel selective photocatalytic syntheses.

Analogously to the above mentioned report, the dye molecule is catalytically regenerated after oxidizing a substrate also in the visible light-induced selective oxidation of alcohols to aldehydes or ketones devoid of any redox mediator.[154] The reaction afforded selectivity values close of ca. 99% in different organic solvents, but the highest conversion (ca. 70%) was obtained in acetonitrile. Quenching of the excited state of the dye results in electrons injection into the conduction band of TiO_2 and in the generation of the corresponding radical cations. The latter are restored to their ground state by oxidizing benzyl alcohol to the corresponding radicals, which in turn are transformed into the corresponding aldehyde molecules through interaction with superoxide radical anions.

Oxidation of aliphatic alcohols to the corresponding aldehydes has been carried out in gas phase under solar light irradiation by modifying commercial TiO_2 (P25) with a perylene derivative. In this case, yields to formaldehyde, acetaldehyde and acetone were 67, 70 and 96%, respectively.[155]

In the above mentioned examples the organic modifier plays the role of the light absorbing species. However, in other cases the shutter molecule initiates redox reaction by mediating between the excited semiconductor and the target substrate. For instance, Zhang et al.[156] reported the selective oxidation of methyl phenyl sulfide and other substituted aromatics sulphides to sulfoxides by means of mesoporous graphitic C_3N_4 (mpg-C_3N_4) modified with aldehyde molecules such as isobutyraldehyde (IBA) (Figure 25). Bare C_3N_4 afforded only 8% conversion, although selectivity was remarkable (99%), while IBA modified C_3N_4 showed a significantly increased conversion by maintaining a high selectivity. In particular, 100 mol % IBA concentration, afforded 51% conversion with methyl phenyl sulfoxide as the sole product. When 200 mol % of IBA was used, the conversion and selectivity were 97% and 98%, respectively. With higher IBA concentrations the main product changed from methyl phenyl sulfoxide to methyl phenyl sulfone with a selectivity of 92%. The aldehyde grafted on the surface was oxidized by the photogenerated superoxide anions to peroxide radicals or peracids which in turn oxidized sulphides to sulfoxides.
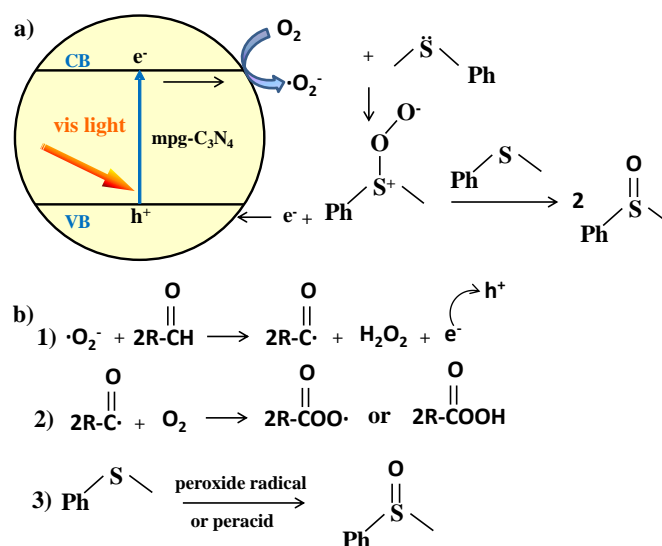

Figure 25: A possible reaction mechanism for the catalytic cycle of the mpg-C_3N_4 and mpg-C_3N_4–aldehyde system.

A similar mechanism has been invoked for the selective allylic oxidation of cholesteryl acetate to 7-ketocholesteryl acetate (7-KOCA), a key step in the production of vitamin D3.[157]

The organic compound grafted on the surface of the semiconductor can be highly beneficial for the conversion and selectivity of the process by improving the spatial charge separation.

Graphene modified semiconductors have been synthesized to this aim due to the remarkable conducting properties of this 2D carbon material. Ma et al.[158] reported the selective (100% selectivity) hydrogenation of nitroaromatics by using CoS_2/graphene composites under visible light irradiation and mild conditions. Graphene rapidly trapped the photoexcited electrons and efficiently suppressed charge recombination.

Abd-Elaal et al.[159] modified home prepared TiO_2 with a conjugated diol molecule and silver nanoparticles. The coupled use of the organic molecule and the silver nanoparticles enabled fast electron transfer from the conduction band of the semiconductor to the outer shell of the composite, thus facilitating oxidation of aromatic alcohols to aldehyde which occurred with a high selectivity (ca. 90%) in aqueous suspension.

The selectivity of the photocatalytic reduction of nitrobenzene to aniline has been significantly improved in the presence of TiO_2 modified with electron-donating aminoacids such as asparagine (Asp), serine (Ser), phenylalanine (Phe), and tyrosine (Tyr).[160-162] The aminoacids acted as hole traps on the surface of TiO_2, thus hindering charges recombination. However, other factors synergistically act along with their electron donating effect, positively contributing to the performance of the reaction. In fact, at alkaline pH values the positively charged amine group of the aminoacid efficiently reacted

with the negatively charged nitrophenol molecules thus improving its reduction. As a consequence, modified Ag-TiO$_2$ samples selectively reduced NBz, even in the presence of chemically similar molecules such as phenol. Furthermore, modification with aminoacids strongly improved the nitrobenzene adsorption capability due to hydrogen bonding, n-π and π-π interactions.

Surface modification with organo silane (silylation) influences the physico-chemical features of the surface in order to enhance its affinity to target molecules. The selectivity towards cyclohexanone in the photooxidation of cyclohexane on anatase TiO$_2$ was greatly improved by sililation.[163] In fact, the higher hydrophobicity of the surface facilitated cyclohexanone desorption, thus preventing its further oxidation and enhancing selectivity up to 97%. Surface silylation is reported as a powerful tool to address the photocatalytic mechanism by limiting the charge transfer efficiency in favor of energy transfer-based mechanisms. For instance, silylation of TiO$_2$ allowed to highlight that the photocatalytic isomerisation of caffeic acid occurs by means of energy transfer from the excited TiO$_2$.[164] Janczyk et al.[165] reported that surface silylation promoted energy transfer from the excited semiconductor to oxygen, forming singlet oxygen. Recently, this mechanism has been invoked in the limonene oxidation to limonene epoxide occurring with high selectivity (ca. 90%) in the presence of silylated TiO$_2$.[166] Nevertheless, it is worth reminding that the use of organics to modify the surface properties of a photocatalyst should imply a careful check of their stability under irradiation.

1.7.3 Ion Modification

Surface modification by metal and non-metal ions is reported to enhance the selectivity of photocatalytic processes by modulating the adsorption of target molecules. Higashimoto et al.[167] studied the influence of metal ions loading (Fe, Ag, Ce, Pt, or Cu) for the TiO$_2$ induced oxidation of aromatic alcohols to the corresponding aldehydes. Modification by Fe (III) afforded the highest photocatalytic performances giving rise to ca. 99% selectivity towards benzaldehyde. The enhanced performances are mainly attributed to the hybridization of the O2p orbitals of the adsorbed alcohols molecules with the Fe 3d orbitals, which improved electron transfer to the conduction band of TiO$_2$.

The presence of the superoxide radical (O$_2^{\bullet-}$) could depress the selectivity of photocatalytic syntheses, being it an active oxidizing species. Therefore, inhibiting its formation generally improves the performances of the selective processes. Marotta et al.[168] added Cu^{2+} cations efficiently competing with oxygen as electron scavengers. In this way superoxide radical formation was inhibited. The cycle was closed by oxygen mediated oxidation of the formed Cu(0) in the dark. The authors reported an approximately 50% selectivity for the photocatalytic oxidation of benzyl alcohol to benzaldehyde. A further paper of the same authors reports a scale up of this process in a solar pilot plant using a compound parabolic collector reactor (CPC),[169] with ca. 50% yield towards benzaldehyde (ca. 60% selectivity). Authors found that the amount of Cu^{2+}, the incident solar radiation and the temperature were key parameters for the reported process, which is a rare example of a photocatalytic synthesis at a pilot scale.

Ti^{3+}-containing TiO$_2$ has shown higher selectivity for the production of ketones than P25 and rutile, due to the high defectivity and to the enhanced affinity for water.[170]

The effects of the presence of fluoride ions on the TiO$_2$ surface has been often investigated for photocatalytic degradation reactions. Indeed, fluorination is reported to enhance the production of highly oxidizing OH radicals which unselectively degrade almost every organic compound with few exceptions.[171] For this reason selective synthetic applications are rare. Maurino et al.[172] investigated the influence of TiO$_2$ surface fluorination in the partial oxidation of glycerol. Fluorination determined a decrease in the glycerol conversion rate with respect to bare TiO$_2$ at low substrate concentration, but a fivefold increase at high concentrations. Furthermore, the production of value-added compounds such as 1,3-dihydroxyacetone and glyceraldehyde increased.

Enhancing the hydroxyl ions concentration on the surface of TiO$_2$ has been proved to be an efficient way for increasing the conversion of glucose and xylose to formate. The presence of hydroxyl ions not only accelerated the formation of active oxygen species, but also influenced adsorption of glucose and desorption of formic acid.[173]

1.7.4 Mixed Photocatalysts

Mixed semiconductor oxides have been reported to improve performances with respect to the single components. The synergistic effect has been often justified by taking into account the improved spatial charge separation due to the relative energetic positions of the valence and conduction bands of the semiconductor components. The direct contact between the two semiconductors is essential and coupling or capping them are the mainly used techniques.[174] Regardless of which component is the light absorbing species, both of them act as direct or indirect photocatalysts. Therefore, the opto-electronic features of the components should be carefully considered in order to design efficient systems.

Liu et al.[175] presented a mini-review on the use of core-shell nanostructures for selective organic transformations.

Solvent free oxidation of toluene to benzaldehyde has been selectively carried out under visible light by using a hybrid composite comprised of CdS and a coordination polymer Cd$_3$(C$_3$N$_3$S$_3$)$_2$. The resulting heterojunction facilitates separation and transfer of the photogenerated electrons, thus increasing the stability of CdS against corrosion, while the porous structure and the large surface area enabled surface enrichment of adsorbed toluene.[176]

Among the coupled systems different organic assemblies have been tested. A hybrid system, containing TiO$_2$ anatase and HKUST-1, a porous metal-organic framework (MOF), was used for the CO$_2$ photocatalytic reduction under solar light irradiation.[177] The close contact between the two components, favouring an effective electron transfer, proved to be essential as its efficiency was much higher than those of the single constituents. By using a similar coupled photocatalyst, He et al.[178] found an improved CO$_2$ photoreduction to CO, in comparison with pristine TiO$_2$. In this case no electron transfer

proces between the two components was observed and the enhanced photoactivity was attributed only to the improved CO_2 adsorption on the catalyst due to the MOF presence. Coupling an inorganic photocatalyst with MOF can be very advantageous as it combines features of the former with the peculiar properties of the latter (porous structure, presence of organic linkers and metal atoms).

CdS nanoparticles supported on 2-D graphene scaffold were used for selectively oxidizing a series of alcohols to the corresponding aldehydes under visible light irradiation and ambient conditions.[179] The good performance of the system was attributed to the coupling of the photocatalytic properties of CdS with the features of graphene (high electron conductivity, enhanced light absorption, porous structure).

Also ternary systems have been investigated for synthetic applications. Han et al.[180] designed a very stable hierarchical nanostructure in which the three components (CdS, ZnO, and graphene) electronically interacted thus providing excellent charge separation and resistance to photocorrosion. The composite has been used for selective photo-hydrogenation of nitro aromatics. The presence of CdS warranted visible light absorption while graphene and ZnO afforded efficient spatial charge separation.

Notably, even if charge separation is a key factor determining photocatalytic performances, the selectivity of the process was mainly determined by surface factors as pointed out by Hamrouni et al.[181] The photodegradation of 4-nitrophenol occurred with an efficiency related to that of the charge transfer separation, while the selectivity towards PAA in the 4-MBA photocatalytic oxidation was mainly influenced by the surface properties.

The effects of the surface features have been highlighted by Tsukamoto et al.[182] and Di Paola et al.[183] for selective oxidation of aromatic alcohols and ferulic acid, respectively, in the presence of WO_3/TiO_2 photocatalysts. In both reports the higher selectivity towards aldehydes obtained with respect to the bare components was explained by considering the change in adsorption properties of the WO_3/TiO_2 photocatalysts compared to the bare TiO_2 rather than the electronic effects. In fact, the produced aldehyde did not undergo further oxidation on the WO_3 phase, thus increasing the selectivity of the process.

A selectivity enhancement in alcohol photooxidation has been obtained by using TiO_2 covered with Nb_2O_5.[184] Unlike the case of WO_3 modified TiO_2, the authors attributed the enhancement in the selectivity to the inhibition in the generation of ozonide radical O_3^- as shown by ESR analyses. In this way overoxidation of the desired intermediate was avoided.

Photocatalytic and catalytic partial oxidation of 2-propanol to acetone were compared over mixed TiO_2–CeO_2-based catalysts. The mixed samples showed higher catalytic conversion compared to the single oxides. Decoration with gold nanoparticles further increased the conversion. The catalytic oxidation was mainly directed by the presence of CeO_2 acting as a reducible oxide support enabling a strong interaction with gold nanoparticles and providing very active lattice oxygen atoms. The use of mixed oxides favored mineralization of the alcohol to CO_2, while the interaction of gold with bare TiO_2 was responsible for the highest selectivity towards acetone.[185]

By coupling a photocatalyst with non-photoactive compounds has been also demonstrated a viable tool to enhance the selectivity towards valuable compounds.

Magdziarz et al.[186] reported the partial oxidation of benzyl alcohol to benzaldehyde in the presence of an iron doped TiO_2/zeolite photocatalyst synthesized by a sonophotodeposition method. This material allowed to obtain higher yield in benzaldehyde with respect to the corresponding photocatalyst prepared by means of wet-impregnation methods.

Photoactive Bi_2WO_6 was entrapped into silica and allowed the selective oxidation of trans-ferulic acid and trans-cinnamic acid into a mixture of acid and aldehyde derivatives (vanillic acid, vanillin, and benzoic acid). The sol–gel encapsulation of the photocatalyst enhanced significantly the selectivity towards the aldehyde or the acid, depending on the nature of the substrate.[187]

The role of the silica component in non-photocatalytic reaction steps was hypothesized for reduction of nitroaromatics by alcohols in the presence of TiO_2 loaded onto silica grafted with arylsulfonic acid groups.[188] Silica acted as a thermally active catalyst while the TiO_2 component as the photocatalyst (Figure 26). m-Nitrotoluene (17) was reduced to the corresponding aniline (18) while the alcohol (19) was oxidized to the corresponding aldehyde (20). Condensation of amine and aldehyde afforded an intermediate imine (21), while condensation of aldehyde (20) and alcohol (19) produced the enolether (22). The following steps were thermally catalyzed on the acidic surface of silica. In particular, the imine (21) reacted with the enolether (22) affording the intermediate (23). The latter, on the acidic sites of the modified silica, evolved to the intermediate (24) which in turn disproportionated eventually affording products (25) and (26).
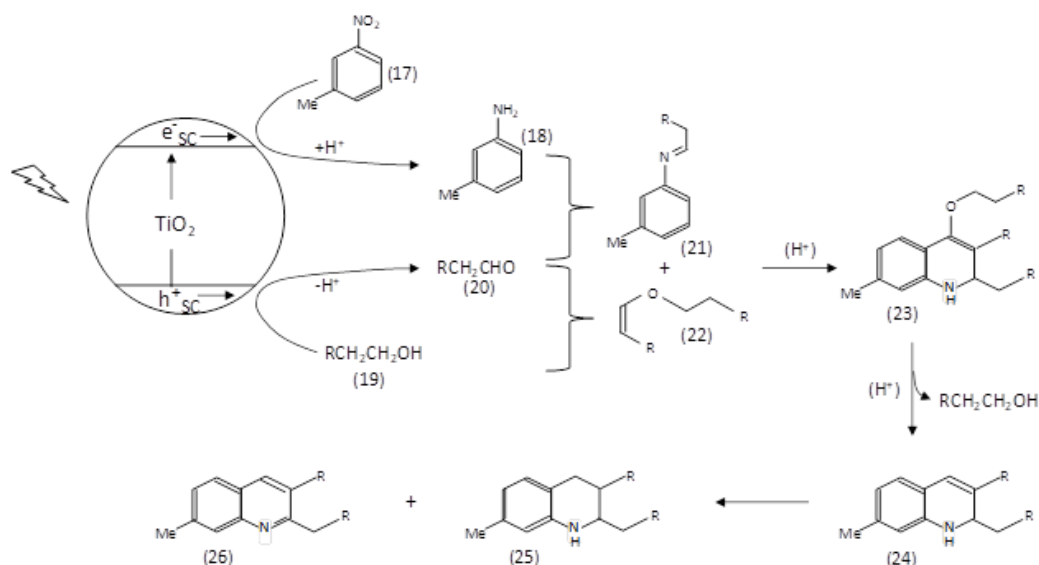
Figure 26: Mechanism of the reduction reaction of nitroaromatics by alcohols. Reproduced with permission from ref 188. Copyright 2013 American Chemical Society.

1.7.5 Metal loading

Decorating the surface of a semiconductor with metal nanoparticles is a viable tool to reduce charge recombination, to tailor the optical properties of the composite, and to address preferential adsorption of target compounds and the selectivity of the reaction.

When the semiconductor is the light absorbing species, metal nanoparticles behave as co-catalysts and act as sinks for the photogenerated electrons so that they provide selective active sites for the reaction to occur. For instance, Kominami et al.[189] performed deoxygenation of epoxides in alcoholic suspensions in the presence of TiO_2 loaded with silver, gold, or copper nanoparticles. Gold or copper addressed the reaction towards hydrogen production, while Ag nanoparticles promoted selective reduction of (2,3-epoxypropyl)benzene epoxide to allylbenzene (99% yield).

In other cases the nanoparticles themselves act as catalysts by absorbing radiation and generating charges by means of localized surface plasmon resonance (LSPR), i.e. the collective oscillations of electrons of the metal nanoparticle upon electromagnetic radiation absorption.[190]

For instance, noble metals such as silver and gold give rise to LSPR resonance in the visible region of spectrum. As summarized by Kochuveedu et al.,[191] the mechanisms of LSPR induced photocatalytic reactions are (i) transfer of electrons generated at the metal nanoparticle to the semiconductor and (ii) excitation of LSPR that causes chemical transformations of adsorbates on the surface of the metal nanoparticles itself. The first mechanism has been invoked for addition reactions such as hydroamination of alkynes to imines,[192] whilst reduction reactions are often catalysed by the second one. For instance, gold nanoparticles on different supports allow to reduce nitro-aromatics to azo compounds, hydrogenate azobenzene to hydroazobenzene, reduce ketones to alcohols, and deoxygenate epoxides to alkenes.[193,194] In particular, plasmon electrons abstract hydrogen atoms from the solvent giving rise to Au-H species which then transfer hydrogen to the substrate. In some cases, a combination of direct and indirect photocatalysis takes place, whereby both the semiconductor and the metal nanoparticles activate the reactants. Oxidations such as visible light epoxidation of ethylene in the presence of Ag nanoparticles on α-Al_2O_3 support have been reported to occur by means of this mechanism as well. [195]

Metal deposition could also favor adsorption of organic substrates onto the photocatalyst surface. Tada et al.[196,197] reported a remarkable increase in both activity and selectivity of the photocatalytic reduction of nitrobenzene to aniline due to an increase in the amount of adsorbed nitrobenzene on Ag and Pt-Ag modified TiO_2 with respect to non-modified TiO_2.

Decoration with Au nanoparticles is reported to decrease the hydroxylation degree of the TiO_2 surface.[198,199] For instance the mineralization of phenol to CO_2 is suppressed in favor of the partial oxidation to hydroquinone in the presence of TiO_2 P25 modified with gold nanoparticles.[199] This behavior has been attributed to the reduced affinity of the hydroquinone towards the gold nanoparticles and to the reduced hydroxylation degree of the Au modified photocatalysts. The same reasons have been invoked by Ide et al.[200] to justify the enhancement of selectivity of the photocatalytic oxidation of cyclohexane towards the formation of cyclohexanone and cyclohexanol employing Au-modified Fe/Ni/TiO_2 as the photocatalyst. Pt and Pd deposited on $CdS_{1-x}Se_x$ ($0 < x < 1$) nanorods induced the photocatalytic alcohol dehydrogenation and hydrogenolysis under sunlight irradiation.[201] In particular, benzyl alcohol was converted under sunlight illumination to benzaldehyde, being toluene and H_2 the byproducts. The presence of Pt favored dehydrogenation (H_2) over hydrogenolysis (toluene) 8:1, whereas the presence of Pd favored hydrogenolysis over dehydrogenation 3:1.

The photocatalytic properties of silver nanoparticles (Ag NPs) coupled with tungsten oxide (WO_3) nanocrystals were investigated to understand structural effects of the WO_3 nanocrystals in selective oxidation of cyclohexane (C_yH). The photocatalytic activity of monolayer hydrated WO_3 nanosheet-Ag nanoparticle composites (WO_3 NSs-Ag NPs) was 1.3 times higher than that of WO_3 nanocube-Ag nanoparticle composites (WO_3 NCs-Ag NPs). The highest cyclohexane conversion of 40.2% with cyclohexanol and cylohexanone (KA oil) selectivity of 97.0% were achieved by WO_3

NSs-Ag NPs photocatalyst under solar-light irradiation at room temperature. WO$_3$ NSs-Ag NPs showed good photocatalytic stability. The improved photocatalytic activity for the oxidation of cyclohexane was mainly due to the facilitated generation of highly reactive hydroxyl radicals caused by surface plasmon resonance (SPR) effect of Ag NPs, and to the effective charge transfer to WO$_3$. The design and structural analysis of the WO$_3$ NSs-Ag NPs in this research can provide a novel approach for the further development of high-performance photocatalysts.[202]

2. Selectivity enhancement by tuning various reaction conditions not related to the photocatalyst

2.1 Effect of the solvent

Water is the "green" solvent *par excellence* and one of the strengths of heterogeneous photocatalysis compared to other synthetic processes. The advantages of using water are related to environmental and economic reasons, by taking into account that the organic compounds can not be generally used in food industries due to their toxicity, and the purification of the obtained products is less expensive in the presence of water.

Several papers report on the photocatalytic synthesis of valuable organic compounds by using water as the solvent[20,53,66,182,127,128,41,203-209] obtaining, in some cases, good selectivity values. In one of their first papers on selective photocatalysis, Yurdakal et al.[41] reported the partial photocatalytic oxidation of benzyl alcohol (BA) and p-methoxybenzyl alcohol (MBA) to their corresponding aldehydes (benzaldehyde (BAD) and 4-methoxybenzaldehyde (PAA)) in aqueous solution by using home made TiO$_2$ samples. The best selectivity was 38 % for BAD and 60% for PAA. The higher MBA conversion and PAA selectivity was explained by considering the presence of the electron-donating methoxy group which stabilizes the aromatic ring favoring the aldehyde formation, whilst the lower selectivity to BAD was ascribed to the simultaneous formation of hydroxylated aldehydes (Figure 27). Subsequently, a PAA selectivity enhancement up to 90 % was obtained under simulated solar irradiation by using N-doped TiO$_2$ samples.[66]
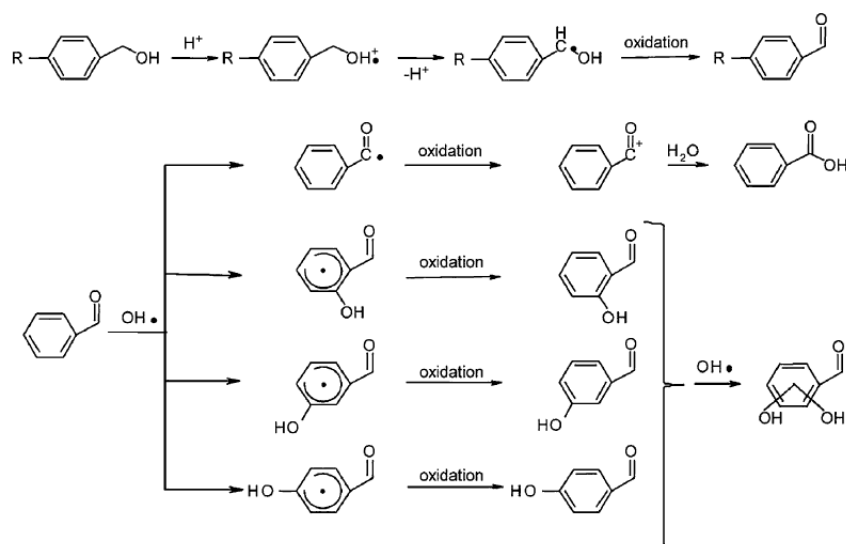

Figure 27: Proposed reaction schemes. R=H, OCH$_3$. Reproduced with permission from ref 203. Copyright 2011 John Wiley and Sons.

Spasiano et al.[169] verified the selective production of BAD (selectivity of ca. 63%) from BA in a solar pilot plant, by using TiO$_2$ in aqueous cupric ion solutions. A further enhancement was achieved using a hybrid RuCat/Pt-g-C$_3$N$_4$ system in the presence of solar light irradiation with over 99% of selectivity to BAD and contemporary H$_2$ evolution.[205] The improved aldehyde selectivity was attributed to the presence of Ru catalyst and the combination of homogeneous and heterogeneous catalysis.

Selective oxidation of piperonyl alcohol (PA) to piperonal was carried out in water by using both commercial and home-prepared TiO$_2$ samples with a selectivity of ca. 35% (piperonyl alcohol initial concentration 0.5 mM).[24] Starting from higher concentrated solutions also traces of 1,3-bis(3,4-(methylenedioxy)benzyl) ether, deriving from the condensation of two alcohol molecules, were found. In this case, the separation of the products by a chromatographic procedure allowed to separate the reaction mixture obtaining unreacted PA (49% with respect to the starting amount), piperonal (10% isolated yield based on the starting amount of alcohol; 20% yield, based on the converted amount of alcohol) and negligible amounts of 1,3-bis(3,4-(methylenedioxy)benzyl) ether (0.6%isolated yield based on the starting amount of alcohol).

Recently, the selective oxidation of three aromatic alcohols BA, 4-MBA and PA in aqueous suspension was carried out by using pristine and P-doped g-C$_3$N$_4$ samples both under UV and visible light irradiation.[204] The selectivity to the corresponding aldehydes reached 100 % (with some samples) for BA and 4-MBA, whilst the maximum value reached for PA was 46%. g-C$_3$N$_4$ was used also for conversion of HMF to 2,5-furandicarboxaldehyde (FDC) in aqueous medium under UV and natural irradiation, with ca. 30 % and 50% selectivity, respectively, at 50% conversion.[210] The high activity of these samples was attributed to the absence of ˙OH radicals on the C$_3$N$_4$ surface. The selectivity under natural irradiation was enhanced up to 88% (at 20% of HMF conversion) by using a polymeric carbon nitride-hydrogen peroxide adduct as the photocatalyst.[206]

However, it is generally difficult to perform selective photocatalytic oxidation in pure water because very reactive ·OH radicals are formed in the presence of water. These species are highly unselective and cause over-oxidation of the products present in the solution. The replacement of water with organic solvents enhances the selectivity, as in this case organic peroxides are formed instead of OH radicals. The conversion and selectivity values depend on solvent, substrate and photocatalyst type. The most used solvents are acetonitrile,[44,154,167,211,212] trifluorotoluene,[213-217] benzotrifluoride,[130,218,219] while less common solvents are dimethyl carbonate (DMC),[25] methanol,[220] 2-propanol,[50,221] carbon tetrachloride.[222] In some cases no additional solvents are used.[223-225]

Imamura et al.[211] studied the oxidation of BA to BAD with the simultaneous production of H_2 in acetonitrile solution by using metal loaded TiO_2 P25. BAD and H_2 evolved with a molar ratio of 1:1 and the best performance, with a total conversion of BA to BAD, was obtained in the presence of Pt-TiO_2 samples. The results suggested that BA dehydrogenation occurred in the absence of water practically quantitatively without over-oxidation. A selectivity to BAD over 99% in acetonitrile solution was also found by using rutile TiO_2 nanorods under visible light irradiation.[44] The activation of the photocatalyst was explained by considering the formation of a surface complex ($PhCH_2O$) between the -OH group of BA and TiO_2–OH group capable to absorb visible-light, thus generating electrons and holes (Figure 28).
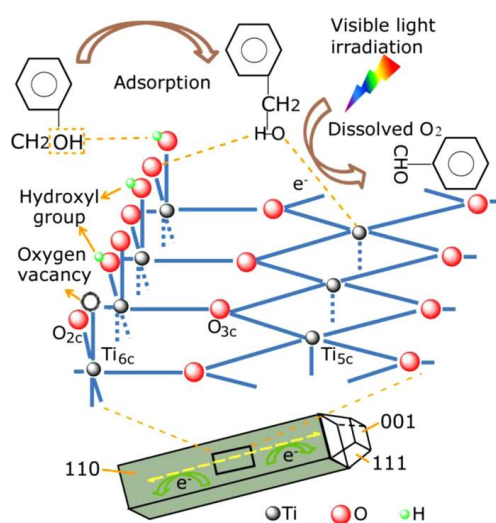

Figure 28: Hypothesized scheme for the partial oxidation of BA to BDA in acetonitrile solution. Reproduced with permission from ref 44. Copyright 2012 Elsevier.

Almquist and Biswas[226] compared the TiO_2 (commercial Degussa P25) photocatalytic oxidation of cyclohexane to cyclohexanol and cyclohexanone in different solvents. The results showed that the formation rate and the distribution of the two products are related to the solvent nature because of the different extent of adsorption of all of the species present in the reaction mixture onto the catalyst surface (also the solvent can be adsorbed). Generally, the higher the degree of absorption of a species, the greater the interaction with the photocatalyst and, therefore, its oxidation degree. In this case cyclohexanol is better adsorbed by the catalyst in the presence of non-polar solvents, whilst the amount of adsorption is lower in polar solvent. The best performance, in fact, was observed by using dichloromethane (Figure 29), because of the less significant adsorption. It suggests, furthermore, that also chlorine atoms influence the photocatalytic activity. Additionally, different products deriving from the organic solvents oxidation have been identified. This finding suggests that the use of organic solvents can make the reaction mixture more complex by increasing the separation cost for products of interest.
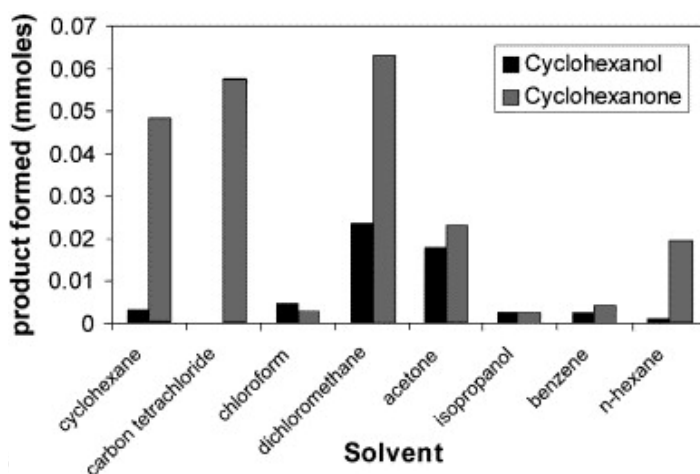
Figure 29: Amount of cyclohexanol and cyclohexanone formed in the various solvents after 1 h of irradiation with 450W xenon lamp. Reproduced with permission from ref 226. Copyright 2001 Elsevier.

Coupling of TiO_2 (P25) with a MOF (Metal Organic Framework) (NH_2-MIL-125(Ti)) in the presence of CCl_4 as the solvent, allowed to carry out the selective oxidation of cyclohexane to cyclohexanol and cyclohexanone under visible light irradiation, working the MOF as a sensitizer for TiO_2.[222] $Ru(bpy)_3^{2+}$-based MOF showed good photocatalytic performances towards aerobic coupling of various amines in CH_3CN and photo-oxidation of thioanisole to methyl phenyl sulfoxide in methanol solution.[227]

During the reduction of nitrobenzene to aniline in 2-propanol TiO_2 suspension, acetone (the oxidation product of the solvent) was observed in almost stoichiometric amount along with aniline.[221]

The mixture DMC/3%H_2O proved to be a good solvent for the degradation/partial oxidation of phenanthrene.[25] Water was necessary as phenanthrene conversion was negligible in pure DMC. By using ethanol, 1-propanol or 2-propanol as the solvents many oxidation by-products were found due to the attack of phenanthrene by ˙OH radicals and by insertion of ethyl, ethanoate, propyl or propylate groups. Even if phenanthrene reaction rate was faster in the alcohols than in DMC, in the latter case only two products were obtained, allowing a higher selectivity and a simpler reaction system. The yields at 60% conversion (after 250 h of UV irradiation) for 9-fluorenone and 6H-benzo[c]chromen-6-one were 19% and 23% w/w, respectively. When organic solvents are employed, another parameter which should be taken into account is the dispersibility of the catalyst, which is very low in aprotic solvents such as DMC. In fact, in the case of phenanthrene, to overcome this drawback the catalyst was immobilized on Pyrex spheres packed in a fixed bed.

By using V_2O_5@TiO_2 as the photocatalyst under simulated solar light irradiation, the selectivity to cyclohexanol and cyclohexanone was 15.5% and 84.5%, respectively in a mixture of acetonitrile/water (volume ratio 10/1) with a substrate conversion of 12.4 % and no formation of others by-products.[228] In pure acetonitrile the total selectivity to the two products was ca. 100%, but the cyclohexane conversion was only 0.5%. The presence of water was necessary to increase the conversion, but when its amount exceeded certain levels selectivity decreased due to formation of other by-products. Moreover, as the solubility of cyclohexanol and cyclohexanone in water is very low, acetonitrile favored the desorption of these products from the catalyst surface. Mixed solvents demonstrated to be very efficient also in the valorization of biomasses. Colmenares et al.[229] achieved a total selectivity of 71 % in conversion of glucose to organic high value-added compounds (glucaric acid, gluconic acid and arabitol) in 50% H_2O/50% ACN mixture at 11% of conversion. The effect of the solvent type was investigated in the selective visible light photo-oxidation of 5-hydroxymethylfurfural (HMF) to 2,5-diformylfuran (DFF) on g-C_3N_4.[230] The best results in terms of HMF conversion were found by using benzotrifluoride (PhCF$_3$) as the solvent, whilst the highest selectivity (and yield) to DFF (Figure 30) was obtained in acetonitrile (ACN)/benzotrifluoride mixture. The great conversion was attributed to the low polarity of PhCF$_3$ and to its superior capability to dissolve O_2. The addition of polar solvents lowered the conversion and, consequently, increased the selectivity. The above reported results indicate that the different solvents can improve the selectivity values by acting in various ways, depending on the nature of the substrate and of the formed products.
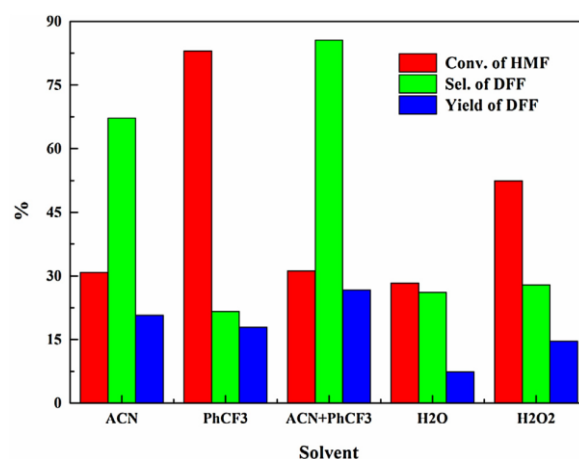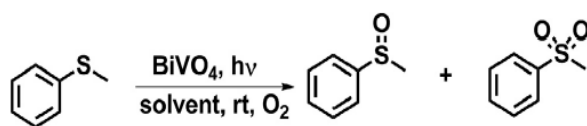

Figure 30: Effect of the solvent on the photocatalytic selective oxidation of HMF by using g-C_3N_4 under solar light irradiation. Reproduced with permission from ref 230. Copyright 2017 Elsevier.

$CdLa_2S_4$, a ternary chalcogenide active under visible light, was used for the contemporary selective reduction of nitroarenes and oxidation of aromatic alcohols in benzotrifluoride under deaerated conditions with a good efficiency.[219]

The photocatalytic selective oxidation of sulfides (thioanisole) to sulfoxides under visible light irradiation in different solvents and in the presence of $BiVO_4$ or Pt/$BiVO_4$ photocatalysts (Figure 31), showed that the best results were obtained by using a mixture of CH_3CN/H_2O (2:1 v/v) as the solvent. The presence of H_2O was beneficial as the conversion raised up to 70% with selectivity of 98% and 2% to sulfoxide and sulfone, respectively, without formation of over-oxidation products.[231] A further increase of H_2O amount had a negative effect due to the low solubility of thioanisole. By isotopic labelling, moreover, it was demonstrated that oxygen present in the oxidation products derived from H_2O.

Figure 31: Photocatalytic results for selective oxidation of thioanisole. Reproduced with permission from ref 231. Copyright 2015 Elsevier.

Solvent	Photocatalyst	Conv. (%)[a]	Sel. (% sulfoxide:sulfone)[a]
CH_3CN	$BiVO_4$	3	>99:1
CH_3CH_2OH	$BiVO_4$	<1	–
$C_6H_5CF_3$	$BiVO_4$	<1	–
CH_3CN	$Pt/BiVO_4$[b]	4	>99:1
CH_3CN/H_2O[c]	$BiVO_4$	7	99:1
CH_3CN/H_2O[c]	$Pt/BiVO_4$[d]	<1	–
CH_3CN/H_2O[c]	$Pt/BiVO_4$[b]	70	98:2

Notes: Reaction conditions: catalyst 50 mg, thioanisole 50 μmol, total volume 1.5 mL, O_2 0.1 MPa, reaction temperature 20 °C, λ > 420 nm, reaction time 5 h.

[a] Based on GC.
[b] 0.1 wt.% Pt loading.
[c] H_2O (0.5 mL).
[d] Under Ar.

Chen et al.[151] carried out the photo-reduction of nitro-compounds in organic solvents (CCl_4 and $CHCl_3$) and in the presence of alcohols (both aliphatic and aromatic) as scavengers, by using TiO_2 (Figure 32a) and dye-sensitized/TiO_2 (Figure 32b) systems under UV and visible light irradiation, respectively. Whilst an almost complete reduction of the nitro compound to aniline followed by alcohol mineralization was observed with TiO_2 and UV light, in the presence of the TiO_2/dye sample and visible light, alcohols were selectively partially oxidized, with a good efficiency, to the corresponding aldehydes, regardeless of the solvent type. In the latter case, alcohols selective oxidation and nitro-aromatics reduction occurred simultaneously, although the reduction efficiency was not high.
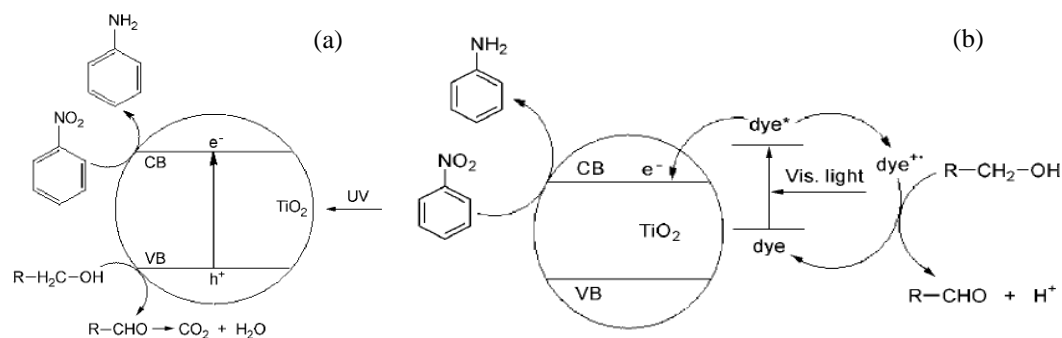
Figure 32: Schematic diagram of photocatalytic reduction of nitrobenzene in (a) UV/TiO_2/holes scavenger system and (b) Vis/TiO_2/dye-sensitized system. Reproduced with permission from ref 151. Copyright 2011 John Wiley and Sons.

2.2 Photoreactors

The reactor geometry, configuration and modes of operation could influence the efficiency of the reacting system. Figure 33 schematizes some of these parameters.

Figure 33: Scheme of reaction system operative parameters.

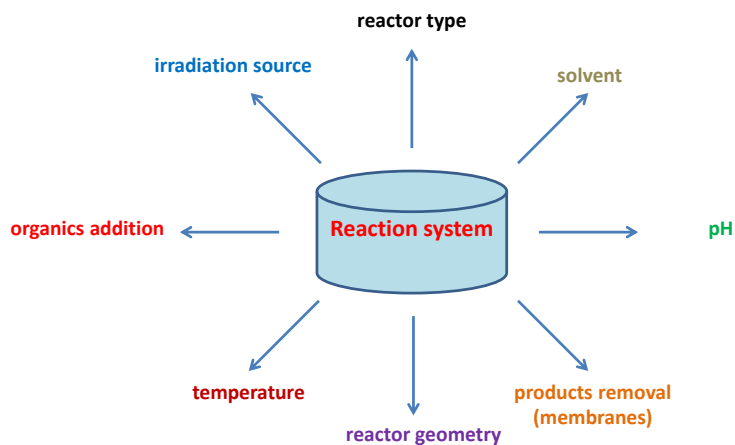In order to enhance the selectivity towards the target compound, the residence time must be carefully optimized. In a batch system this can be achieved only by stopping the reaction when the target compound concentration reaches its maximum, with relevant disadvantages in terms of plant flexibility and operational costs. On the other hand, the residence time distribution in a continuous reactor can be simply controlled by optimizing the fluid dynamics of the system. However, the relevance of this issue is even more evident in synthetic applications, especially in cases where the back reaction of the products is faster than their formation, as for instance in the semiconductor induced photocatalytic CO_2 activation. In this case the back reaction can be avoided by using a photoelectrochemical device in which the involved species are generated in separate compartments.

This reaction, also known as artificial photosynthesis, has recently attracted great interest due to the environmental implications of reducing emissions of the waste CO_2 and using it as "green" building block for the synthesis of high value-added products such as fuels.

Formation of methane and methanol is thermodynamically favoured, but the need of multiple electron transfer generally favors the production of carbon monoxide, formaldehyde and formic acid.[232,233] The low conversion values (less than 1%) obtained up to now for CO_2 reduction is the main drawback for its practical applications. The influence of various parameters (reaction phase, temperature, pressure, reagents ratio, properties of the photocatalysts, etc.) affecting the reactivity has been considered so far in other reviews. However, only some aspects related to the reactor configuration were presented. In general, to increase the CO_2 conversion the reactor configuration should optimise the irradiation and enable the fast removal of the reduction products from the reacting mixture before they could be further transformed.

Even if batch systems have been often applied for CO_2 photo-reduction, fluidised bed reactors and fixed bed reactors are generally the most efficient configurations. In fluidised bed reactors the photocatalyst is dispersed in a fluid-like state so that substrate adsorption and reaction rate are maximized. However, the fixed bed configuration allows to better control the residence time which is a key parameter. The problem of product separation is negligible in this case by considering the rather volatile nature of the obtained compounds. Olivo et al.[234] compared methane formation in a fixed bed reactor and in a thin film reactor, demonstrating that in the latter case a methane production resulted three order of magnitude higher. In general, in fixed bed reactors only a small fraction of the photocatalyst is activated by light, decreasing the effectiveness of the whole process.[235] The use of honeycomb monoliths and optical fibers could solve the problem.[236] For instance Wu[237] optimized the absorbed photons in a fixed bed reactor where the photocatalyst was deposited on optical fibers (the fixed bed) and the fluidodynamic parameters chosen to generate a plug-flow. The yield in methanol obtained in this reactor was 14 times higher with respect to a conventional batch reactor.[238] Accordingly, Lee et al.[239] reported in similar conditions quantum efficiency (0.049%) ca. 25 times higher than in a conventional batch reactor (0.002%), owing to the fact that the photocatalyst supported on an optical fiber, probably was mainly irradiated by the total reflection evanescent wave having very low intensity, thus allowing higher quantum efficiency due to a lower recombination rate. Generally speaking, it is possible to ascertain whether recombination negatively affects the process efficiency by plotting the reaction rate versus the light intensity; recombination dominates if the reaction rate is proportional to the square root of the intensity, while if the relationship is linear this does not happen.

An appealing alternative is the impregnation of the photocatalyst on a moist quartz wool, as reported by Bazzo and Urawaka,[240] although the missing control of the ratio CO_2/H_2O led to hardly comparable results. These results agree with a recent report on the comparison between batch and continuous systems for the photodegradation of organic pollutants.[241] Authors highlight the higher flexibility of a continuous system in which the photocatalytic activity increased up to 110% compared to that of a batch system. Notably, it would be highly desirable to find similar investigations focused on synthetic reactions, by comparing not only conversion but also selectivity values in the two configurations, and by critically evaluating results in terms of possible applications. To the best of our knowledge this approach has been only rarely considered.

A good compromise between batch and continuous flow reactors is a closed system in which recirculation is used to introduce the advantages of a flow-through process. For instance, the photocatalytic synthesis of vanillin has been performed in a similar reactor where the photocatalytic suspension exiting the reactor was continuously recycled back by a peristaltic pump to the reactor after passing through a perfectly mixed tank.[242] This configuration has been often used for photodegradation purposes, although, in view of real applications, it does not easily allow to treat the high volumes typically required in water remediation processes. For instance, some authors have used such configuration for the photodegradation of model pollutants in the presence of a fixed bed TiO_2 based catalyst.[243,244] Notably, whilst in these cases the photocatalytic reaction rate increased with increasing flow rate, Meshram et al.[245] found that phenol photodegradation decreased at increasing flow rate by using a dispersed photocatalyst. These results highlight that the highly specific nature of the interaction of light and matter and of the substrate with the photocatalyst, along with the differences in the experimental set up, may afford results whose generality is rather questionable. This is particularly true for synthetic applications which, in addition, present a long-felt need of similar studies.

Continuous-flow systems may assume two extreme configurations, named continuous stirred tank reactor (CSTR) and plug flow reactor (PFR). In the CSTR system the flow is perfectly mixed so that the concentration is basically constant throughout the reactor. On the other hand, the concentration decreases along the flow direction in the PFR configuration. Although PFR has been chosen as the configuration used in the ISO norms for standardization of photocatalytic reactions, CSTR presents relevant advantages. A PFR is more efficient than a CSTR having the same volume,[246] but all the catalyst surface in a CSTR is exposed to the same (output) concentration.[247] On the other hand, while the rate values obtained in PFR may be seen as mean values, the CSTR configuration affords an evaluation of the photocatalytic rate closer to the intrinsic one. For these reasons, the European Standard Organization (CEN) is currently working on standard test methods performed in CSTR configurations. However, while classical PFR and

CSTR configurations have been used in photocatalytic degradation processes, micro-fluidic systems have been generally reported for synthetic applications. In the latter case, the configuration can be theoretically considered as a PFR due to the reduced size of the system, although the above mentioned disadvantages can be significantly reduced as will be discussed in the next section.

2.3 Photocatalytic microreactors

The selectivity of some organic reactions has been recently improved by performing them in microreactors which can be defined as devices where the reacting medium flows through channels with at least one dimension smaller than 1 mm.[248] Figure 34 reports some microreactor configurations. Photocatalytic applications in micro reactors present various advantages with respect to conventional configurations.[249] Indeed, confining photocatalytic reactions in micro sized spaces allows to reduce mass and heat transfer limitation due to the reduction of molecular diffusion distances, to large surface-to-volume ratios and to reduced residence time. In this way reaction parameters can be better controlled, with a fast response to operational changes.
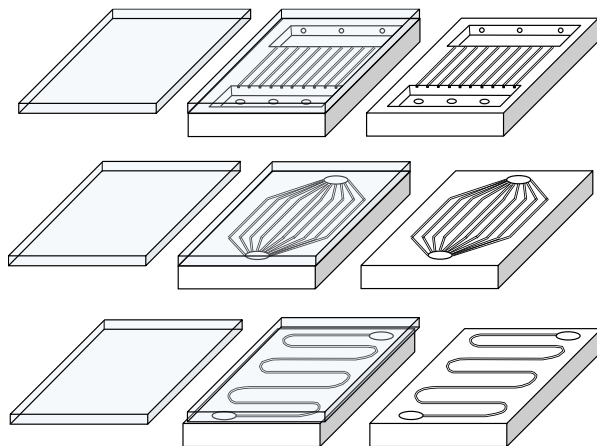

Figure 34: Different microreactor configurations.

Furthermore, light induced processes may benefit of high spatial illumination homogeneity and good light penetration, resulting in optimized reaction conditions and better controlled kinetics of the process.[250-253] As a matter of fact, reaction rates observed in microreactors are generally at least one order of magnitude higher than those correspondingly reported in conventional reactors. However, the most appealing feature of microreactors consists in the possibility of scale-up the process by simply numbering up the microreactors in parallel. This avoids risks and high capital costs related to scaling from laboratory to production plant, allowing faster transfer of results from research to production.

The design and operation of microreactor with immobilized thin-film photocatalyst can be justified because it does not require photocatalyst separation steps, while maintaining large illumination surface area per volume. Generally, the photocatalyst has been supported on the internal part of the microchannels. In some cases TiO₂ nanotubes or nanoparticles have been deposited on a titanium foil in situ by anodic oxidation followed by a hydrothermal treatment.[250]

Recently, optical elements such as for instance waveguides and lasers, have been integrated into microfluidic devices, giving rise to efficiency enhancements of ca. two orders of magnitude.[254] Most of the investigations deal with photocatalytic degradations as model reactions used to approach fluid-dynamic issues.[255] Figure 35 shows some optofluidic microreactor schemes.
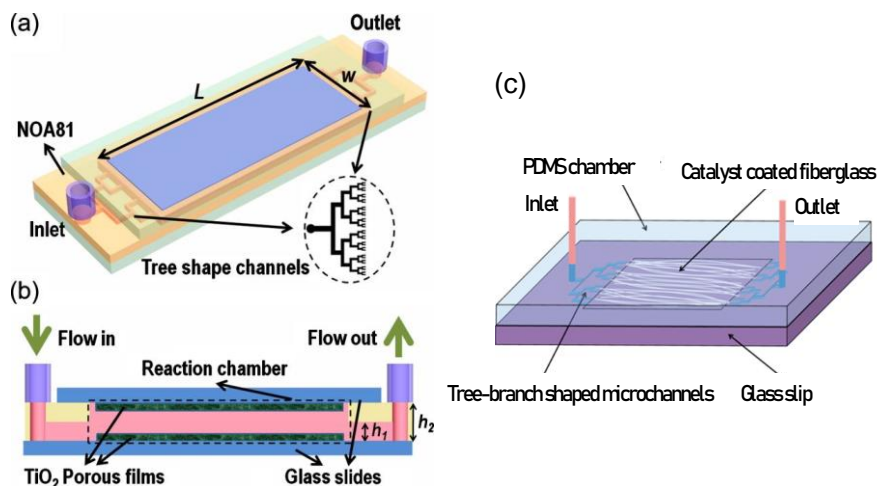
Figure 35: Schemes of optofluidic microreactors: (a) schematic and (b) cross sectional view of photocatalytic microfluidic reactor. Reproduced with permission from ref 254. Copyright 2010 American Institute of Physics; c) schematic of the optofluidic microreactor with the catalyst coated fiberglass. Reproduced with permission from ref 255. Copyright 2013 American Chemical Society.

As far as synthetic applications are concerned, photochemical reactions in homogeneous phase have been often reported in microfluidic systems, whereas heterogeneous photocatalysis for synthetic purposes has been more rarely reported.[256]

Matsushita et al.[257] reported the reduction of benzaldehyde and nitrotoluene in ethanol, under nitrogen atmosphere, in the presence of TiO_2 in a quartz microreactor irradiated with UV-LEDs. Benzyl alcohol and p-amino toluene were obtained with a yield of 11 and 46%, respectively, after 60 s.

Takei et al.[258] reported the cyclization of L-lysine to L-pipecolinic acid (Figure 36) in a self-fabricated micro reactor. Platinum (0.2 wt%) modified TiO_2 was deposited into the channels (770 μm wide and 3.5 μm depth) and a high-pressure Hg lamp was used as the irradiation source. The L-lysine conversion in the microstructured reactor was 87% after a residence time of ca. 52 s, which was 70 times greater than that obtained in a batch reactor. In this case the selectivity of the reaction did not depend on the reaction time.

Even if reactions are not optimised, these pioneering works demonstrate the potentialities of microstructured reactors with respect to conventional ones.
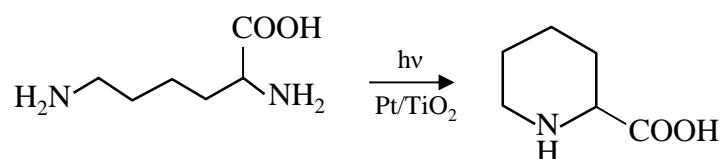

Figure 36: Photocatalytic synthesis of L-pipecolinic acid.

N-ethylation of benzylamine was carried out in a quartz microreactor (width 500 μm, 40 mm length) whose channels were coated with TiO_2 (with and without Pt), irradiated with UV-LEDs (365 nm), by using ethanol as the solvent.[259]

The alkylated product was detected in yields of up to 43% in only 90 s. Other amines such as aniline and piperidine were also alkylated.[260] Increasing the depth of the channels resulted in reduced reaction efficiency due to reduced surface to volume ratio. While reaction proceeded with bare TiO_2 in the microstructured reactor, the presence of Pt was required in the batch system. Notably, the continuous mode allowed to prevent the undesired bis-alkylation reaction.

The additive cyclization of N-methylmaleimide and N,N-dimethylaniline has been carried out in a spiral of PFA capillary (ID 760 μm, 650 μL) irradiated with UV-LEDs at 365 nm, in the presence of TiO_2 nanocrystals capped with oleic acid.[261] The product (tetrahydroquinoline) was obtained in 91% yield after 5 h of reaction time (see Figure 37).

Microflow conditions:
PFA-tubing (760 μm ID, 650 μL)
UV-A source (λ_{max}: 365 nm)
Solvent: DCM (0,08 M)

91%
5 hours
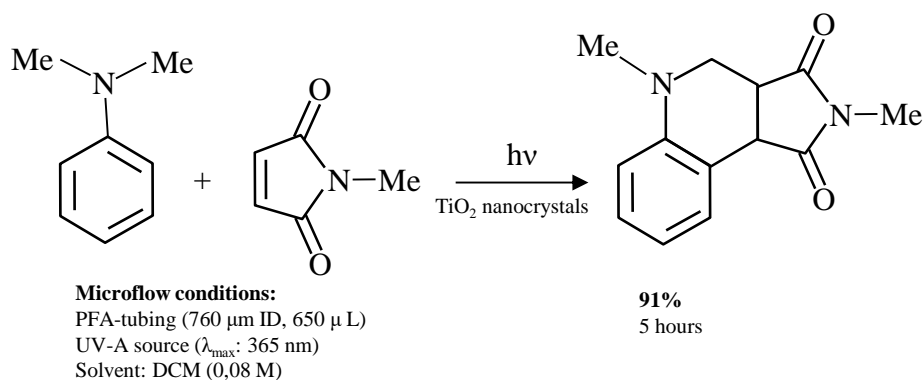
Figure 37: Photocatalytic addition of N,N-dimethylaniline to N-methylmaleimide.

Symmetrical and unsymmetrical disulfides, useful molecules employed as drugs, anti-oxidants or pesticides as well as rubber vulcanizing agents, were prepared through TiO_2 induced oxidation of thiols under visible light irradiation in organic solvents (acetonitrile or ethanol) (Figure 38).[262,263] The reaction was carried out both in batch and in continuous flow systems. Switching from batch to a continuous-flow packed-bed reactor substantially reduced the reaction times. Furthermore, biocompatible reaction conditions and the facile catalyst separation, makes this method particularly appealing for biomolecule modification protocols.[264]

Figure 38: Scheme of disulfides production by TiO_2 photocatalysis.

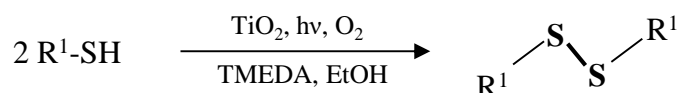Recently, the continuous-flow radical cyclization of bromomalonates catalyzed by graphitic carbon nitride in a packed-bed reactor (ID 2 mm, 620 μL) has been reported (Figure 39).[265,266] The photocatalyst suffered only a slight reduction in efficiency after ca. 70 cycles. Various bromomalonates were cyclized in high yield (74−99%).
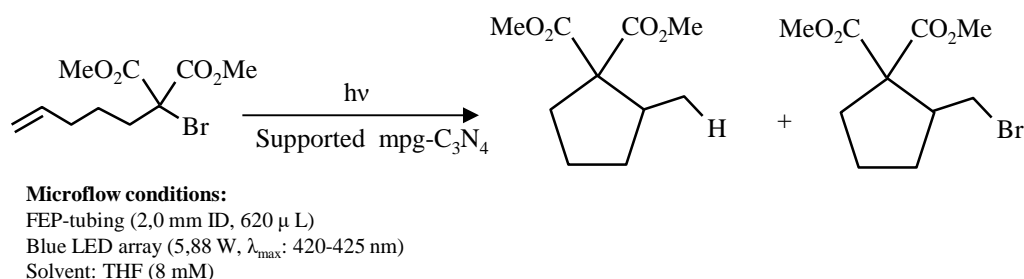

Microflow conditions:
FEP-tubing (2,0 mm ID, 620 μ L)
Blue LED array (5,88 W, λ_{max}: 420-425 nm)
Solvent: THF (8 mM)

Figure 39: Continuous flow radical cyclization photocatalyzed by graphitic carbon nitride.

Katayama et al.[267] recently summarized methods for TiO_2 and WO_3 induced photocatalytic syntheses (oxidation of benzyl alcohol and reduction of benzaldehyde and nitrobenzene) in microflow reactors. In this case the photocatalysts were coated inside a fused silica capillary (inner diameter 1.1 mm, outer diameter 1.4 mm) and irradiated with UV-LEDs or with visible light.

High yield photoisomerization and photooxygenation reactions of trans- and cis-1,2-bis(4-methoxyphenyl) cyclopropanes to trans- and cis-3,5-bis(4-methoxyphenyl)-1,2-dioxolanes were performed in a TiO_2 thin film-coated microflow reactor.[268,269] These photoreactions (see Figure 40), which are likely initiated by electron transfer from 1,2-diarylcyclopropanes to excited TiO_2, were accelerated by $Mg(ClO_4)_2$ because of its ability to stabilize the cyclopropane radical cation intermediates, therefore suppressing back-electron transfer.
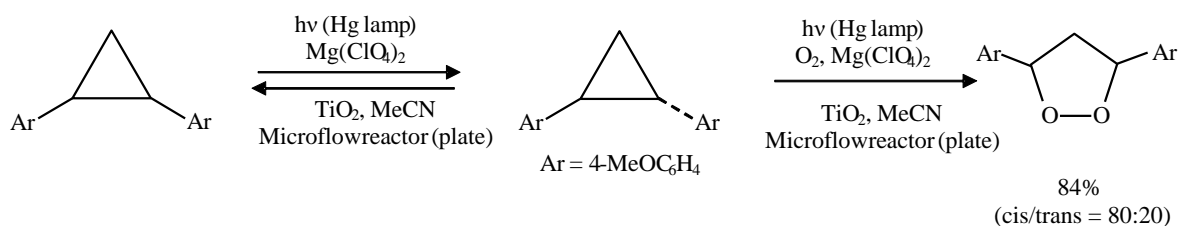

Figure 40: Photoisomerization and photo-oxygenation of trans-bis(4-methoxyphenyl)cyclopropanes by using TiO_2 catalysts in the presence of $Mg(ClO_4)_2$.

Recently the cleavage of photo-labile 2-nitrobenzyl linkers in Merrifield type solid phase synthesis was carried out in a continuous microflow photoreactor.[270] Interestingly, unlike the batch system, where the photoreaction resulted in incomplete cleavage of the linkers, the reaction reached yields of 86% in the continuous flow microreactor (Figure 41).
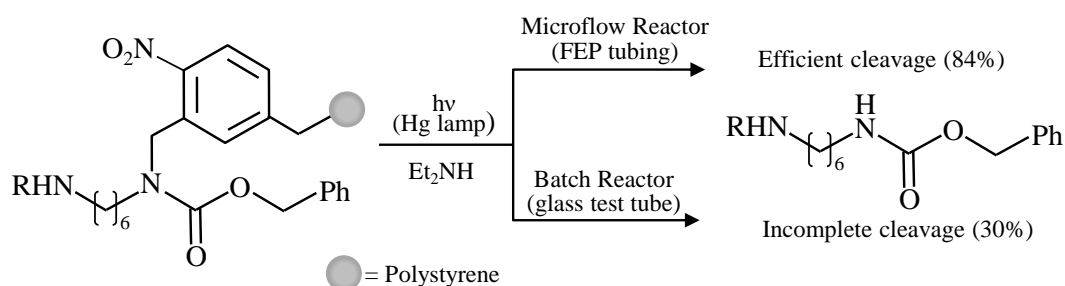
Figure 41: Scheme of cleavage of photo-labile 2-nitrobenzyl linkers in Merrifield type solid phase synthesis.

2.4 Photocatalytic membrane reactors
The integration of photocatalysis with a membrane-based separation unit has been proposed as a promising tool to transfer photocatalytic syntheses from lab to industrial scale. The reason why photocatalytic membrane reactors (PMRs) could produce great advantages is based on a simple idea. The target molecule, generally a reaction intermediate, can be continuously separated from the photocatalytic system by means of suitable membranes in order to avoid its further transformation. This not only provides higher selectivity and efficiency with respect to the sole photocatalytic process, but also enables direct separation of the product of interest. Furthermore, the dense membranes are generally not affected by possible fouling and allow the complete retention of the photocatalytic powder by avoiding further separation steps, and reducing the operative costs. Finally, the possibility of operating in a continuous or semi-continuous mode, the easy control and the modularity of the system endow the integrated process with versatility and

flexibility. It is worth to note that the integration of the two processes is straightforward due to the similar operative conditions at which they generally work (mild temperature, low pressure, diluted solutions, low energy demand). This solution has been often applied for environmental purposes by considering the synergistic effects of the integration, i.e. the possibility of pollutant removal with rates higher than the sum of those obtained by the single technologies.[271] Indeed, coupling membrane filtration with photocatalysis enables the oxidation of organic compounds transforming them into smaller compounds reducing membrane fouling and/or eliminating the threat of emerging contaminants. Moreover, other advantages are the chemical-free disinfection of microorganisms and the self-cleaning of the catalyst which enables to maintain constant the permeation flux reducing the cleaning procedure frequency along with the cost of cleaning agents.

On the other hand, applications for the synthesis of high value-added compounds can be still defined at a nascent level. While some interesting syntheses have been investigated from a "chemical" point of view, in fact, the highly specific engineering issues related to them should be still approached. Therefore, various competences and different research approaches must be interdisciplinary connected, and scientific collaborations are often required to prove the applicative viability of PMRs for synthetic purposes. It is therefore understandable why the relevant literature reports only a limited number of photocatalytic syntheses of high added value chemicals carried out in PMRs. Few photo-oxidation reactions (partial oxidation of benzene to phenol, alcohols to aldehydes and the synthesis of vanillin) and only two photocatalytic synthetic reductions (CO_2 to fuels and the synthesis of phenylethanol) have been carried out in PMRs, to the best of our knowledge. By taking into account the above considerations, some engineering issues related to these reactions will be reported hereby.

Photocatalytic oxidation of benzene to phenol occured with poor selectivity in batch conditions due to further hydroxylation of the aromatic ring.[272-276] Molinari et al.[277] investigated the direct benzene conversion to phenol in a hybrid PMR (Figure 42), by using TiO_2 as the suspended catalyst.
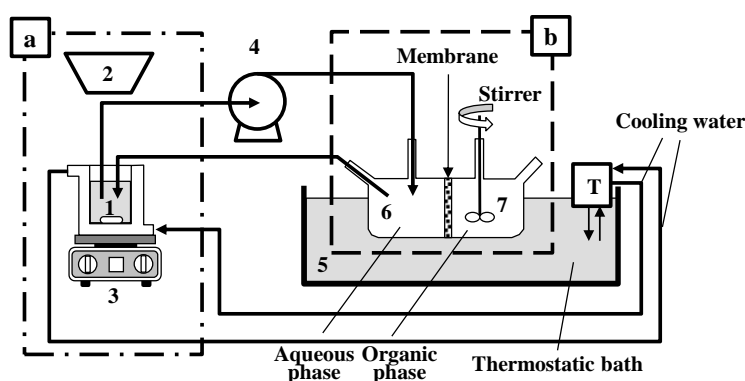

Figure 42: Scheme of the system for the photocatalytic oxidation of benzene. Reproduced with permission from ref 277. Copyright 2009 Elesevier.

Briefly, the system consisted of a batch photocatalytic reactor (a) coupled with a membrane contactor module (b) by means of recirculation. Benzene acted both as reactant (permeating from the organic phase to the aqueous phase) and as the extraction solvent (phenol, once produced in the reacting mixture, permeated to the organic phase). This system allowed to limit the phenol further oxidation and afforded 40% higher phenol production with respect to batch systems. From these results it is evident that the ratio between the rate of photocatalytic phenol production and that of phenol permeation through the membrane is crucial and a systematic optimization study would be useful for the scale-up on a bench scale.

The photocatalytic hydrogenation of acetophenone to phenylethanol has been proposed by Molinari et al.[278] The same authors integrated the acetophenone reduction in a PMR similar to that shown in Figure 42.[279] The phenylethanol produced in the aqueous reacting phase diffused through the membrane and then dissolved into the organic extracting phase, where it was protected from successive over-hydrogenation. The integrated system showed better conversion, selectivity, yield and overall produced amount of phenylethanol than the sole photocatalytic system.

Aromatic aldehydes can be photocatalytically produced by partial oxidation of the corresponding alcohols under mild experimental conditions and in water as the solvent.[42,159] Even if a good selectivity towards aldehydes has been reported in batch systems, the yield generally can decrease due to further oxidation of the produced aldehyde molecules. Furthermore, the photocatalyst must be separated and it is hard to operate the reaction in a continuous mode. These issues have been approached by integrating the reaction step (4-methoxybenzyl alcohol partial oxidation to 4-methoxybenzaldehyde) with a pervaporation membrane contactor.[280] Unlike the above mentioned phenol production, the aldehyde permeated through a non-porous membrane from the retentate (reacting suspension) to the permeate side (vapour phase at low pressure) where it was condensed by means of liquid nitrogen traps.[281] The experimental set-up is shown in Figure 43.
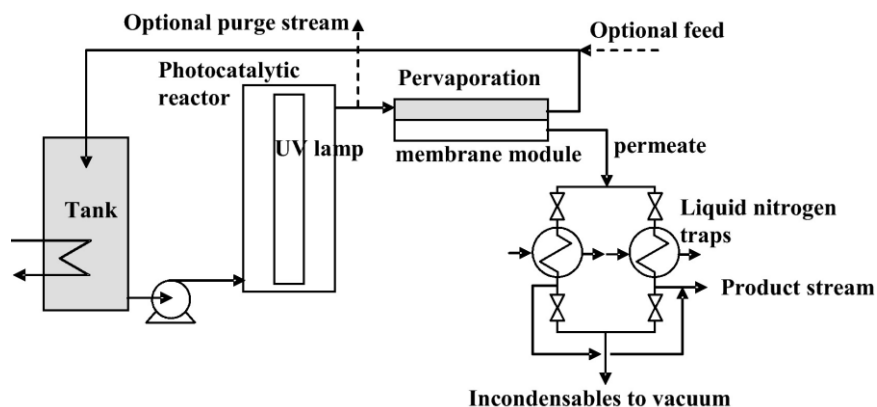
Figure 43: Photocatalytic reaction system integrated with a pervaporation membrane contactor. Reproduced with permission from ref 280. Copyright 2011 Elesevier.

By using a suitable membrane with a high affinity to the aldehyde and a significant rejection to the alcohol, efficient separation without relevant reactant losses could be obtained.

Furthermore, the photocatalyst was completely retained in the reacting mixture and its presence did not affect the membrane performance even after very long times. Figure 44 shows yield, conversion and selectivity of the photocatalytic process alone (a) and integrated with the pervaporation module (b). Notably, while by means of the sole photocatalysis the yield of the process reached a plateau, it monotonically increased by coupling the reaction with pervaporation.
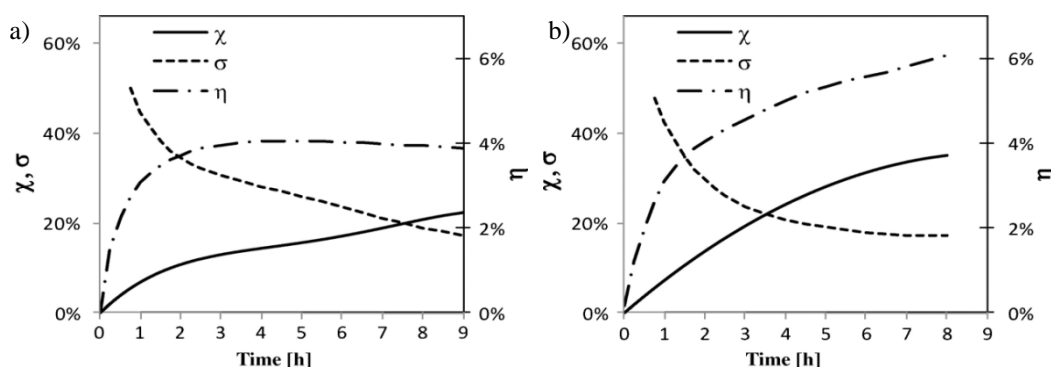

Figure 44: Yield (η), conversion (χ) and selectivity (σ) versus time of the photocatalytic process alone (a) and integrated with the pervaporation module (b). Reproduced with permission from ref 280. Copyright 2011 Elesevier.

A similar system was used for the TiO_2 induced photocatalytic synthesis of vanillin from precursors of natural origin as trans-ferulic acid, isoeugenol, eugenol or vanillyl alcohol.[207,242] The reaction carried out in batch afforded selectivity values towards vanillin ranging from 1.4 to 21 %, depending on the substrate and on the type of photocatalyst. On the other hand, the yield doubled in the photocatalysis-pervaporation integrated process. Furthermore, the permeated vanillin was recovered as highly pure crystals ($\geq$ 99.8%) by freezing downstream in a liquid nitrogen trap, without further separation and purification steps. Due to the industrial relevance of vanillin,[282-287] the process was carefully optimized, kinetically modelled, and some engineering aspects was deeply approached.

Systems in which the photocatalyst was dispersed generally presented not very high performances. This is confirmed by the results of Pathak et al.[288] which performed CO_2 photoreduction in liquid CO_2 in a reactor at high pressure, equipped with a quartz window to provide irradiation (Figure 45). Authors compared the system performances when TiO_2 was dispersed in the porous cavities of a Nafion membrane and when it was suspended in liquid CO_2. Few hundreds of micromoles of methanol and formic acid were obtained per gram of photocatalyst in the immobilized system and their amounts increased with increasing TiO_2 loading onto the membrane. Lower amount of formic acid and traces of methanol were detected when TiO_2 was suspended. Authors justified this result by considering the negative role played by particle aggregation in the suspended system.
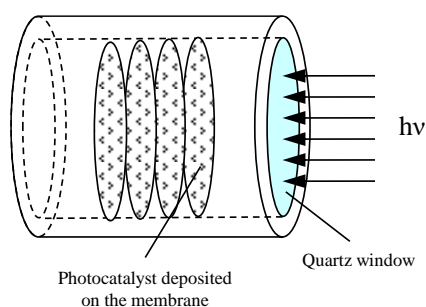
Figure 45: High pressure photoreactor equipped with a quartz window.

Notably, the same authors observed in a successive report that the presence of metal silver nanoparticles on the surface of TiO_2 enhanced the CO_2 conversion and favored the formation of methanol.[289]

Rarely particular structures of the photocatalyst itself work as an inorganic membrane. A nanoporous structured wafer comprised of the photocatalyst itself has been used as a flow-through membrane for gas phase CO_2 photoreduction under sunlight irradiation. The effect of the presence of Cu or Pt metal nanoparticels, the relative humidity, and the exposure time was investigated.[290] Methane, hydrogen and carbon monoxide were the main products. Notably, ca. 25% higher formation of reduction products was obtained when the TiO_2 wafers were used in flow-through configuration. In this case the reduced residence time allowed to avoid re-oxidation of the products, due to removal of them from the surface of the catalyst.

The photocatalyst has been also immobilized in non-polymeric membranes. For instance, a particular optofluidic membrane microreactor system was used by Cheng et al.[291] The membrane was comprised of carbon paper coated with TiO_2 on one side and treated with poly-tetrafluoroethylene on the other side in order to confer hydrophobicity. The membrane separated two chambers in which circulated water and gaseous CO_2, respectively (Figure 46). UV irradiation of the TiO_2 containing membrane side resulted in methanol production of ca. 100 μmoles per hour and gram of photocatalyst in the optimised conditions. The influence of water flow rate, light intensity and catalyst loading on the performance of the system was investigated. The microsized dimensions coupled with the presence of a membrane provided high surface area/volume ratio, improved the light distribution inside the reactor and the proton transfer. However, despite blank tests, the inertness of the carbon paper may be questionable. Furthermore, the ratio H_2O/CO_2 could be hardly controlled.
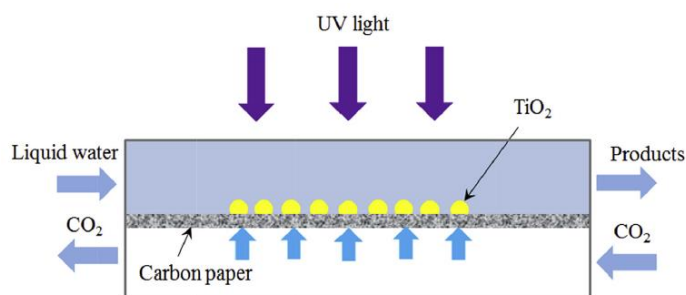

Figure 46: Scheme of the optofluidic membrane microreactor system. Reproduced with permission from ref 291. Copyright 2016 Elsevier.

However the most used membrane systems for CO_2 photoreduction use polymeric membranes. The catalyst immobilization into polymeric membrane supports offers several advantages such as a better catalyst exposition to UV light, the possibility of tuning and control the contact between reactants and catalyst, the reduction of catalyst aggregation and the possibility of reusing it, and a better control of fluid dynamics. Nafion is the most used polymer due to its transparency and resistance to heat and irradiation.[292]

Sellaro et al.[293] performed the photocatalytic CO_2 reduction in a continuous photocatalytic membrane reactor in which TiO_2 was embedded in a Nafion membrane. Runs were carried out in continuous or in batch mode under UV light and by using water as the reducing agent. The best results were obtained in continuous mode, with a H_2O/CO_2 stream with a molar ratio equal to 5:1. The system worked at a transmembrane pressure of 2 bar. The main photoreduction product was methanol whose further oxidation was limited in continuous mode so that its flow rate/catalyst weight reached 45 μmoles per gram of photocatalyst per hour. This value is among the highest reported in literature for systems under mild pressure conditions. The reason of this result lies in the continuous operating mode promoting conversion and avoiding further oxidation of the products. In a successive work exfoliated C_3N_4 was used instead of TiO_2 in a similar system configuration.[294] In fact, exfoliated C_3N_4 presented a high specific surface area and maintained its physico-chemical properties when embedded in Nafion membranes. Furthermore, it could generate electrons with a more negative potential, thus thermodynamically favoring CO_2 reduction with respect to TiO_2. In this case the membrane reactor converted at least 10 times more carbon than the batch system, as a result of the continuous operation mode and the improved dispersion of catalyst once embedded in the Nafion matrix. In the presence of C_3N_4, CO_2 was converted in a different set of products compared to the system with TiO_2, i.e. methanol, ethanol, formaldehyde and acetone, whose distribution strongly depended on H_2O/CO_2 feed molar ratio and residence time.

3. Conclusions and perspectives

Photocatalysis has been often proposed as a promising tool for water purification purposes. However, after ca. 30 years of scientific investigation and many attempts to transfer processes on a larger scale than the bench one, photocatalytic water treatments show the widest disconnection between academic research and the actual needs of the water industry with respect to other technologies. As a matter of fact, in this field photocatalysis alone can hardly survive outside the lab. Coupling photocatalysis with other processes (already applied) such as ozonation or membrane technologies may fill the above mentioned gap by increasing the efficiency of the overall process with respect to the single technologies (synergistic effects), thus making the integration appealing for large scale applications. Consequently, we believe that further scientific efforts should be done in the field of photocatalysis for water treatments, but a neat change of direction is required. Stable, reusable and visible light active materials are needed more than elegant, high performing and complex photocatalysts, which are often unstable giving rise to leaching problems. Moreover, engineering issues related to the design of reactors, to radiant field distribution and to process intensification aspects should be deeper investigated, and, above all, greater collaborations with industries would be desirable.

The situation is different when looking at photocatalysis as a tool for the synthesis of high value-added compounds. In this field, basic research is still necessary to develop novel syntheses and niche applications which, although intrinsically at small scale, could be of wide diffusion. Notably, the possibility of using abundant solar light, water as the solvent and mild operating conditions, make photocatalysis an appealing alternative to the traditional chemical syntheses.

Photocatalysis has been long believed to be an unselective oxidation process due to the presence of highly oxidizing radicals. However, plenty of reports demonstrate that high selectivity towards the target compounds may be achieved by carefully tailoring crystallinity, surface properties of the photocatalyst, and its interaction with the substrates. For this reason, the field has recently spawned a growing number of synthetic applications with novel and admirable insights into mechanistic and physico-chemical aspects. In this framework we would like to note that photocatalytic formation of target compounds does not strictly implies their synthesis. Unfortunately, under the label of "syntheses" reactions have been often reported in which the desired products have been only chromatographically detected, and whose separation, purification or isolation in gram scale has not been performed. Furthermore, we believe that more attention should be paid on reactor design and other engineering issues in order to optimize the most economically promising syntheses. To this aim, interdisciplinary collaborations are needed and various specific hurdles could arise, but it is time to stop basking in lab successes, turning a blind eye on fatal implementation problems. This is the driving force of the present review which focus not only on relevant physico-chemical aspects, but also on some engineering issues which can improve the efficiency of photocatalytic syntheses. We surveyed the rare photocatalytic syntheses performed in continuous reacting systems, in microreactors and in membrane reactors, which we envisaged as promising tools to enhance the performances of the syntheses and whose investigation in this field is only at a very early stage. In some cases, the high yields obtained and the appealing mild operating conditions make engaging the competition between photocatalysis and the applied synthetic routes, whereby the existence of traditional and still operating plants seems to be the only (merely economic) reason hindering the implementation of novel and "greener" systems. Microreactors can be good candidates to facilitate the transfer from laboratory to bigger scales. In fact, this can be obtained simply by increasing the number of devices arranged in series, thus avoiding risky and costly scale up procedures. Moreover, along with other remarkable points of strength, it is possible to take advantage of the typically small residence times to increase the selectivity of the process. However, high fabrication costs, low throughput, and operating problems related to the use of specific low pulse or pulseless pumps and to clogging of solid particles, still cause poor industrial acceptance. The use of membranes also determines remarkable improvements in terms of yield of the process, by separating the target compounds directly from the photocatalytic suspension. Other benefits are the possibility to simultaneously separate the photocatalyst and to operate continuously and in modular arrangements.

We think that the integration of different systems can mitigate the hurdles related to the single technologies and that an interdisciplinary vision of the processes can be a viable way towards the industrial application of some photocatalytic syntheses.

References

(1) Ciamician, G. The Photochemistry of the Future. *Science* **1912**, *36*, 385-394.
(2) Renz, C. Lichtreaktionen der Oxyde des Titans, Cers und der Erdsäuren. *Helv. Chim. Acta* **1921**, *4*, 691-968.
(3) Schwab, G. M. Photochemical and Kinetic Studies of Electronic Reaction Mechanisms. *Adv. Catal.* **1957**, *9*, 229-237.
(4) Fujishima, A.; Honda, K. Electrochemical Evidence for the Mechanism of the Primary Stage of Photosynthesis. *Bull. Chem. Soc. Japan* **1971**, *44*, 1148-1150.
(5) Fujishima, A.; Honda, K. Electrochemical Photolysis of Water at a Semiconductor Electrode. *Nature* **1972**, *238*, 37-38.
(6) Schiavello, M. *Photocatalysis and Environment. Trends and Applications;* Kluwer, Dordrecht, 1988.
(7) Fox, M. A.; Dulay, M. Heterogeneous Photocatalysis. *Chem. Rev.* **1995**, *83*, 341-357.
(8) Mills, A.; Le Hunte, S. An Overview of Semiconductor Photocatalysis. *J. Photochem. Photobiol. A* **1997**, *108*, 1-35.
(9) Hermann, J. -M. Heterogeneous Photocatalysis: Fundamentals and Applications to the Removal of Various Types of Aqueous Pollutants. *Catal. Today* **1999**, *53*, 115-129.
(10) Friedmann, D.; Hakki, A.; Kim, H.; Choi, W.; Bahnemann, D. W. Heterogeneous Photocatalytic Organic Synthesis: State-of-the-Art and Future Perspectives. *Green Chem.* **2016**, *18*, 5391-5411.
(11) Lang, X.; Chen, X.; Zhao, J. Heterogeneous Visible Light Photocatalysis for Selective Organic Transformations. *Chem. Soc. Rev.* **2014**, *43*, 473-486.

(12) Augugliaro, V.; Camera-Roda, G.; Loddo, V.; Palmisano, G.; Palmisano, L.; Soria, J.; Yurdakal, S. Heterogeneous Photocatalysis and Photoelectrocatalysis: from Unselective Abatement of Noxious Species to Selective Production of High-Value Chemicals. *J. Phys. Chem. Lett.* **2015**, *6*, 1968-1981.

(13) Shiraishi, Y.; Hirai, T. Selective Organic Transformations on Titanium Oxide-Based Photocatalysts. *J. Photochem. Photobiol. C* **2008**, *9*, 157-170.

(14) Habisreutinger, S. N.; Schmidt-Mende, L.; Stolarczyk, J. K. Photocatalytic Reduction of CO_2 on TiO_2 and Other Semiconductors. *Angew. Chem. Int. Ed.* **2013**, *52*, 7372-7408.

(15) Lu, H.; Zhao, J.; Li, L.; Gong, L.; Zheng, J.; Zhang, L.; Wang, Z.; Zhang, J.; Zhu, Z. Selective Oxidation of Sacrificial Ethanol over TiO_2-Based Photocatalysts During Water Splitting. *Energy Environ. Sci.* **2011**, *4*, 3384-3388.

(16) Fagnoni, M.; Dondi, D.; Ravelli, D.; Albini, A. Photocatalysis for the Formation of the C−C Bond. *Chem. Rev.* **2007**, *107*, 2725-2756.

(17) Ma, Y.; Wang, X.; Jia, Y.; Chen, X.; Han, H.; Li, C. Titanium Dioxide-Based Nanomaterials for Photocatalytic Fuel Generations. *Chem. Rev.* **2014**, *114*, 9987-10043.

(18) Herrmann, J. -M. Fundamentals and Misconceptions in Photocatalysis. *J. Photochem. Photobiol. A* **2010**, *216*, 85-93.

(19) Kou, J.; Lu, C.; Wang, J.; Chen, Y.; Xu, Z.; Varma, R. S. Selectivity Enhancement in Heterogeneous Photocatalytic Transformations. *Chem. Rev.* **2017**, *117*, 1445-1514.

(20) Parrino, F.; Camera-Roda, G.; Loddo, V.; Palmisano, L. Elemental Bromine Production by TiO_2 Photocatalysis and/or Ozonation. *Angew. Chem. Int. Ed.* **2016**, *55*, 10391-10395.

(21) Kuenneth, R.; Feldmer, C.; Knoch, F.; Kisch, H. Heterogeneous Photocatalysis. XIII. Semiconductor-Catalyzed Photoaddition of Olefins and Enol Ethers to 1,2-Diazenes: A New Route to Allylhydrazines. *Chem. Eur. J.* **1995**, *1*, 441-448.

(22) Hoerner, G.; Johne, P.; Kunneth, R.; Twardzik, G.; Roth, H.; Clark, T.; Kisch, H. Heterogeneous Photocatalysis, Part XIX: Semiconductor Type A Photocatalysis: Role of Substrate Adsorption and the Nature of Photoreactive Surface Sites in Zinc Sulfide Catalyzed C-C Coupling Reactions. *Chem. Eur. J.* **1999**, *5*, 208-217.

(23) Parrino, F.; Ramakrishnan, A.; Kisch, H. Semiconductor Photocatalyzed Sulfoxidation of Alkanes. *Angew. Chem. Int. Ed.* **2008**, *47*, 7107-7109.

(24) Bellardita, M.; Loddo, V.; Palmisano, G.; Pibiri, I.; Palmisano, L.; Augugliaro, V. Photocatalytic Green Synthesis of Piperonal in Aqueous TiO_2 Suspension. *Appl. Catal. B.* **2014**, *144*, 607-613.

(25) Bellardita, M.; Loddo, V.; Mele, A.; Panzeri, W.; Pibiri, I.; Parrino, F.; Palmisano, L. Photocatalysis in Dimethyl Carbonate Green Solvent: Degradation and Partial Oxidation of Phenanthrene on Supported TiO_2. *RSC Adv.* **2014**, *4*, 40859-40864.

(26) Lazar, M. A.; Daoud, W. A. Achieving Selectivity in TiO_2-Based Photocatalysts. *RSC Adv.* **2013**, *3*, 4130-4140.

(27) Granone, L. I.; Sieland, F.; Zheng, N.; Dillert, R.; Bahnemann, D. W. Photocatalytic Conversion of Biomass Into Valuable Products: A Meaningful Approach?. *Green Chem.* **2018**, *20*, 1169-1192.

(28) Yang, M. -Q.; Zhang, N.; Pagliaro, M.; Xu, Y. -J. Artificial Photosynthesis Over Graphene–Semiconductor Composites. Are we Getting Better?. *Chem. Soc. Rev.* **2014**, *43*, 8240-8254.

(29) Molinari, R.; Argurio, P.; Lavorato, C. Review on Reduction and Partial Oxidation of Organics in Photocatalytic (Membrane) Reactors. *Curr. Org. Chem.* **2013***, 17*, 2516-2537.

(30) Kisch, H. Semiconductor Photocatalysis for Chemoselective Radical Coupling Reactions. *Acc. Chem. Res.*, **2017**, *50*, 1002-1010.

(31) Ma, D.; Liu, A.; Li, S.; Lu, C.; Chen, C. TiO_2 Photocatalysis for C-C Bond Formation. *Catal. Sci. Technol.* **2018**, *8*, 2030-2045.

(32) Spasiano, D.; Marotta, R.; Malato, S.; Fernandez-Ibanez, P.; Di Somma, I. Solar Photocatalysis: Materials, Reactors, Some Commercial, and Pre-Industrialized Applications. A Comprehensive Approach. *Appl. Catal. B* **2015**, *170*, 90-123.

(33) Schenck, G. O. Problems in Photochemical Synthesis. *Angew. Chem.* **1952**, *64*, 12-23.

(34) Di Paola, A.; Bellardita, M.; Ceccato, R.; Palmisano, L.; Parrino, F. Highly Active Photocatalytic TiO_2 Powders Obtained by Thermohydrolysis of $TiCl_4$ In Water. *J. Phys. Chem. C* **2009**, *113*, 15166-15174.

(35) Carp, O.; Huisman, C. L.; Reller, A. Photoinduced Reactivity of Titanium Dioxide. *Progress Solid State Chem.* **2004**, *32*, 33-177.

(36) Mo, S. -D.; Ching, W. Y. Electronic and Optical Properties of Three Phases of Titanium Dioxide: Rutile, Anatase, and Brookite. *Phys. Rev. B* **2015**, *51*, 13023-13032.

(37) Wang, X. L.; Kafizas, A.; Li, X. O.; Moniz, S. J. A.; Reardon, P. J. T.; Tang, J. W.; Parkin, I. P.; Durrant, J. R. Transient Absorption Spectroscopy of Anatase and Rutile: The Impact of Morphology and Phase on Photocatalytic Activity. *J. Phys. Chem. C* **2015**, *119*, 10439-10447.

(38) Li, Y. -F.; Aschauer, U.; Chen, J.; Selloni, A. Adsorption and Reactions of O_2 on Anatase TiO_2. *Acc. Chem. Res.* **2014**, *47*, 3361-3368.

(39) Buchalska, M.; Kobielusz, M.; Matuszek, A.; Pacia, M.; Wojtyła, S.; Macyk, W. On Oxygen Activation at Rutile and Anatase-TiO_2. *ACS Catal.* **2015**, *5*, 7424-7431.

(40) Di Paola, A.; Cufalo, G.; Addamo, M.; Bellardita, M.; Campostrini, R.; Ischia, M.; Ceccato, R.; Palmisano, L. Photocatalytic Activity of Nanocrystalline TiO_2 (Brookite, Rutile and Brookite-Based) Powders Prepared by Thermohydrolysis of $TiCl_4$ in Aqueous Chloride Solutions. *Colloid Surf. A* **2008**, *317*, 366-376.

(41) Yurdakal, S.; Palmisano, G.; Loddo, V.; Augugliaro, V.; Palmisano, L. Nanostructured Rutile TiO_2 for Selective Photocatalytic Oxidation of Aromatic Alcohols to Aldehydes in Water. *J. Am. Chem. Soc.* **2008**, *130*, 1568-1569.

(42) Addamo, M.; Augugliaro, V.; Bellardita, M.; Di Paola, A.; Loddo, V.; Palmisano, G.; Palmisano, L. Yurdakal S., Environmentally Friendly Photocatalytic Oxidation of Aromatic Alcohol to Aldehyde in Aqueous Suspension of Brookite TiO_2. *Catal. Lett.* **2008**, *126,* 58-62.

(43) Augugliaro, V.; Loddo, V.; Lopez-Munoz, M. J.; Marquez-Alvarez, C.; Palmisano, G.; Palmisano, L.; Yurdakal S. Home-Prepared Anatase, Rutile, and Brookite TiO_2 for Selective Photocatalytic Oxidation of 4-Methoxybenzyl Alcohol in Water: Reactivity and ATR-FTIR Study. *Photochem. Photobiol. Sci.* **2009**, *8*, 663-669.

(44) Li, C. -J.; Xu, G. -R.; Zhang, B.; Gong, J. R. High Selectivity in Visible-Light-Driven Partial Photocatalytic Oxidation of Benzyl Alcohol into Benzaldehyde over Single-Crystalline Rutile TiO_2 Nanorods. *Appl. Catal. B* **2012**, *115*, 201-208.

(45) Zhao, J.; Ke, X.; Liu, H.; Huang, Y.; Chen, C.; Bo, A.; Sheng, X.; Zhu, H. Comparing the Contribution of Visible-Light Irradiation, Gold Nanoparticles, and Titania Supports in Photocatalytic Nitroaromatic Coupling and Aromatic Alcohol Oxidation. *Part. Part. Syst. Charact.* **2016**, *33*, 628-634.

(46) Wei, Z.; Liu, D.; Wei, W.; Chen, X.; Han, Q.; Yao, W.; Ma, X.; Zhu, Y. Ultrathin TiO_2(B) Nanosheets as the Inductive Agent for Transferring H_2O_2 into Superoxide Radicals. *ACS Appl. Mater. Interfaces* **2017**, *9*, 15533-15540.

(47) Ohno, T.; Mitsui, T.; Matsumura, M. TiO_2-Photocatalyzed Oxidation of Adamantane in Solutions Containing Oxygen or Hydrogen Peroxide. *J. Photochem. Photobiol. A* **2003**, *160*, 3-9.

(48) Hirakawa, T.; Yawata, K.; Nosaka, Y. Photocatalytic Reactivity for $O_2^{.-}$ and OH· Radical Formation in Anatase and Rutile TiO_2 Suspension as the Effect of H_2O_2 Addition**. *Appl. Catal. A* **2007**, *325*, 105-111.

(49) Lv, K.; Lu, C. Different Effects of Fluoride Surface Modification on The Photocatalytic Oxidation of Phenol in Anatase and Rutile TiO_2 Suspensions. *Chem. Eng. Technol.* **2008**, *31*, 1272-1276.

(50) Kaur, J.; Pal, B. 100% Selective Yield of m-Nitroaniline by Rutile TiO_2 and m-Phenylenediamine by P25-TiO_2 during m-Dinitrobenzene Photoreduction. *Catal. Commun.* **2014**, *53*, 25-28.

(51) Matsushita, M.; Tran, T. H.; Nosaka, A. Y.; Nosaka, Y. Photo-oxidation Mechanism of L-Alanine in TiO_2 Photocatalytic Systems as Studied by Proton NMR Spectroscopy. *Catal. Today* **2007**, *120*, 240-244.

(52) Bui, T. D.; Kimura, A.; Ikeda, S.; Matsumura, M. Determination of Oxygen Sources for Oxidation of Benzene on TiO_2 Photocatalysts in Aqueous Solutions Containing Molecular Oxygen. *J. Am. Chem. Soc.* **2010**, *132*, 8453-8458.

(53) Bellardita, M.; García-López, E.; Marcì, G.; Palmisano, L. Photocatalytic Formation of H_2 and Value-Added Chemicals in Aqueous Glucose (Pt)-TiO_2 Suspension. *Int. J. Hydrogen Energ*. **2016**, *41*, 5934-5947.

(54) Chong, R.; Li, J.; Ma, Y.; Zhang, B.; Han, H.; Li, C. Selective Conversion of Aqueous Glucose to Value-Added Sugar Aldose on TiO_2-Based Photocatalysts. *J. Catal*. **2014**, *314*, 101-108.

(55) Da Vià, L.; Recchi, C.; Gonzalez-Yañez, E. O.; Davies, T. E.; Lopez-Sanchez, J. A. Visible Light Selective Photocatalytic Conversion of Glucose by TiO_2. *Appl. Catal. B* **2017**, *202*, 281-288.

(56) Shiraishi, Y.; Togawa, Y.; Tsukamoto, D.; Tanaka, S.; Hirai, T. Highly Efficient and Selective Hydrogenation of Nitroaromatics on Photoactivated Rutile Titanium Dioxide. *ACS Catal*. **2012**, *2*, 2475-2481.

(57) Yurdakal, S.; Augugliaro, V.; Sanz, J.; Soria, J.; Sobrados, I.; Torralvo, M. J. The Influence of the Anatase Nanoparticles Boundaries on the Titania Activity Performance. *J. Catal*. **2014**, *309*, 97-104.

(58) Jensen, H.; Joensen, K. D.; Jørgensen, J. -E.; Pedersen, J. S.; Søgaard, E. G. Characterization of Nanosized Partly Crystalline Photocatalysts. *J. Nanopart. Res*. **2004**, *6*, 519-526.

(59) Ohtani, B.; Ogawa, Y.; Nishimoto, S. -I. Photocatalytic Activity of Amorphous Anatase Mixture of Titanium(IV) Oxide Particles Suspended in Aqueous Solutions. *J. Phys. Chem. B* **1997**, *101*, 3746-3752.

(60) Bertoni, G.; Beyers, E.; Verbeeck, J.; Mertens, M.; Cool, P.; Vansant, E. F.; Van Tendeloo, G. Quantification of Crystalline and Amorphous Content in Porous TiO_2 Samples from Electron Energy Loss Spectroscopy. *Ultramicroscopy* **2006**, *106*, 630-635.

(61) Bellardita, M.; Di Paola, A.; Megna, B.; Palmisano, L. Absolute Crystallinity and Photocatalytic Activity of Brookite TiO_2 Samples. *Appl. Catal. B* **2017**, *201*, 150-158.

(62) Lebedev, V. A.; Kozlov, D. A.; Kolesnik, I. V.; Poluboyarinov, A. S.; Becerikli, A. E.; Grünert, W.; Garshev, A. V. The Amorphous Phase in Titania and its Influence on Photocatalytic Properties. *Appl. Catal. B* **2016**, *195*, 39-47.

(63) Tobaldi, D. M.; Pullar, R. C.; Seabra, M. P.; Labrincha, J. A. Fully Quantitative X-ray Characterization of Evonik Aeroxide TiO_2 P25®. *Mater. Lett*. **2014**, *122*, 345-347.

(64) Bellardita, M.; Di Paola, A.; Megna, B.; Palmisano, L. Determination of the Crystallinity of TiO_2 Photocatalysts. *J. Photochem. Photobiol. A* **2018**, *367*, 312-320.

(65) Zhang, L.; Miller, B. K.; Crozier, P. A. Atomic Level In-Situ Observation of Surface Amorphization in Anatase Nanocrystals During Light Irradiation in Water Vapor. *Nano Lett*. **2013**, *13*, 679-684.

(66) Yurdakal, S.; Augugliaro, V.; Loddo, V.; Palmisano, G.; Palmisano, L. Enhancing Selectivity in Photocatalytic Formation of P-Anisaldehyde in Aqueous Suspension under Solar Light Irradiation via TiO_2 N-Doping. *New J. Chem*. **2012**, *36*, 1762-1768.

(67) Yurdakal, S.; Yanar, Ş. Ö.; Çetinkaya, S.; Alagöz, O.; Yalçın, P.; Özcan, L. Green Photocatalytic Synthesis of Vitamin B_3 by Pt Loaded TiO_2 Photocatalysts. *Appl. Catal. B* **2017**, *202*, 500-508.

(68) Carneiro, J. T.; Almeida, A. R.; Moulijn, J. A.; Mul, G. Cyclohexane Selective Photocatalytic Oxidation by Anatase TiO_2: Influence of Particle Size and Crystallinity. *Phys. Chem. Chem. Phys*. **2010**, *12*, 2744-2750.

(69) Bellardita, M.; Augugliaro, V.; Loddo, V.; Megna, B.; Palmisano, G.; Palmisano, L.; Puma, M. A. Selective Oxidation of Phenol and Benzoic Acid in Water via Home-Prepared TiO_2 Photocatalysts: Distribution of Hydroxylation Products. *Appl. Catal. A* **2012**, *441-442*, 79-89.

(70) Augugliaro, V.; El Nazer, H. A.; Loddo, V.; Mele, A.; Palmisano, G.; Palmisano, L.; Yurdakal, S. Partial Photocatalytic Oxidation of Glycerol in TiO_2 Water Suspensions. *Catal. Today* **2010**, *151*, 21-28.

(71) Liu, G.; Yang, H. G.; Pan, J.; Yang, Y. Q.; Lu, G. Q.; Cheng, H. -M. Titanium Dioxide Crystals with Tailored Facets. *Chem. Rev*. **2014**, *114*, 9559-9612.

(72) Dozzi, M. V.; Selli, E. Specific Facets-Dominated Anatase TiO_2: Fluorine-Mediated Synthesis and Photoactivity. *Catalysts* **2013**, *3*, 455-485.

(73) Wang, J.; Rao, P.; An, W.; Xu, J.; Men, Y. Boosting Photocatalytic Activity of Pd Decorated TiO_2 Nanocrystal with Exposed (001) Facets for Selective Alcohol Oxidations. *Appl. Catal. B* **2016**, *195*, 141-148.

(74) Bellardita, M.; Garlisi, C.; Venezia, A. M.; Palmisano, G.; Palmisano, L. Influence of Fluorine on the Synthesis of Anatase TiO_2 for Photocatalytic Partial Oxidation: Are Exposed Facets the Main Actors?. *Catal. Sci. Technol*. **2018**, *8*, 1606-1620.

(75) Yu, J.; Low, J.; Xiao, W.; Zhou, P.; Jaroniec, M. Enhanced Photocatalytic CO_2-Reduction Activity of Anatase TiO_2 by Coexposed {001} and {101} Facets. *J. Am. Chem. Soc*. **2014**, *136*, 8839-8842.

(76) Cao, Y.; Lia, Q.; Lia, C.; Li, J.; Yang, J. Surface Heterojunction between (001) and (101) facets of Ultrafine Anatase TiO_2 Nanocrystals for Highly Efficient Photoreduction CO_2 to CH_4. *Appl. Catal. B* **2016**, *198*, 378-388.

(77) Mao, J.; Ye, L.; Li, K.; Zhang, X.; Liu, J.; Peng, T.; Zan, L. Pt-Loading Reverses the Photocatalytic Activity Order of Anatase TiO_2{001} and {010} Facets for Photoreduction of CO_2 to CH_4. *Appl. Catal. B* **2014**, *144*, 855-862.

(78) Li, K.; Peng, T.; Ying, Z.; Song, S.; Zhang, J. Ag-Loading on Brookite TiO_2 Quasi Nanocubes with Exposed {210} and {001} Facets: Activity and Selectivity of CO_2 Photoreduction to CO/CH_4. *Appl. Catal. B* **2016**, *180*, 130-138.

(79) Lei, Z.; Xiong, Z.; Wang, Y.; Chen, Y.; Cao, D.; Zhao, Y.; Zhang, J.; Zheng, C. Photocatalytic Reduction of CO_2 over Facet Engineered TiO_2 Nanocrystals Supported by Carbon Nanofibers under Simulated Sunlight Irradiation. *Catal. Commun*. **2018**, *108*, 27-32.

(80) Liu, L.; Gu, X.; Ji, Z.; Zou, W.; Tang, C.; Gao, F.; Dong, L. Anion-Assisted Synthesis of TiO_2 Nanocrystals with Tunable Crystal Forms and Crystal Facets and Their Photocatalytic Redox Activities in Organic Reactions. *J. Phys. Chem. C* **2013**, *117*, 18578-18587.

(81) Sun, D.; Yang, W.; Zhou, L.; Sun, W.; Lia, Q.; Shang, J. K. The Selective Deposition of Silver Nanoparticles onto {101} Facets of TiO_2 Nanocrystals with Co-Exposed {001}/{101} Facets, and their Enhanced Photocatalytic Reduction of Aqueous Nitrate under Simulated Solar Illumination. *Appl. Catal. B* **2016**, *182*, 85-93.

(82) Chong, R.; Li, J.; Zhou, X.; Ma, Y.; Yang, J.; Huang, L.; Han, H.; Zhang, F.; Li, C. Selective Photocatalytic Conversion of Glycerol to Hydroxyacetaldehyde in Aqueous Solution on Facet Tuned TiO_2-Based Catalysts. *Chem. Commun*. **2014**, *50*, 165-167.

(83) Zhou, Y.; Tian, Z.; Zhao, Z.; Liu, Q.; Kou, J.; Chen, X.; Gao, J.; Yan, S.; Zou, Z. High-Yield Synthesis of Ultrathin and Uniform Bi_2WO_6 Square Nanoplates Benefitting from Photocatalytic Reduction of CO_2 into Renewable Hydrocarbon Fuel under Visible Light. *ACS Appl. Mater. Interfaces* **2011**, *3*, 3594-3601.

(84) Bai, S.; Wang, X.; Hu, C.; Xie, M.; Jiang, J.; Xiong, Y. Two-Dimensional g-C_3N_4: An Ideal Platform for Examining Facet Selectivity of Metal Co-Catalysts in Photocatalysis. *Chem. Commun*. **2014**, *50*, 6094-6097.

(85) Tan, H. L.; Wen, X.; Amal, R.; Ng, Y. H. $BiVO_4$ {010} and {110} Relative Exposure Extent: Governing Factor of Surface Charge Population and Photocatalytic Activity. *J. Phys. Chem. Lett*. **2016**, *7*, 1400-1405.

(86) Gao, B.; Wang, T.; Fan, X.; Gong, H.; Meng, X.; Li, P.; Feng, Y.; Huang, X.; He, J.; Ye, J. Selective Deposition of Ag_3PO_4 on Specific Facet of $BiVO_4$ Nanoplate for Enhanced Photoelectrochemical Performance. *Sol. RRL* **2018**, 1800102.

(87) Wang, D.; Jiang, H.; Zong, X.; Xu, Q.; Ma, Y.; Li, G.; Li, C. Crystal Facet Dependence of Water Oxidation on $BiVO_4$ Sheets under Visible Light Irradiation. *Chem. Eur. J*. **2011**, *17*, 1275-1282.

(88) Xie, S.; Shen, Z.; Zhang, H.; Cheng, J.; Zhang, Q.; Wang, Y. Photocatalytic Coupling of Formaldehyde to Ethylene Glycol and Glycolaldehyde over Bismuth Vanadate with Controllable Facets and Cocatalysts. *Catal. Sci. Technol*. **2017**, *7*, 923-933.

(89) Zhao, G.; Liu, W.; Hao, Y.; Zhang, Z.; Li, Q.; Zang, S. Nanostructured Shuriken-Like $BiVO_4$ with Preferentially Exposed {010} Facets: Preparation, Formation Mechanism, and Enhanced Photocatalytic Performance. *Dalton Trans*. **2018**, *47*, 1325-1336.

(90) Li, X.; Yu, J.; Jaroniec, M. Hierarchical Photocatalysts. *Chem. Soc. Rev*. **2016**, *45*, 2603-2636.

(91) Brahimi, R.; Bessekhouad, Y.; Bouguelia, A.; Trari, M. Visible Light Induced Hydrogen Evolution over the Heterosystem Bi_2S_3/TiO_2. *Catal. Today* **2007**, *122*, 62-65.

(92) Weber, H.; Kirchner, B. Ionic Liquid Induced Band Shift of Titanium Dioxide. *ChemSusChem* **2016**, *9*, 2505-2514.

(93) Bickley, R. I.; Gonzalez-Carreno, T.; Lees, J. S.; Palmisano, L.; Tilley, R. J. D. A Structural Investigation of Titanium Dioxide Photocatalysts. *J. Solid State Chem.* **1991**, *92*, 178-190.

(94) Kho, Y. K.; Iwase, A.; Teoh, W. Y.; Mädler, L.; Kudo, A.; Amal, R. Photocatalytic H_2 Evolution over TiO_2 Nanoparticles. The Synergistic Effect of Anatase and Rutile. *J. Phys. Chem. C* **2010**, *114*, 2821-2829.

(95) Scanlon, D. O.; Dunnill, C. W.; Buckeridge, J.; Shevlin, S. A.; Logsdail, A. J.; Woodley, S. M.; Catlow, C. R. A.; Powell, M. J.; Palgrave, R. G.; Parkin, I. P.; Watson, G. W.; Keal, T. W.; Sherwood, P.; Walsh, A.; Sokol, A. A. Band Alignment of Rutile and Anatase TiO_2. *Nat. Mater.* **2013**, *12*, 798-801.

(96) Kullgren, J.; Aradi, B.; Frauenheim, T.; Kavan, L.; Deák, P. Resolving the Controversy about the Band Alignment between Rutile and Anatase: The Role of OH^-/H^+ Adsorption. *J. Phys. Chem.* C **2015**, *119*, 21952-21958.

(97) Wilcoxon, J. P.; Newcomer, P. P.; Samara, G. A. Synthesis and Optical Properties of MoS_2 and Isomorphous Nanoclusters in the Quantum Confinement Regime. *J. Appl. Phys.* **1997**, *81*, 7934-7944.

(98) Torimoto, T.; Kontani, H.; Shibutani, Y.; Kuwabata, S.; Sakata, T.; Mori, H.; Yoneyama, H. Characterization of Ultrasmall CdS Nanoparticles Prepared by the Size-Selective Photoetching Technique. *J. Phys. Chem. B* **2001**, *105*, 6838-6845.

(99) Xia, P.; Zhu, B.; Yu, J.; Cao, S.; Jaroniec, M. Ultra-Thin Nanosheet Assemblies of Graphitic Carbon Nitride for Enhanced Photocatalytic CO_2 Reduction. *J. Mater. Chem. A* **2017**, *5*, 3230-3238.

(100) Xu, Q.; Yu, J.; Zhang, J.; Zhang, J.; Liu, G. Cubic Anatase TiO_2 Nanocrystals with Enhanced Photocatalytic CO_2 Reduction Activity. *Chem. Commun.* **2015**, *51*, 7950-7953.

(101) Chen, X.; Zhou, Y.; Liu, Q.; Li, Z.; Liu, J.; Zou, Z. Ultrathin, Single-Crystal WO_3 Nanosheets by Two-Dimensional Oriented Attachment toward Enhanced Photocatalystic Reduction of CO_2 into Hydrocarbon Fuels under Visible Light. *ACS Appl. Mater. Interfaces* **2012**, *4*, 3372-3377.

(102) Bellardita, M.; Di Paola, A.; García-López, E.; Loddo, V.; Marcì, G.; Palmisano, L. Photocatalytic CO_2 Reduction in Gas-Solid Regime in the Presence of Bare, SiO_2 Supported or Cu-Loaded TiO_2 Samples. *Curr. Org. Chem.* **2013**, *17*, 2440-2448.

(103) Marcì, G.; García-López, E.; Palmisano, L. Photocatalytic CO_2 Reduction in Gas–Solid Regime in the Presence of H_2O by Using GaP/TiO_2 Composite as Photocatalyst under Simulated Solar Light. *Catal. Commun.* **2014**, *53*, 38-41.

(104) Tripathy, J.; Lee, K.; Schmuki, P. Tuning the Selectivity of Photocatalytic Synthetic Reactions Using Modified TiO_2 Nanotubes. *Angew. Chem. Int. Ed.* **2014**, *53*, 12605-12608.

(105) Zheng, C.; He, G.; Xiao, X.; Lu, M.; Zhong, H.; Zuo, X.; Nan, J. Selective Photocatalytic Oxidation of Benzyl Alcohol into Benzaldehyde with High Selectivity and Conversion Ratio over $Bi_4O_5Br_2$ Nanoflakes under Blue LED Irradiation. *App. Catal. B* **2017**, *205*, 201-210.

(106) Xiao, X.; Zheng, C.; Lu, M.; Zhang, L.; Fei, L.; Zuo, X.; Nan, J. Deficient $Bi_{24}O_{31}Br_{10}$ as a Highly Efficient Photocatalyst for Selective Oxidation of Benzyl Alcohol into Benzaldehyde under Blue LED Irradiation. *App. Catal. B* **2018**, *228*, 142-151.

(107) Yu, J.; Hai, Y.; Jaroniec, M. Photocatalytic Hydrogen Production over CuO-Modified Titania. *J. Colloid Interface Sci.* **2011**, *357*, 223-228.

(108) Li, X. -B.; Li, Z. -J.; Gao, Y. -J.; Meng, Q. -Y.; Yu, S.; Weiss, R. -G.; Tung, C. -H.; Wu, L. -Z. Mechanistic Insights into the Interface-Directed Transformation of Thiols into Disulfides and Molecular Hydrogen by Visible-Light Irradiation of Quantum Dots. *Angew. Chem. Int. Ed.* **2014**, *53*, 2085-2089.

(109) Zhao, L. -M.; Meng, Q. -Y.; Fan, X. -B.; Ye, C.; Li, X. -B.; Chen, B.; Ramamurthy, V.; Tung, C. -H.; Wu, L. -Z. Photocatalysis with Quantum Dots and Visible Light: Selective and Efficient Oxidation of Alcohols to Carbonyl Compounds through a Radical Relay Process in Water. *Angew. Chem. Int. Ed.* **2017**, *56*, 3020-3024.

(110) Caputo, J. A.; Frenette, L. C.; Zhao, N.; Sowers, K. L.; Krauss, T. D.; Weix, D. J. General and Efficient C–C Bond Forming Photoredox Catalysis with Semiconductor Quantum Dots. *J. Am. Chem. Soc.* **2017**, *139*, 4250-4253.

(111) Warrier, M.; Lo, M. K. F.; Monbouquette, H.; Garcia-Garibay, M. A. Photocatalytic Reduction of Aromatic Azides to Amines Using CdS And CdSe Nanoparticles. *Photochem. Photobiol. Sci.* **2004**, *3*, 859-863.

(112) Jensen, S. C.; Homan, S. B.; Weiss, E. A. Photocatalytic Conversion of Nitrobenzene to Aniline through Sequential Proton-Coupled One-Electron Transfers from a Cadmium Sulfide Quantum Dot. *J. Am. Chem. Soc.* **2016**, *138*, 1591-1600.

(113) Marcì, G.; García-López, E.; Palmisano, L.; Carriazo, D.; Martín, C.; Rives, V. Preparation, Characterization and Photocatalytic Activity of TiO_2 Impregnated with the Heteropolyacid $H_3PW_{12}O_{40}$: Photo-Assisted Degradation of 2-Propanol in Gas-Solid Regime. *Appl. Catal. B* **2009**, *90*, 497-506.

(114) Marcì, G.; García-López, E.; Bellardita, M.; Parisi, F.; Colbeau-Justin, C.; Sorgues, S.; Liotta, L. F.; Palmisano, L. Keggin Heteropolyacid $H_3PW_{12}O_{40}$ Supported on Different Oxides for Catalytic and Catalytic Photoassisted Propene Hydration. *Phys. Chem. Chem. Phys.* **2013**, *15*, 13329-13342.

(115) Marcì, G.; García-López, E.; Vaiano, V.; Sarno, G.; Sannino, D.; Palmisano, L. Keggin Heteropolyacids Supported on TiO_2 Used in Gas-Solid (Photo)Catalytic Propene Hydration and in Liquid-Solid Photocatalytic Glycerol Dehydration. *Catal. Today* **2017**, *281*, 60-70.

(116) Bellardita, M.; García-López, E. I.; Marcì, G.; Megna, B.; Pomilla, F. R.; Palmisano, L. Photocatalytic Conversion of Glucose in Aqueous Suspensions of Heteropolyacid–TiO_2 Composites. *RSC Adv.* **2015**, *5*, 59037-59047.

(117) Hirakawa, H.; Hashimoto, M.; Shiraishi, Y.; Hirai, T. Selective Nitrate-to-Ammonia Transformation on Surface Defects of Titanium Dioxide Photocatalysts. *ACS Catal.* **2017**, *7*, 3713-3720.

(118) Ma, B.; Xie, H.; Li, J.; Zhan, H.; Lin, K.; Liu, W. Bifunctional Solid Acid Photocatalyst $TiO_2/AC/SO_3H$ with High Acid Density for Pure Green Photosynthesis of 2-Quinoline Carboxamide. *J. Mol. Catal. A* **2016**, *420*, 290-293.

(119) Hakki, A.; Dillert, R.; Bahnemann, D. W. Factors Affecting the Selectivity of the Photocatalytic Conversion of Nitroaromatic Compounds over TiO_2 to Valuable Nitrogen-Containing Organic Compounds. *Phys. Chem. Chem. Phys.* **2013**, *5*, 2992-3002.

(120) Liang, S.; Wen, L.; Lin, S.; Bi, J.; Feng, P.; Fu, X.; Wu, L. Monolayer HNb_3O_8 for Selective Photocatalytic Oxidation of Benzylic Alcohols with Visible Light Response. *Angew. Chem. Int. Ed.* **2014**, *53*, 2951-2955.

(121) Leow, W. R.; Ng, W. K. H.; Peng, T.; Liu, X.; Li, B.; Shi, W.; Lum, Y.; Wang, X.; Lang, X.; Li, S.; Mathews, N.; Ager, J. W.; Sum, T. C.; Hirao, H.; Chen, X. Al_2O_3 Surface Complexation for Photocatalytic Organic Transformations. *J. Am. Chem. Soc.* **2017**, *139*, 269-276.

(122) Leow, W. R.; Yu, J.; Li, B.; Hu, B.; Li, W.; Chen, X. Correlating the Surface Basicity of Metal Oxides with Photocatalytic Hydroxylation of Boronic Acids to Alcohols. *Angew. Chem. Int. Ed.* **2018**, *57*, 9780-9784.

(123) Sclafani, A.; Palmisano, L.; Schiavello, M. Influence of the Preparation Methods of TiO_2 on the Photocatalytic Degradation of Phenol in Aqueous Dispersion. *J. Phys. Chem.* **1990**, *94*, 829-832.

(124) Nosaka, Y.; Kishimoto, M.; Nishino, J. Factors Governing the Initial Process of TiO_2 Photocatalysis Studied by Means of In-Situ Electron Spin Resonance Measurements. *J. Phys. Chem. B* **1998**, *102*, 10279-10283.

(125) Di Paola, A.; Bellardita, M.; Palmisano, L.; Barbieriková, Z.; Brezová, V. Influence of Crystallinity and OH Surface Density on the Photocatalytic Activity of TiO_2 Powders. *J. Photochem. Photobiol. A* **2014**, *273*, 59-67.

(126) Du, P.; Moulijn, J. A.; Mul, G. Selective Photo(Catalytic)-Oxidation of Cyclohexane: Effect of Wavelength and TiO_2 Structure on Product Yields. *J. Catal.* **2006**, *238*, 342-352.

(127) Cano-Casanova, L.; Amorós-Pérez, A.; Ouzzine, M.; Lillo-Ródenas, M. A.; Román-Martínez, M. C. One Step Hydrothermal Synthesis of TiO_2 with Variable HCl Concentration: Detailed Characterization and Photocatalytic Activity in Propene Oxidation. *Appl. Catal. B* **2018**, *220*, 645-653.

(128) Augugliaro, V.; Coluccia, S.; Loddo, V.; Marchese, L.; Martra, G.; Palmisano, L.; Schiavello, M. Photocatalytic Oxidation of Gaseous Toluene on Anatase TiO_2 Catalyst: Mechanistic Aspects and FT-IR Investigation. *Appl. Catal. B* **1999**, *20*, 15-27.

(129) Liu, S.; Liu, C.; Wang, W.; Cheng, B.; Yu, J. Unique Photocatalytic Oxidation Reactivity and Selectivity of TiO₂-Graphene Nanocomposites. *Nanoscale* **2012**, *4*, 3193-3200.

(130) Wang, Q.; Zhang, M.; Chen, C.; Ma, W.; Zhao, J. Photocatalytic Aerobic Oxidation of Alcohols on TiO₂: The Acceleration Effect of a Brønsted Acid. *Angew. Chem. Int. Ed.* **2010**, *49*, 7976-7979.

(131) Higashimoto, S.; Kitao, N.; Yoshida, N.; Sakura, T.; Azuma, M.; Ohue, H.; Sakata, Y. Selective Photocatalytic Oxidation of Benzyl Alcohol and its Derivatives into Corresponding Aldehydes by Molecular Oxygen on Titanium Dioxide Under Visible Light Irradiation. *J. Catal.* **2009**, *266*, 279-285.

(132) Li, R.; Kobayashi, H.; Guo, J.; Fan, J. Visible-Light Induced High-Yielding Benzyl Alcohol-to-Benzaldehyde Transformation over Mesoporous Crystalline TiO₂: A Self-Adjustable Photo-Oxidation System with Controllable Hole-Generation. *J. Phys. Chem. C* **2011**, *115*, 23408-23416.

(133) Tang, Z. R.; Yin, X.; Zhang, Y.; Xu, Y. J. One-Pot, High-Yield Synthesis of One-Dimensional ZnO Nanorods with Well-Defined Morphology as a Highly Selective Photocatalyst. *RSC Adv.* **2013**, *3*, 5956-5965.

(134) Shiraishi, Y.; Hirai, T. Titanium Oxide-Based Photocatalysts for Selective Organic Transformations, *J. Jap. Petrol. Inst.* **2012**, *55*, 287-298.

(135) Nishimoto, S.; Ohtani, B.; Yoshikawa, T.; Kagiya, T. Photocatalytic Conversion of Primary Amines to Secondary Amines and Cyclization of Polymethylene-α,ω-Diamines by an Aqueous Suspension of Titanium(IV) Oxide/Platinum. *J. Am. Chem. Soc.* **1983**, *105*, 7180-7182.

(136) Pal, B.; Ikeda, S.; Kominami, H.; Kera, Y.; Ohtani, B. Photocatalytic Redox-Combined Synthesis of L-Pipecolinic Acid from L-Lysine by Suspended Titania Particles: Effect of Noble Metal Loading on the Selectivity and Optical Purity of the Product. *J. Catal.* **2003**, *217*, 152-159.

(137) Ohtani, B.; Tsuru, S.; Nishimoto, S.; Kagiya, T.; Izawa, K. Photocatalytic One-Step Syntheses of Cyclic Imino Acids by Aqueous Semiconductor Suspensions. *J. Org. Chem.* **1990**, *55*, 5551-5553.

(138) Augugliaro, V.; Kisch, H.; Loddo, V.; López-Munoz, M. J.; Marquez-Alvarez, C.; Palmisano, G.; Palmisano, L.; Parrino, F.; Yurdakal, S. Photocatalytic Oxidation of Aromatic Alcohols to Aldehydes in Aqueous Suspension of Home-Prepared Titanium Dioxide 1. Selectivity Enhancement by Aliphatic Alcohols. *Appl. Catal. A* **2008**, *349*, 182-188.

(139) Augugliaro, V.; Kisch, H.; Loddo, V.; López-Munoz, M. J.; Marquez-Alvarez, C.; Palmisano, G.; Palmisano, L.; Parrino, F.; Yurdakal, S. Photocatalytic Oxidation of Aromatic Alcohols to Aldehydes in Aqueous Suspension of Home-Prepared Titanium Dioxide 2. Intrinsic and Surface Features of Catalysts. *Appl. Catal. A* **2008**, *349*, 189-197.

(140) Parrino, F.; Conte, P.; De Pasquale, C.; Laudicina, V. A.; Loddo, V.; Palmisano, L. Influence of Adsorbed Water on the Activation Energy of Model Photocatalytic Reactions. *J. Phys. Chem. C* **2017**, *151*, 2258-2267.

(141) Renckens, T. J. A.; Almeida, A. R.; Damen, M. R.; Kreutzer, M. T.; Mul, G. Product Desorption Limitations in Selective Photocatalytic Oxidation. *Catal. Today* **2010**, *155*, 302-310.

(142) Maira, A. J.; Coronado, J. M.; Augugliaro, V.; Yeung, K. L.; Conesa, J. C.; Soria, J. Fourier Transform Infrared Study of the Performance of Nanostructured TiO₂ Particles for the Photocatalytic Oxidation of Gaseous Toluene. *J. Catal.* 2001, *202*, 413-420.

(143) Maldotti, A.; Molinari, A. Design of Heterogeneous Photocatalysts Based on Metal Oxides to Control the Selectivity of Chemical Reactions. *Top. Curr. Chem.* **2011**, *303*, 185-216.

(144) Weng, B.; Liu, S.; Tang, Z. -R.; Xu, Y. -J. One-Dimensional Nanostructure-Based Materials for Versatile Photocatalytic Applications. *RSC Adv.* **2014**, *4*, 12685-12700.

(145) Chen, L.; Wang, X.; Lu, W.; Wu, X.; Li, J. Molecular Imprinting: Perspectives and Applications. *Chem. Soc. Rev.*, **2016**, *45*, 2137-2211.

(146) Shen, X.; Zhu, L.; Wang, N.; Ye, L.; Tang, H. Molecular Imprinting for Removing Highly Toxic Organic Pollutants. *Chem. Commun.* **2012**, *48*, 788-798.

(147) Ghosh-Mukerji, S.; Haick, H.; Schvartzman, M.; Paz, Y. Selective Photocatalysis by Means of Molecular Recognition. *J. Am. Chem. Soc.* **2001**, *123*, 10776-10777.

(148) Shen, X.; Zhu, L.; Huang, C.; Tang, H.; Yu, Z.; Deng, F. Inorganic Molecular Imprinted Titanium Dioxide Photocatalyst: Synthesis, Characterization and its Application for Efficient and Selective Degradation of Phthalate Esters. *J. Mater. Chem.* **2009**, *19*, 4843-4851.

(149) Canlas, C.; Lu, J.; Ray, N.; Grosso-Giordano, N.; Lee, S.; Elam, J.; Winans, R.; Van Duyne, R.; Stair, P.; Notestein, J. Shape-Selective Sieving Layers on an Oxide Catalyst Surface. *Nat. Chem.* **2012**, *4*, 1030-1036.

(150) Martin-Esteban, A.; Tadeo, J. L. Selective Molecularly Imprinted Polymer Obtained from a Combinatorial Library for the Extraction of Bisphenol A. *Comb. Chem. High Throughput Screen* **2006**, *9*, 747-751.

(151) Chen, S.; Zhang, H.; Yu, X.; Liu, W. Photocatalytic Reduction of Nitro Compounds Using TiO₂ Photocatalyst by UV and Vis Dye sensitized Systems. *Chin. J. Chem.* **2011**, *29*, 399-404.

(152) Wang, Z.; Lang, X. Visible Light Photocatalysis of Dye-Sensitized TiO₂: The Selective Aerobic Oxidation of Amines to Imines. *Appl. Catal. B* **2018**, *224*, 404-409.

(153) Ma, S. S. K.; Hisatomi, T.; Domen, K. Hydrogen Production by Photocatalytic Water Splitting. *J. Jap. Petrol. Inst.* **2013**, *56*, 280-287.

(154) Li, X.; Shi, J. -L.; Hao, H.; Lang, X. Visible Light-Induced Selective Oxidation of Alcohols with Air by Dye Sensitized TiO₂ Photocatalysis. *Appl. Catal. B* **2018**, *232*, 260-267.

(155) Guarisco, C.; Palmisano, G.; Calogero, G.; Ciriminna, R.; Di Marco, G.; Loddo, V.; Pagliaro, M.; Parrino, F. Visible-Light Driven Oxidation of Gaseous Aliphatic Alcohols to the Corresponding Carbonyls via TiO₂ Sensitized by a Perylene Derivative. *Environ. Sci. Pollut. Res.* **2014**, *21*, 11135-11141.

(156) Zhang, P.; Wang, Y.; Li, H.; Antonietti, M. Metal-Free Oxidation of Sulfides by Carbon Nitride with Visible Light Illumination at Room Temperature. *Green Chem.* **2012**, *14*, 1904-1908.

(157) Zhang, P.; Wang, Y.; Yao, J.; Wang, C.; Yan, C.; Antonietti, M.; Li, H. Visible-Light-Induced Metal-Free Allylic Oxidation Utilizing a Coupled Photocatalytic System of g-C₃N₄ and N-Hydroxy Compounds. *Adv. Synth. Catal.* **2011**, *353*, 1447-1451.

(158) Ma, B.; Wang, Y.; Tong, X.; Guo, X.; Zhenga, Z.; Guo, X. Graphene-Supported CoS₂ Particles: An Efficient Photocatalyst for Selective Hydrogenation of Nitroaromatics in Visible Light. *Catal. Sci. Technol.* **2017**, *7*, 2805-2812.

(159) Abd-Elaal, A.; Parrino, F.; Ciriminna, R.; Loddo, V.; Palmisano, L.; Pagliaro, M. Alcohol-Selective Oxidation in Water Under Mild Conditions via a Novel Approach to Hybrid Composite Photocatalysts. *Chemistryopen* **2015**, *4*, 779-785.

(160) Huang, H.; Zhou, J.; Liu, H.; Zhou, Y.; Feng, Y. Selective Photoreduction of Nitrobenzene to Aniline on TiO₂ Nanoparticles Modified with Aminoacid. *J. Hazard. Mater.* **2010**, *178*, 994-998.

(161) Ahn, W. -Y.; Sheeley, S. A.; Rajh, T.; Cropek, D. M. Photocatalytic Reduction of 4-Nitrophenol with Arginine-Modified Titanium Dioxide Nanoparticles. *Appl. Catal. B* **2007**, *74*, 103-110.

(162) Makarova, O. V.; Rajh, T.; Thurnauer, M. C.; Martin, A.; Kemme, P. A.; Cropek, D. Surface Modification of TiO₂ Nanoparticles for Photochemical Reduction of Nitrobenzene. *Environ. Sci. Technol.* **2000**, *34*, 4797-4803.

(163) Almeida, A. R.; Carneiro, J. T.; Moulijn, J. A.; Mul, G. Improved Performance of TiO₂ in the Selective Photo-Catalytic Oxidation of Cyclohexane by Increasing the Rate of Desorption through Surface Silylation. *J. Catal.* **2010**, *273*, 116-124.

(164) Parrino, F.; Di Paola, A.; Loddo, V.; Pibiri, I.; Bellardita, M.; Palmisano, L. Photochemical and Photocatalytic Isomerization of Trans-Caffeic Acid and Cyclization of Cis-Caffeic Acid to Esculetin. *Appl. Catal. B* **2016**, *182*, 347-355.

(165) Janczyk, A.; Krakowska, E.; Stochel, G.; Macyk, W. Singlet Oxygen Photogeneration at Surface Modified Titanium Dioxide. *J. Am. Chem. Soc.* **2006**, *128*, 15574-15575.

(166) Ciriminna, R.; Parrino, F.; De Pasquale, C.; Palmisano, L.; Pagliaro, M. Photocatalytic Partial Oxidation of Limonene to 1,2 Limonene Oxide. *Chem. Commun.* **2018**, *54*, 1008.

(167) Higashimoto, S.; Shirai, R.; Osano, Y.; Azuma, M.; Ohue, H.; Sakata, Y.; Kobayashi, H. Influence of Metal Ions on the Photocatalytic Activity: Selective Oxidation of Benzyl Alcohol on Iron (III) Ion-Modified TiO_2 Using Visible Light. *J. Catal.* **2014**, *311*, 137-143.

(168) Marotta, R.; Di Somma, I.; Spasiano, D.; Andreozzi, R.; Caprio, V. Selective Oxidation of Benzyl Alcohol to Benzaldehyde in Water by TiO_2/Cu(II)/UV Solar System. *Chem. Eng. J.* **2011**, *172*, 243-249.

(169) Spasiano, D.; Del Pilar Prieto Rodriguez, L.; Olleros, J.; Malato, S.; Marotta, R.; Andreozzi, R. TiO_2/Cu(II) Photocatalytic Production of Benzaldehyde from Benzyl Alcohol in Solar Pilot Plant Reactor. *Appl. Catal. B* **2013**, *136-137*, 56-63.

(170) Hamdy, M. S.; Amrollahi, R.; Mul, G. Surface Ti^{3+}-Containing (Blue) Titania: A Unique Photocatalyst with High Activity and Selectivity in Visible Light-Stimulated Selective Oxidation. *ACS Catal.* **2012**, *2*, 2641-2647.

(171) Mrowetz, M.; Selli, E. Enhanced Photocatalytic Formation of Hydroxyl Radicals on Fluorinated TiO_2. *Phys. Chem. Chem. Phys.* **2005**, *7*, 1100-1102.

(172) Maurino, V.; Bedini, A.; Minella, M.; Rubertelli, F.; Pelizzetti, E.; Minero, C. Glycerol Transformation through Photocatalysis: A Possible Route to Value Added Chemicals. *J. Adv. Oxid. Technol.* **2008**, *11*, 184-192.

(173) Jin, B.; Yao, G.; Wang, X.; Ding, K.; Jin, F. Photocatalytic Oxidation of Glucose into Formate on Nano TiO_2 Catalyst. *ACS Sustainable Chem. Eng.* **2017**, *5*, 6377-6381.

(174) Beydoun, D.; Amal, R.; Low, G.; McEvoy, S. Novel Photocatalyst: Titania-Coated Magnetite. Activity and Photodissolution. *J. Phys. Chem. B* **2000**, *104*, 4387-4396.

(175) Liu, S.; Zhang, N.; Xu, Y. -J. Core–Shell Structured Nanocomposites for Photocatalytic Selective Organic Transformations. *Part. Part. Syst. Char.* **2014**, *31*, 540-556.

(176) He, J.; Chen, L.; Ding, D.; Yang, Y. -K.; Au, C. -T.; Yin, S. -F. Facile Fabrication of Novel $Cd_3(C_3N_3S_3)_2$/CdS Porous Composites and their Photocatalytic Performance for Toluene Selective Oxidation under Visible Light Irradiation. *Appl. Catal. B* **2018**, *233*, 243-249.

(177) Di Credico, B.; Redaelli, M.; Bellardita, M.; Calamante, M.; Cepek, C.; Cobani, E.; D'Arienzo, M.; Evangelisti, C.; Marelli, M.; Moret, M.; Palmisano, L.; Scotti, R. Step-By-Step Growth of HKUST-1 on Functionalized TiO_2 Surface: An Efficient Material for CO_2 Capture and Solar Photoreduction. *Catalysts* **2018**, *8*, 353.

(178) He, X.; Gan, Z.; Fisenko, S.; Wang, D.; El-Kaderi, H. M.; Wang, W. -N. Rapid Formation of Metal Organic Frameworks (MOFs) Based Nanocomposites in Microdroplets and their Applications for CO_2 Photoreduction. *ACS Appl. Mater. Interfaces* **2017**, *9*, 9688-9698.

(179) Zhang, N.; Zhang, Y.; Pan, X.; Fu, X.; Liu, S.; Xu, Y. -J. Assembly of CdS Nanoparticles on the Two-Dimensional Graphene Scaffold as Visible-Light-Driven Photocatalyst for Selective Organic Transformation under Ambient Conditions. *J. Phys. Chem. C* **2011**, *115*, 23501-23511.

(180) Han, C.; Chen, Z.; Zhang, N.; Colmenares, J.; Xu, Y. -J. Hierarchically CdS Decorated 1D ZnO Nanorods-2D Graphene Hybrids: Low Temperature Synthesis and Enhanced Photocatalytic Performance. *Adv. Funct. Mater.* **2015**, *2*, 221-229.

(181) Hamrouni, A.; Moussa, N.; Di Paola, A.; Palmisano, L.; Houas, A.; Parrino, F. Photocatalytic Activity of Binary and Ternary SnO_2–ZnO–$ZnWO_4$ Nanocomposites. *J. Photochem. Photobiol. A* **2015**, *309*, 47-54.

(182) Tsukamoto, D.; Ikeda, M.; Shiraishi, Y.; Hara, T.; Ichikuni, N.; Tanaka, S.; Hirai, T. Selective Photocatalytic Oxidation of Alcohols to Aldehydes in Water by TiO_2 Partially Coated with WO_3. *Chem. Eur. J.* **2011**, *17*, 9816-9824.

(183) Di Paola, A.; Bellardita, M.; Megna, B.; Parrino, F.; Palmisano, L. Photocatalytic Oxidation of Trans-Ferulic Acid to Vanillin on TiO_2 and WO_3-Loaded TiO_2 Catalysts. *Catal. Today* **2015**, *252*, 195-200.

(184) Furukawa, S.; Shishido, T.; Teramura, K.; Tanaka, T. Photocatalytic Oxidation of Alcohols over TiO_2 Covered with Nb_2O_5. *ACS Catal.* **2012**, *2*, 175-179.

(185) Fiorenza, R.; Bellardita, M.; Palmisano, L.; Scirè, S. A Comparison between Photocatalytic and Catalytic Oxidation of 2-Propanol over Au/TiO_2–CeO_2 Catalysts. *J. Mol. Catal. A* **2016**, *415*, 56-64.

(186) Magdziarz, A.; Colmenares, J.; Chernyayeva, O.; Kurzydłowski, K.; Grzonka, J. Iron-Containing Titania Photocatalyst Prepared by the Sonophotodeposition Method for the Oxidation of Benzyl Alcohol. *ChemCatChem* **2016**, *8*, 536-539.

(187) Ciriminna, R.; Delisi, R.; Parrino, F.; Palmisano, L.; Pagliaro, M. Tuning the Photocatalytic Activity of Bismuth Wolframate: Towards Selective Oxidations for the Biorefinery Driven by Solar-Light. *Chem. Commun.* **2017**, *53*, 7521-7524.

(188) Hakki, A.; Dillert, R.; Bahnemann, D. W. Arenesulfonic Acid Functionalized Mesoporous Silica Decorated with Titania: A Heterogeneous Catalyst for the One-Pot Photocatalytic Synthesis of Quinolines from Nitroaromatic Compounds and Alcohols. *ACS Catal.* **2013**, 3, 565-572.

(189) Kominami, H.; Yamamoto, S.; Imamura, K.; Tanaka, A.; Hashimoto, K. Photocatalytic Chemoselective Reduction of Epoxides to Alkenes along with Formation of Ketones in Alcoholic Suspensions of Silver-Loaded Titanium (IV) Oxide at Room Temperature without the Use of Reducing Gases. *Chem Commun.* **2014**, *50*, 4558-4560.

(190) Mie, G. Beiträge zur Optik Trüber Medien, Speziell Kolloidaler Metallösungen. *Ann. Phys.* **1908**, *25*, 377-445.

(191) Kochuveedu, S. T.; Kim, D. -P.; Kim, D. H. Surface-Plasmon Induced Visible Light Photocatalytic Activity of TiO_2 Nanospheres Decorated by Au Nanoparticles with Controlled Configuration. *J. Phys. Chem. C* **2012**, *116*, 2500-2506.

(192) Zhao, J.; Zheng, Z.; Bottle, S.; Chou, A.; Sarina, S.; Zhu, H. Highly Efficient and Selective Photocatalytic Hydroamination of Alkynes by Supported Gold Nanoparticles Using Visible Light at Ambient Temperature. *Chem. Commun.* **2013**, *49*, 2676-2678.

(193) Ke, X.; Sarina, S.; Zhao, J.; Zhang, X.; Chang, J.; Zhu, H. Tuning the Reduction Power of Supported Gold Nanoparticle Photocatalysts for Selective Reductions by Manipulating Wavelength of Visible Light Irradiation. *Chem. Commun.* **2012**, *48*, 3509-3511.

(194) Ke, X.; Zhang, X.; Zhao, J.; Sarina, S.; Barry, J.; Zhu, H. Selective Reductions Using Visible Light Photocatalysts of Supported Gold Nanoparticles. *Green Chem.* **2013**, *15*, 236-244.

(195) Christopher, P.; Xin, H.; Linic, S. Visible-Light-Enhanced Catalytic Oxidation Reactions on Plasmonic Silver Nanostructures. *Nat. Chem.* **2011**, *3*, 467-472.

(196) Tada, H.; Ishida, T.; Takao, A.; Ito, S.; Mukhopadhyay, S.; Akita, T.; Tanaka, K.; Kobayashi, H. Kinetic and DFT Studies on the Ag/TiO_2-Photocatalyzed Selective Reduction of Nitrobenzene to Aniline. *ChemPhysChem* **2005**, *6*, 1537-1543.

(197) Tada, H.; Takao, A.; Akita, T.; Tanaka, K. Surface Properties and Photocatalytic Activity of Pt Core/Ag Shell Nanoparticle-Loaded TiO_2. *ChemPhysChem* **2006**, *7*, 1687-1691.

(198) Carneiro, J.; Yang, C. -C.; Moma, J.; Moulijn, J.; Mul, G. How Gold Deposition Affects Anatase Performance in the Photo-Catalytic Oxidation of Cyclohexane. *Catalysis Lett.* **2009**, *129*, 12-19.

(199) Ide, Y.; Kawamoto, N.; Bando, Y.; Hattori, H.; Sadakane, M.; Sano, T. Ternary Modified TiO_2 as a Simple and Efficient Photocatalyst for Green Organic Synthesis, *Chem. Commun.* **2013**, *49*, 3652-3654.

(200) Ide, Y.; Ogino, R.; Sadakane, M.; Sano, T. Effects of Au Loading and CO_2 Addition on photocatalytic selective phenol oxidation over TiO_2-Supported Au nanoparticles. *ChemCatChem* **2013**, *5*, 766-773.

(201) Ruberu, T.; Nelson, N.; Slowing, I.; Vela, J. Selective Alcohol Dehydrogenation and Hydrogenolysis with Semiconductor-Metal Photocatalysts: Toward solar-to-chemical energy conversion of biomass-relevant substrates. *J. Phys. Chem. Lett.* **2012**, *3*, 2798-2802.

(202) Xiao, Y.; Liu, J.; Mai, J.; Pan, C.; Cai, X.; Fang, Y. High-Performance Silver Nanoparticles Coupled with Monolayer Hydrated Tungsten Oxide Nanosheets: The Structural Effects in Photocatalytic Oxidation of Cyclohexane. *J. Colloid Interface Sci.* **2018**, *516*, 172-181.

(203) Palmisano, L.; Augugliaro, V.; Bellardita, M.; Di Paola, A.; García López, E.; Loddo, V.; Marcì, G.; Palmisano, G.; Yurdakal, S. Titania Photocatalysts for Selective Oxidations in Water. *ChemSusChem* **2011**, *4*, 1431-1438.

(204) Bellardita, M.; García-López, E. I.; Marcì, G.; Krivtsov, I.; García, J. R.; Palmisano, L. Selective Photocatalytic Oxidation of Aromatic Alcohols in Water by Using P-Doped g-C₃N₄. *Appl. Catal. B* **2018**, *220*, 222-233.

(205) Li, F.; Wang, Y.; Du, J.; Zhu, Y.; Xu, C.; Sun, L. Simultaneous Oxidation of Alcohols and Hydrogen Evolution in a Hybrid System under Visible Light Irradiation. *Appl. Catal. B* **2018**, *225*, 258-263.

(206) Ilkaeva, M.; Krivtsov, I.; García-López, E. I.; Marcì, G.; Khainakova, O.; García, J. R.; Palmisano, L.; Díaz, E.; Ordóñez, S. Selective Photocatalytic Oxidation of 5-Hydroxymethylfurfural to 2,5-Furandicarboxaldehyde by Polymeric Carbon Nitride-Hydrogen Peroxide Adduct. *J. Catal*. **2018**, *359*, 212-222.

(207) Augugliaro, V.; Camera-Roda, G.; Loddo, V.; Palmisano, G.; Palmisano, L.; Parrino, F.; Puma, M. A. Synthesis of Vanillin in Water by TiO₂ Photocatalysis. *Appl. Catal. B* **2012**, *111-112*, 555-561.

(208) Parrino, F; Palmisano, L. Reactions in the Presence of Irradiated Semiconductors: Are They Simply Photocatalytic?. *MiniRev. Org. Chem.* **2018**, *15*, 157-164.

(209) Tanaka, A.; Hashimoto, K.; Kominami, H. Selective Photocatalytic Oxidation of Aromatic Alcohols to Aldehydes in an Aqueous Suspension of Gold Nanoparticles Supported on Cerium(IV) Oxide under Irradiation of Green Light. *Chem. Commun*. **2011**, *47*, 10446-10448.

(210) Krivtsov, I.; García-López, E. I.; Marcì, G.; Palmisano, L.; Amghouz, Z.; García, J. R.; Ordóñez, S.; Díaz, E. Selective Photocatalytic Oxidation of 5-Hydroxymethyl-2-Furfural to 2,5-Furandicarboxaldehyde in Aqueous Suspension of g-C₃N₄. *Appl. Catal. B* **2017**, *204*, 430- 439.

(211) Imamura, K.; Tsukahara, H.; Hamamichi, K.; Seto, N.; Hashimoto, K.; Kominami, H. Simultaneous Production of Aromatic Aldehydes and Dihydrogen by Photocatalytic Dehydrogenation of Liquid Alcohols over Metal-Loaded Titanium(IV) Oxide under Oxidant- and Solvent-Free Conditions. *Appl. Catal. A* **2013**, *450*, 28-33.

(212) Mao, C.; Cheng, H.; Tian, H.; Li, H.; Xiao, W. -J.; Xu, H.; Zhao, J.; Zhang, L. Visible Light Driven Selective Oxidation of Amines to Imines with BiOCl: Does Oxygen Vacancy Concentration Matter?. *Applied Catal. B* **2018**, *228*, 87-96.

(213) Liu, S.; Zhang, N.; Tang, Z. -R.; Xu, Y. -J. Synthesis of One-Dimensional CdS@TiO₂ Core-Shell Nanocomposites Photocatalyst for Selective Redox: The Dual Role of TiO₂ Shell. *ACS Appl. Mater. Interfaces* **2012**, *4*, 6378-6385.

(214) Zhang, Y.; Zhang, N.; Tang, Z. -R.; Xu, Y. -J. Transforming CdS into an Efficient Visible Light Photocatalyst for Selective Oxidation of Saturated Primary C-H Bonds under Ambient Conditions. *Chem. Sci*. **2012**, *3*, 2812-2822.

(215) Chen, Z.; Wu, Y.; Xu, J.; Wang, F.; Wang, J.; Zhang, J.; Ren, Z.; He, Y.; Xiao, G. Synthesis of C-Coated ZnIn₂S₄ Nanocomposites with Enhanced Visible Light Photocatalytic Selective Oxidation Activity. *J. Mol. Catal. A* **2015**, *401*, 66-72.

(216) Zhang, N.; Liu, S.; Fu, X.; Xu, Y. -J. A Simple Strategy for Fabrication of ″Plum-Pudding″ Type Pd@CeO₂ Semiconductor Nanocomposite as a Visible-Light-Driven Photocatalyst for Selective Oxidation. *J. Phys. Chem. C* **2011**, *115*, 22901-22909.

(217) Zavahir, S.; Xiao, Q.; Sarina, S.; Zhao, J.; Bottle, S.; Wellard, M.; Jia, J.; Jing, L.; Huang, Y.; Blinco, J. P.; Wu, H.; Zhu, H. -Y. Selective Oxidation of Aliphatic Alcohols Using Molecular Oxygen at Ambient Temperature: Mixed-Valence Vanadium Oxide Photocatalysts. *ACS Catal*. **2016**, *6*, 3580-3588.

(218) Meng, S.; Ning, X.; Chang, S.; Fu, X.; Ye, X.; Chen, S. Simultaneous Dehydrogenation and Hydrogenolysis of Aromatic Alcohols in one Reaction System via Visible-Light-Driven Heterogeneous Photocatalysis. *J. Catal*. **2018**, *357*, 247-256.

(219) Zhang, S.; Huang, W.; Fu, X.; Zheng, X.; Meng, S.; Ye, X.; Chen, S. Photocatalytic Organic Transformations: Simultaneous Oxidation of Aromatic Alcohols and Reduction of Nitroarenes on CdLa₂S₄ in One Reaction System. *Appl. Catal. B* **2018**, *233*, 1-10.

(220) Wang, H.; Yan, J.; Chang, W.; Zhang, Z. Practical Synthesis of Aromatic Amines by Photocatalytic Reduction of Aromatic Nitro Compounds on Nanoparticles N-Doped TiO₂. *Catal. Commun*. **2009**, *10*, 989-994.

(221) Imamura, K.; Yoshikawa, T.; Hashimoto, K.; Kominami, H. Stoichiometric Production of Aminobenzenes and Ketones by Photocatalytic Reduction of Nitrobenzenes in Secondary Alcoholic Suspension of Titanium (IV) Oxide under Metal-Free Conditions. *Appl. Catal. B* **2013**, *134-135*, 193-197.

(222) Zhao, X.; Zhang, Y.; Wen, P.; Xu, G.; Ma, D.; Qiu, P. NH₂-MIL-125(Ti)/TiO₂ Composites as Superior Visible-Light Photocatalysts for Selective Oxidation of Cyclohexane. *Mol. Catal*. **2018**, *452*, 175-183.

(223) Henríquez, A.; Mansilla, H. D.; Martínez-de la Cruz, A. M.; Freer, J.; Contreras, D. Selective Oxofunctionalization of Cyclohexane over Titanium dioxide–Based and Bismuth Oxyhalide (BiOX, X = Cl⁻, Br⁻, I⁻) Photocatalysts by Visible Light Irradiation. *Appl. Catal. B* **2017**, *206*, 252-262.

(224) Ueyama, K.; Hatta, T.; Okemoto, A.; Taniya, K.; Ichihashi, Y.; Nishiyama, S. Cyclohexane Photooxidation under Visible Light Irradiation by WO₃-TiO₂ Mixed Catalysts. *Res. Chem. Intermed*. **2018**, *44*, 629-638.

(225) Yang, J.; Mou, C. -Y. Ordered Mesoporous Au/TiO₂ Nanospheres for Solvent-Free Visible-Light Driven Plasmonic Oxidative Coupling Reactions of Amines. *Appl. Catal. B* **2018**, *231*, 283-291.

(226) Almquist, C. B.; Biswas, P. The Photo-Oxidation of Cyclohexane on Titanium Dioxide: An Investigation of Competitive Adsorption and its Effects on Product Formation and Selectivity. *Appl. Catal. A* **2001**, *214*, 259-271.

(227) Wang, C.; Xie, Z.; De Krafft, K. E.; Lin, W. Doping Metal-Organic Frameworks for Water Oxidation, Carbon Dioxide Reduction, and Organic Photocatalysis. *J. Am. Chem. Soc*. **2011**, *133*, 13445-13454.

(228) Yang, D.; Wu, T.; Chen, C.; Guo, W.; Liu, H.; Han, B. The Highly Selective Aerobic Oxidation of Cyclohexane to Cyclohexanone and Cyclohexanol over V₂O₅@TiO₂ under Simulated Solar Light Irradiation. *Green Chem*. **2017**, *19*, 311-318.

(229) Colmenares, J. C.; Magdziarz, A.; Bielejewska, A. High-Value Chemicals Obtained from Selective Photo-Oxidation of Glucose in the Presence of Nanostructured Titanium Photocatalysts. *Bioresource Technol*. **2011**, *102*, 11254-11257.

(230) Wu, Q.; He, Y.; Zhang, H.; Feng, Z.; Wu, Y.; Wu, T. Photocatalytic Selective Oxidation of Biomass-Derived 5-Hydroxymethylfurfural to 2,5-Diformylfuran on Metal-Free g-C₃N₄ under Visible Light Irradiation. *Mol. Catal*. **2017**, *436*, 10-18.

(231) Zhang, B.; Li, J.; Zhang, B.; Chong, R.; Li, R.; Yuan, B.; Lu, S. -M.; Li, C. Selective Oxidation of Sulfides on Pt/BiVO₄ Photocatalyst under Visible Light Irradiation Using Water as the Oxygen Source and Dioxygen as the Electron Acceptor. *J. Catal*. **2015**, *332*, 95-100.

(232) Kubacka, A.; Fernandez-García, M.; Colon, G. Advanced Nanoarchitectures for Solar Photocatalytic Applications. *Chem. Rev*. **2012**, *112*, 1555-1614.

(233) Navalon, S.; Dhakshinamoorthy, A.; Alvaro, M.; Garcia, H. Photocatalytic CO₂ Reduction Using non-Titanium Metal Oxides and Sulfides. *ChemSusChem* **2013**, *6*, 562-577.

(234) Olivo, A.; Ghedini, E.; Pascalicchio, P.; Manzoli, M.; Cruciani, G.; Signoretto, M. Sustainable Carbon Dioxide Photoreduction by a Cooperative Effect of Reactor Design and Titania Metal Promotion. *Catalysts* **2018**, *8*, 41.

(235) Lo, C. C.; Hung, C. H.; Yuan, C. S.; Wu, J. F. Parameter Effects and Reaction Pathways of Photoreduction of CO₂ over TiO₂/SO₄²⁻ Photocatalyst. *Sol. Energy Mater. Sol. Cells* **2007**, *91*, 1765-1774

(236) Wang, T.; Yang, L.; Du, X.; Yang, Y. Numerical Investigation on CO₂ Photocatalytic Reduction in Optical Fiber Monolith Reactor. *Energy Convers. Manag.* **2013**, *65*, 299-307.

(237) Wu, J. C. S. Photocatalytic Reduction of Greenhouse Gas CO₂ to Fuel. *Catal. Surv. Asia* **2009**, *13*, 30-40.

(238) Liu, Y.; Huang, B.; Dai, Y.; Zhang, X.; Qin, X.; Jiang, M.; Whangbo, M. -H. Selective Ethanol Formation from Photocatalytic Reduction of Carbon Dioxide in Water with BiVO₄ Photocatalyst. *Catal. Commun*. **2009**, *11*, 210-213.

(239) Lee, W. H.; Liao, C. H.; Tsai, M. F.; Huang, C. W.; Wu, J. C. S. A Novel Twin Reactor for CO₂ Photoreduction to Mimic Artificial Photosynthesis. *Appl. Catal. B* **2013**, *132-133*, 445-451.

(240) Bazzo, A.; Urawaka, A. Origin of Photocatalytic Activity in Continuous Gas Phase CO₂ Reduction over Pt/TiO₂. *ChemSusChem* **2013**, *6*, 2095-2102.

41

(241) Colombo, E.; Ashokkumar, M. Comparison of the Photocatalytic Efficiencies of Continuous Stirred Tank Reactor (CSTR) and Batch Systems Using a Dispersed Micron Sized Photocatalyst. *RSC Adv.* **2017**, *7*, 48222-48229.

(242) Camera-Roda, G.; Augugliaro, V.; Cardillo, A.; Loddo, V.; Palmisano, G.; Palmisano, L. A Pervaporation Photocatalytic Reactor for the Green Synthesis of Vanillin. *Chem. Eng. J.* **2013**, *224*, 136-143.

(243) Shargh, M.; Behnajady, M. A. A High-Efficient Batch-Recirculated Photoreactor Packed with Immobilized TiO$_2$-P25 Nanoparticles onto Glass Beads for Photocatalytic Degradation of Phenazopyridine as a Pharmaceutical Contaminant: Artificial Neural Network Modelling. *Water Sci. Technol.* **2016**, *73*, 2804-2814.

(244) Vaiano, V.; Sacco, O.; Sannino, D.; Stoller, M.; Ciambelli, P.; Chianese, A. Photocatalytic Removal of Phenol by Ferromagnetic N-TiO$_2$/SiO$_2$/Fe$_3$O$_4$ Nanoparticles in Presence of Visible Light Irradiation. *Chem. Eng.* **2016**, *47*, 1-6.

(245) Meshram, S.; Limaye, R.; Ghodke, S.; Nigam, S.; Sonawane, S.; Chikate, R. Continuous Flow Photocatalytic Reactor Using ZnO-Bentonite Nanocomposite for Degradation of Phenol. *Chem. Eng. J.* **2011**, *172*, 1008-1015

(246) Levenspiel, O. *Chemical Reactor Engineering*, third Edition, John Wiley & Sons, New York, Chichester, Weinheim, Brisbane, Singapore, Toronto, 1999.

(247) Cassano, A. E.; Martin, C. A.; Brandi, R. J.; Alfano, O. M. Photoreactor Analysis and Design: Fundamentals and Applications. *Ind. Eng. Chem. Res.* **1995**, *34*, 2155-2201.

(248) Yang, Z.; Zhongguo, Y.; Liu, M.; Lin, C. Photocatalytic Activity and Scale-Up Effect in Liquid–Solid Mini-Fluidized Bed Reactor. *Chem. Eng. J.* **2016**, *291*, 254-268.

(249) Heggo, D.; Ookawara, S. Multiphase Photocatalytic Microreactors. *Chem. Eng. Sci.* **2017**, *169*, 67-77.

(250) Krivec, M.; Žagar, K.; Suhadolnik, L.; Čeh, M.; Dražić, G. Highly Efficient TiO$_2$-Based Microreactor for Photocatalytic Applications. *ACS Appl. Mater. Inter.* **2013**, *5*, 9088-9094.

(251) Matsushita, Y.; Ohba, N.; Kumada, S.; Sakeda, K.; Suzuki, T.; Ichimura, T. Photocatalytic Reactions in Microreactors. *Chem. Eng. J.* **2008**, *135*, s303–s308.

(252) Choi, B. -C.; Xu, L. -H.; Kim, H. -T.; Bahnemann, D. W. Photocatalytic Characteristics on Sintered Glass and Microreactors. *J. Ind. Eng. Chem.* **2006**, *12*, 663-672.

(253) Liu, H.; Feng, J.; Zhang, J.; Miller, P.W.; Chen, L.; Su, C. -Y. A Catalytic Chiral Gel Microfluidic Reactor Assembled via Dynamic Covalent Chemistry. *Chem. Sci.* **2015**, *6*, 2292-2296.

(254) Lei, L.; Wang, N.; Zhang, X. M.; Tai, Q.; Tsai, D. P.; Chan, H. L. W. Optofluidic Planar Reactors for Photocatalytic Water Treatment Using Solar Energy. *Biomicrofluidics* **2010**, *4*, 043004.

(255) Li, L.; Chen, R.; Zhu, X.; Wang, H.; Wang, Y.; Liao, Q.; Wang, D. Optofluidic Microreactors with TiO$_2$-Coated Fiberglass. *ACS Appl. Mater. Inter.* **2013**, *5*, 12548-12553.

(256) Cambie, D.; Bottecchia, C.; Straathof, N. J. W.; Hessel, V.; Noel, T. Applications of Continuous-Flow Photochemistry in Organic Synthesis, Material Science, and Water Treatment. *Chem. Rev.* **2016**, *116*, 10276-10341

(257) Matsushita, Y.; Kumada, S.; Wakabayashi, K.; Sakeda, K.; Ichimura, T. Photocatalytic Reduction in Microreactors. *Chem. Lett.* **2006**, *35*, 410–411.

(258) Takei, G.; Kitamori, T.; Kim, H.B. Photocatalytic Redox-Combined Synthesis of L-Pipecolinic Acid with a Titania-Modified Microchannel Chip. *Catal. Commun.* **2005**, *6*, 357-360.

(259) Matsushita, Y.; Ohba, N.; Kumada, S.; Suzuki, T.; Ichimura, T. Photocatalytic N-Alkylation of Benzylamine in Microreactors. *Catal. Commun.* **2007**, *8*, 2194-2197

(260) Matsushita, Y.; Ohba, N.; Suzuki, T.; Ichimura, T. N-Alkylation of Amines by Photocatalytic Reaction in a Microreaction System. *Catal. Today* **2008**, *132*, 153-158

(261) Baghbanzadeh, M.; Glasnov, T. N.; Kappe, C. O. Continuous-Flow Production of Photocatalytically Active Titanium Dioxide Nanocrystals and its Application to the Photocatalytic Addition of N,N-Dimethylaniline to N-Methylmaleimide. *J. Flow Chem.* **2013**, *3*, 109-113.

(262) Cremlyn, R. J. An Introduction to Organosulfur Chemistry. New York: **1996**, Wiley–VCH.

(263) Witt, D. Recent Developments in Disulfide Bond Formation. *Synthesis* **2008**, *16*, 2491-2509.

(264) Bottecchia, C.; Erdmann, N.; Tijssen, P. M.; Milroy, L. G.; Brunsveld, L.; Hessel, V.; Noël, T. Batch and Flow Synthesis of Disulfides by Visible-Light-Induced TiO$_2$ Photocatalysis. *ChemSusChem* **2016**, *9*, 1781-785.

(265) Woźnica, M.; Chaoui, N.; Taabache, S.; Blechert, S. THF: An Efficient Electron Donor in Continuous Flow Radical Cyclization Photocatalyzed by Graphitic Carbon Nitride. *Chem. Eur. J.* **2014**, *20*, 14624-14628.

(266) Tucker, J. W.; Nguyen, J. D.; Narayanam, J. M. R.; Krabbe, S. W.; Stephenson, C. R. J. Tin-Free Radical Cyclization Reactions Initiated by Visible Light Photoredox Catalysis. *Chem. Commun.* **2010**, *46*, 4985-4987.

(267) Katayama, K.; Tanaka, Y.; Shimaoka, K.; Yoshida, K.; Shimizu, R.; Ishikawa, T.; Nakamura, A.; Kuwahara, S.; Mase, A.; Sugita, T.; Mori, M. Novel Method of Screening the Oxidation and Reduction Abilities of Photocatalytic Materials. *Analyst* **2014**, *139*, 1953-1959.

(268) Maeda, H.; Nakagawa, H.; Mizuno, K. Enhancement Effect of Mg(ClO$_4$)$_2$ On TiO$_2$-Catalyzed Photooxygenation of 1,2-Diarylcyclopropanes. *Photochem. Photobiol. Sci.* **2003**, *2*, 1056-1058.

(269) Mizuno, K.; Kamiyama, N.; Ichinose, N.; Otsuji, Y. Photo-Oxygenation of 1,2-Diarylcyclopropanes via Electron Transfer. *Tetrahedron* **1985**, *41*, 2207-2214.

(270) Hurevich, M.; Kandasamy, J.; Ponnappa, B. M.; Collot, M.; Kopetzki, D.; McQuade, D. T.; Seeberger, P. H. Continuous Photochemical Cleavage of Linkers for Solid-Phase Synthesis. *Org. Lett.* **2014**, *16*, 1794-1797.

(271) Camera Roda, G.; Santarelli, F.; Intensification of Water Detoxification by Integrating Photocatalysis and Pervaporation. *J. Sol Energy Eng.* **2007**, *129*, 68-73.

(272) Bianchi, D.; Balducci, L.; Bortolo, R.; D'Aloisio, R.; Ricci, M.; Span, G.; Tassinari, R.; Tonini, C.; Ungarelli, R. Oxidation of Benzene to Phenol with Hydrogen Peroxide Catalyzed by a Modified Titanium Silicalite (TS-1B). *Adv. Synth. Catal.* **2007**, *349*, 979-986.

(273) Bianchi, D.; Bortolo, R.; Tassinari, R.; Ricci, M.; Vignola, R. A Novel Iron-Based Catalyst for the Biphasic Oxidation of Benzene to Phenol with Hydrogen Peroxide. *Angew. Chem. Int. Ed.* **2000**, *39*, 4321-4323.

(274) Itoh, N.; Niwa, S.; Mizukami, F.; Inoue, T.; Igarashi, A.; Namba, T. Catalytic Palladium Membrane for Reductive Oxidation of Benzene to Phenol. *Catal. Commun.* **2003**, *4*, 243-246.

(275) Laufer, W.; Hoelderich, W. F. New Direct Hydroxylation of Benzene with Oxygen in the Presence of Hydrogen over Bifunctional Ion-Exchange Resins. *Chem. Commun.* **2002**, *16*, 1684-1685.

(276) Molinari, R.; Poerio, T. Remarks on Studies for Direct Production of Phenol in Conventional and Membrane Reactors. *Asia-Pac. J. Chem. Eng.* **2010**, *5*, 191-206.

(277) Molinari, R.; Caruso, A.; Poerio, T. Direct Benzene Conversion to Phenol in a Hybrid Photocatalytic Membrane Reactor. *Catal. Today* **2009**, *144*, 81-86.

(278) Molinari, R.; Lavorato, C.; Argurio, P. Photocatalytic Reduction of Acetophenone in Membrane Reactors under UV and Visible Light Using TiO$_2$ and Pd/TiO$_2$ Catalysts. *Chem. Eng. J.* **2015**, *274*, 307-316.

(279) Molinari, R.; Lavorato, C.; Mastropietro, T. F.; Argurio, P.; Drioli, E.; Poerio, T. Preparation of Pd-Loaded Hierarchical FAU Membranes and Testing in Acetophenone Hydrogenation. *Molecules* **2016**, *21*, 394.

(280) Camera-Roda, G.; Santarelli, F.; Augugliaro, V.; Loddo, V.; Palmisano, G.; Palmisano, L.; Yurdakal, S. Photocatalytic Process Intensification by Coupling with Pervaporation. *Catal. Today* **2011**, *161*, 209-213.

(281) Böddeker, K. W. Terminology in Pervaporation. *J. Membr. Sci.* **1990**, *51*, 259-272.

(282) Sinha, A. K.; Sharma, U. K.; Sharma, N. A Comprehensive Review on Vanilla Flavor: Extraction, Isolation and Quantification of Vanillin and others Constituents. *Int. J. Food Sci. Nutr.* **2008**, *59*, 299–326.

(283) Walton, N. J.; Mayer, M. J.; Narbad, A. Vanillin, *Phytochemistry* **2003**, *63*, 505-515.

(284) Korthou, H.; Verpoorte, R. *Vanilla*, in: Berger, R. G. *Flavours and Fragrances*, Springer-Verlag Berlin Heidelberg, 2007, 203-217.

(285) Camera-Roda, G.; Cardillo, A.; Loddo, V.; Palmisano, L.; Parrino, F. Improvement of Membrane Performances to Enhance the Yield of Vanillin in a Pervaporation Reactor. *Membranes* **2014**, *4*, 96-112.

(286) Camera-Roda, G.; Santarelli, F. Design of a Pervaporation Photocatalytic Reactor for Process Intensification. *Chem. Eng. Technol.* **2012**, *35*, 1221-1228.

(287) Camera-Roda, G.; Loddo, V.; Palmisano, L.; Parrino, F.; Santarelli, F. Process Intensification in a Photocatalytic Membrane Reactor: Analysis of the Techniques to Integrate Reaction and Separation. *Chem. Eng. J.* **2017**, *310*, 352-359.

(288) Pathak, P.; Meziani, M. J.; Li, Y.; Cureton, L. T.; Sun, Y. P. Improving Photoreduction of CO_2 with Homogeneously Dispersed Nanoscale TiO_2 Catalysts. *Chem. Commun.* **2004**, 1234-1235.

(289) Pathak, P.; Meziani, M. J.; Castillo, L.; Sun, Y. P. Metal-Coated Nanoscale TiO_2 Catalysts for Enhanced CO_2 Photoreduction. *Green Chem.* **2005**, *7*, 667-670.

(290) Rani, S.; Bao, N.; Roy, S. C. Solar Spectrum Photocatalytic Conversion of CO_2 and Water Vapor into Hydrocarbons Using TiO_2 Nanoparticle Membranes. *Appl. Surf. Sci.* **2014**, *289*, 203-208.

(291) Cheng, X.; Chen, R.; Zhu, X.; Liao, Q.; He, X.; Li, S.; Li, L. Optofluidic Membrane Microreactor for Photocatalytic Reduction of CO_2. *Int. J. Hydrogen Energy* **2016**, *41*, 2457-2465.

(292) Brunetti, A.; Fontananova, E.; Donnadio, A.; Casciola, M.; Di Vona, M. L.; Sgreccia, E.; Drioli, E.; Barbieri, G. New Approach for the Evaluation of Membranes Transport Properties for Polymer Electrolyte Membrane Fuel Cells. *J. Power Sources* **2012**, *205*, 222-230.

(293) Sellaro, M.; Bellardita, M.; Brunetti, A.; Fontananova, E.; Palmisano, L.; Drioli, E.; Barbieri, G. CO_2 Conversion in a Photocatalytic Continuous Membrane Reactor. *RSC Adv.* **2016**, *6*, 67418-67427.

(294) Pomilla, F. R.; Brunetti, A.; Marcì, G.; García-López, E. I.; Fontananova, E.; Palmisano, L.; Barbieri, G. CO_2 to Liquid Fuels: Photocatalytic Conversion in a Continuous Membrane Reactor. *ACS Sustain. Chem. Eng.* **2018**, *6*, 8743-8753.